DIELECTRIC AND RHEOLOGICAL PROPERTIES OF EMULSIONS

A Thesis

Submitted to the Faculty of Graduate Studies
in partial fulfilment of the requirements
for the degree of Master of Science.

by

EDWARD COLLINS

From the Physical Chemistry Laboratory
under the supervision of Dr. L. B. Funt.

University of Manitoba
April, 1952.

ACKNOWLEDGMENT

The author wishes to acknowledge the financial assistance provided by the National Research Council in the form of a summer bursary and research grant. Further he wishes to acknowledge the excellent work done in construction of the cell by Mr. G. Trider, Instrument Shop, University of Manitoba.

TABLE OF CONTENTS

DIELECTRIC AND RHEOLOGICAL PROPERTIES OF EMULSIONS

INTRODUCTION

It has been observed by Voet (1) that as the concentration of the dispersed phase is increased the dielectric constant of liquid dispersions may decrease very considerably upon the application of shearing stresses to the system. An analysis of this phenomenon (1) has yielded the following theory; at relatively low concentration the particles of the dispersion move independently (i.e.) exhibit Newtonian flow but at a value of the concentration greater than some critical value, a tendency to particle agglomeration exists, resulting in the formation of structures and a plastic type of flow. Such particle structures, however, are broken up upon the application of shearing stresses, and as a result the particles move independently at high concentration in these systems. Voet interprets them as accounting for the decrease in the dielectric constant.

The purpose of this investigation was to attempt to verify the theory presented by Voet (1). The results procured by Voet (1) were the only previously existing ones, and for emulsions represented very inconclusive data, certainly inadequate to verify the theory he presented. The work done by the author, however, is the most comprehensive investigation of dielectric and rheological properties of emulsions that has ever been performed and it is on the basis of such results that the validity of the present theories must be judged.

It was further anticipated that the changes in the dielectric constant could be correlated with changes in the viscosity and with this in mind, it was undertaken to measure these two quantities simultaneously.

PART I

DIELECTRIC PROPERTIES OF DISPERSIONS

Even though dispersions made with apparatus such as roller mills, ball mills, colloid mills, etc., usually show a comparatively small particle size on microscopic observation, there are, nevertheless indications that in concentrated dispersions secondary particle agglomeration (or flocculation) occurs. The rheological study of pigment dispersions (2) reveals the existence of plastic and thixotropic systems, the structure of which is thought to be destroyed by the application of shearing stresses. No direct proof of the destruction and rebuilding of such flocculated particle structures has been offered by rheological investigations (2). In addition the phenomenon of plug flow has rendered a proper interpretation of the rheological behavior of pigment dispersions at very low shearing stresses rather uncertain (3) making our knowledge of particle agglomeration at low shearing stresses very incomplete. Rheological investigation offers no knowledge about the progressive particle agglomeration in a dispersion at rest.

The study of the dielectric properties of dispersions at rest as well as when subjected to varying shearing stresses has made it possible to obtain more direct information regarding the existence of such structures.

The theoretical treatment of the dielectric constant of a dispersion was attempted at the end of the last century. Calculations on the basis of the Clausius-Masotti relations became totally inadequate when the dielectric constant of the dispersion medium and dispersed medium were different. The related Lorentz - Lorenz equation is equally invalid (4). The problem was studied theoretically by Bruggeman (5).

An experimental study of the validity of various theoretical considerations was made by Guillien (6) who investigated the dielectric constant of particles of various materials dispersed in air as well as in organic liquids. The results of this study may be summarized as follows: The dielectric constant (ϵ) of a dispersion of a material of dielectric constant ϵ_1, dispersed in a volume fraction, V, in a medium with dielectric constant ϵ_2, depends not only on ϵ_1, ϵ_2 and V but also on the form of the particles and is independent of the size of the particles. The minimum dielectric constant was found for spherical particles, while a considerable increase was found for nonspherical particles.

For spherical particles an equation proposed by Bruggeman (5) appeared to be covering the existing experimental data very well. The equation

$$1 - V = \frac{\epsilon_1 - \epsilon}{\epsilon_1 - \epsilon_2}\left(\frac{\epsilon_2}{\epsilon}\right)^{1/3} \qquad \text{---------- (1)}$$

where V is the volume fraction of the dispersed phase, ϵ is the dielectric constant of the dispersion, ϵ_1 the dielectric constant of the solid particles, and ϵ_2 the dielectric constant of the suspending medium holds for any dispersed phase regardless of its own dielectric constant. It is valid even for infinitely high dielectric constant of the dispersed phase, such as for particles of metals or other conductors. In the latter case the equation is simplified to

$$1-V = \left(\frac{\epsilon_2}{\epsilon}\right)^{1/3} \quad \text{or} \quad \epsilon = \frac{\epsilon_2}{(1-V)^3} \qquad \text{----------(2)}$$

The latter equation may be rewritten as

$$\epsilon = \epsilon_2 (1+3V) \qquad \text{----------(3)}$$

by neglecting the higher terms of V, a procedure which is allowable only for smaller values of V.

The dielectric constant of a dispersion of non-spherical particles is considerably higher than for spherical particles occupying the same volume. In addition, the greater the deviation from the spherical form, the higher is the dielectric constant of the dispersion. Consequently, since particle agglomeration leads to non-spherical chains of particles, these agglomerated particles must show an increase in dielectric constant, which is expected to decrease to the normal value when a shearing stress is applied which breaks up the aggregates. In addition, in a dispersion at rest in which particle structures are in the process of building up, an increase in the dielectric constant is expected, indicating the progressive particle structure formation. A suggestion that such an effect actually exists was found in an observation by Parts (7) that the dielectric constant of a printing ink changed with time. Both effects were verified experimentally and data were obtained for a number of systems Voet (1).

The quantitative evaluation of the dielectric constant of a dispersion of non-spherical particles is very complicated, owing to the fact that the form factor depends not only on the particle form but also on the dielectric constant of both phases. It appeared that none of the many theoretical approaches made in the literature led to a satisfactory equation covering older experiments. Voet (1) extended Bruggeman's equation by introducing a form factor for non-spherical particles in dispersions where the dielectric constant of the dispersed phase is much larger than the dielectric constant of the medium. The modified Bruggeman equation becomes

$$\epsilon = \epsilon_2 \quad (1 + 3fV) \qquad \text{----------} \quad (4)$$

for spherical particles $f = 1$ and for non-spherical particle $f > 1$. Without being able to make any definite prediction about particle shape, it

is possible to state that the larger the experimentally determined factor is, the more the particle shape shows deviation from a spherical form. The form factor can never become smaller than unity.

The form factor for plate-like or needle-shaped particles naturally depends on their orientation. According to the theory of Bruggeman (5) the dielectric constant has a minimum for orientation perpendicular to the field and a maximum for an orientation parallel to the field, while an intermediate factor is valid for random distribution.

Although we are not primarily concerned with dispersions of solids in liquids the conclusion drawn from such experiments aid in the explanations of observed phenomena in liquid dispersions.

On viewing zinc dispersions in mineral oil microscopically, Voet (1) found the particles to be approximately spherical. However, on application of Equation 4, the form factor was found to be 1.4, exhibiting the sensitivity of form factor to the shape of the particles. When the dispersions were allowed to stand, it appeared that at higher concentration the dielectric constant increased, but returned generally to its original value upon agitation.

This change of particle shape, can be explained only by particle agglomeration. Since we have solid zinc particles occupying a constant volume in the dispersion no possibility seemed to exist for a change in the shape of the individual particles.

Where particle agglomeration was found to occur, Voet (1) indicated as the agglomeration factor, A_v, the ratio between the experimentally determined form factor at rest at a given concentration and the form factor of the dispersed phase as determined from the

linear relationship under shearing stresses. Thus

$$\epsilon_v' = \epsilon_2 \left(1 + 3 A_v f V\right) \qquad \text{----------(5)}$$

where ϵ_v' is the value of dielectric constant of the dispersion at rest characterized by the agglomeration factor A_v at the concentration V. Voet gives data in support of the statement that Newtonian flow is characterized by absence of particle agglomeration and hence $A_v = 1$ while a definite particle agglomeration must be associated with plastic flow for which $A_v > 1$.

To study other aspects of flow the dielectric qualities were determined at low shearing stresses corresponding to approximately 8 R.P.M. Dimensions of the double cylindrical capacity cell used were as follows: inside diameter and height of the brass cup were 102 mms. and 96 mms. respectively; outside diameter and height of the brass bob were both 90 mms. It appeared that under these conditions of low shear all the zinc powder dispersions investigated showed a dielectric constant identical with the value obtained at the highest shearing stress corresponding to approximately 250 R.P.M. Thus it is evident that the forces which act to form particle agglomeration in zinc dispersions are weak and very easily removed, and it is desirable to study the progression of particle agglomeration at rest. The dielectric qualities of different zinc dispersions were determined at various time intervals after the dispersion had been thoroughly agitated and the agglomeration factor calculated. It was observed that the particle agglomeration factor changes in dispersions at rest. The upper limit was often not reached in ten minutes and it took sometimes hours before the final stage of maximum agglomeration was reached. This phenomena is closely connected with thixotropy which is believed to

result from the gradual rebuilding of a previously destroyed particle structure.

On investigating dispersion of aluminum leaflets in mineral oil, Voet (1) found the form factor to be 8.2. When viewed under a microscope the aluminum particles deviated much from spherical form. The difference in static and dynamic dielectric behavior was explained as due to differences in particle orientation. This was further backed by showing that the dispersion regained its original random distribution after a short period of time (less than 2 seconds) after agitation was stopped. Even though there is a decrease in the dielectric constant on application of shearing stresses, the agglomeration factor is equal to unity, since the decrease is due to particle orientation, and not particle agglomeration.

Generally speaking particle agglomeration is characterized by a linear relationship between the dielectric constant and concentration under shear and a curve convex towards the abscissa at rest, although the initial part of this curve, at lower concentration may be a straight line. Particle orientation is characterized by a linear relationship in both cases.

As a liquid dispersion, Voet (1) used .5 Normal NaOH (to obtain conducting particles) dispersed by a conventional but a specified emulsifying agent in mineral oil. The form factor was calculated to be 2.0. It was observed that at rest an extremely high agglomeration factor existed. On microscopic observation of these dispersions all the particles appeared to be perfectly spherical. The deviation of the form factor from one was explained by an elongation of the particles under shear, resulting in ellipsoidal particles instead of spheres. The deviation in form factor is due to distortion, here distortion by shear. In very dilute dispersions particle agglomeration, which was microscopically visible did not appear to lead generally to coalescence,

but merely to the formation of particle chains in which individual particles remained visible.

The changes with time in the dispersions are best demonstrated by the change of the agglomeration factor with time calculated by means of equation (5). It was noted that fairly high shearing stresses were needed to break up the particle agglomeration formed; for a 10% dispersion more than 100 R.P.M. was required to obtain the minimum dielectric constant.

Voet (1) checked the validity of the factor 3.0 of the Bruggeman equation (Equation 2) experimentally and justified its use for perfectly spherical particles of conductive material.

PART II

RHEOLOGICAL PROPERTIES OF DISPERSION

The following sections will be a discussion of the Green theory (15) on the rotational viscometer as used in rheological measurements.

Green uses two concepts as the basis for his rheological system. They are:

(1) Newton's concept of viscous flow, $F = \eta \frac{dv}{dr}$ ---------- (6)

Newton assumed that the rate of shear is directly proportional to the tangential shearing stress. The proportionality constant η is the coefficient of viscosity and is defined as the tangential shearing force per unit area that will produce a unit rate of shear. Equation (6) is applicable only to liquids whose molecules are not hampered in their motion by the formation of structure or by molecular alignment

under high rates of shear.

(2) Bingham's concept (modification of Equation (6) for plastic flow or for Bingham bodies).

$$\mu (F - f) = \frac{dv}{dr} \qquad \text{----(7)}$$

For plastic clay suspensions in water, Bingham used Equation (7). He reasoned that plastic flow could not start until the applied shearing stress exceeded the stress arising from frictional resistance between the clay particles. He thus introduced a frictional factor f (which is the tangential force per unit area first required to start flow) into the Newtonian Equation (6). He also replaced $\frac{1}{\eta}$ with μ which he called the mobility.

When Bingham first recognized the significance of an intercept on the pressure axis, he attributed it to friction. This friction existed between the particle of the suspension, and resisted flow to the extent of the pressure designated by the intercept. The letter f was used to symbolize friction. This letter has been retained by many rheologists, even though the name friction is no longer employed. It seemed highly probable that friction might not be the only factor involved in producing the intercept.

The force of suspension flocculation can also prevent flow unless it is exceeded by the applied force. (The transition from plug to laminar flow is sufficient to cause most, if not all, the curvature in the lower end of the consistency curve for Bingham bodies. This is true for rotational as well as for capillary viscometers). Plug flow is that part of the flow where the shearing stress is less than the yield value, laminar flow being orderly flow or flow in parallel layers.

The term "yield value" for f was suggested as a temporary ex-

pedient until something more appropriate could be found. The term yield value appeared for the first time in a joint publication by Bingham and Green in 1918. Several years later the term was definitely adopted by them, though it was realized that it was not entirely satisfactory.

Plastics (Bingham bodies and not synthetic plastics) are distinguished from liquids by having a yield value. When the yield value of a material is sufficiently high, it becomes manifest by comparing to it a shortness or butter-like consistency. Yield values make plasticity possible. Plasticity also includes the concept of flow without rupture; that is, the material must not be brittle.

A Newtonian liquid is defined rheologically by only one constant. That constant is the coefficient of viscosity. Viscosity is directly proportional to the cotangent of the angle made by the consistency curve and the force axis. Numerically it is equal to the number of dynes that will induce a unit rate of shear. This number varies with the temperature of the material; so the temperature at the time of measuring should be given with it. The unit of viscosity is the poise. When a shearing force of one dyne induces a unit rate of shear, the material has a coefficient of viscosity of one poise. Since the rate of flow is directly proportional to the pressure, the coefficient of viscosity for a Newtonian can be obtained by a one-point method from the plot of rate of flow vs. pressure. The measurement is made for any point "a", a straight line is drawn through, "a" to the origin "o" and the result is the consistency curve.

The single-point method is invalid for non-Newtonian fluids. Even so, many rheologists use such a procedure for non-Newtonian fluids. They attempt to make their measurement valid by calling it apparent viscosity. Apparent viscosity is the viscosity a material

would have if it were a Newtonian. But, a non-Newtonian is never a Newtonian. Hence, apparent viscosity is derived from an entirely hypothetical consistency curve.

Plastic viscosity is defined according to Equation (7).

$$U = \frac{F - f}{\frac{dv}{dr}} \qquad \text{----(8)}$$

where U is the coefficient of plastic viscosity and f is the Bingham yield value. Plastic viscosity is the number of dynes per square centimeter of tangential shearing force in excess of the Bingham yield value that will induce a unit rate of shear. Plastic viscosity cannot be determined experimentally by a one-point method. Plastic viscosities are comparable while apparent viscosities are not.

The capillary viscometer is of no use in working with Bingham bodies since it lacks constancy of shear. No method for determining yield values and plastic viscosities other than the use of the Buckingham equation (which was tedious and inaccurate) existed until Reiner and Riwlin published their equation of plastic flow in rotational viscometers (16).

The equation of plastic flow in a rotational viscometer as developed by Reiner and Riwlin (16) is

$$\Omega = \mu \frac{T}{4\pi h}\left(\frac{1}{R_b^2} - \frac{1}{R_c^2}\right) - \mu f \ln \frac{R_c}{R_b} \qquad \text{----(9)}$$

where Ω the angular velocity ω when the torque T (at equilibrium) becomes sufficiently large so that all the material between the wall of the cup and the bob is in laminar flow. R_c and R_b are the radii of the cup and bob respectively, h is the depth of immersion of the bob and f is the yield value.

Equation (9) is the equation of the linear part of the curve,

that is from T_1 upwards (Figure 1).

It is not necessary, to know the equation for the lower end of the curve where transition from plug to laminar flow takes place. In that respect it differs from the Buckingham equation. The curve of Equation 9, on extrapolation to the torque axis, cuts it at the point $\omega = 0$ and $T = T_2$. Then

$$\frac{T_2}{4\pi h}\left(\frac{1}{R_b^2} - \frac{1}{R_c^2}\right) = f \ln \frac{R_c}{R_b} \qquad \text{----(10)}$$

Setting

$$\frac{\frac{1}{R_b^2} - \frac{1}{R_c^2}}{4\pi h} = S \qquad \text{----(11)}$$

and

$$\frac{S}{\ln \frac{R_c}{R_b}} = C \qquad \text{----(12)}$$

gives

$$f = CT_2 \qquad \text{----(13)}$$

Substituting Equations (11), (12), and (13) in Equation (9) and writing μ for $\frac{1}{\mu}$ give

$$\mu = \frac{(T - T_2)\, S}{\Omega} \qquad \text{----(14)}$$

Equations(13)and (14) are the two most important flow equations for plastics of the Bingham-body type where the rotational viscometer is used in making the rheological measureme nts. The constants S and C are instrumental constants.

The amount of torque T is calculated from the number of degrees through which the bob (and the wire) have been deflected multiplied by the wire constant K. This constant then is the torque per degree. Reiner and Riwlin outlined a theoretical method for determining the wire constant but state that its computation requires a knowledge of the amount of inertia of the bob. As this factor is not always known and is somewhat difficult to obtain, they suggest as an alternative pro-

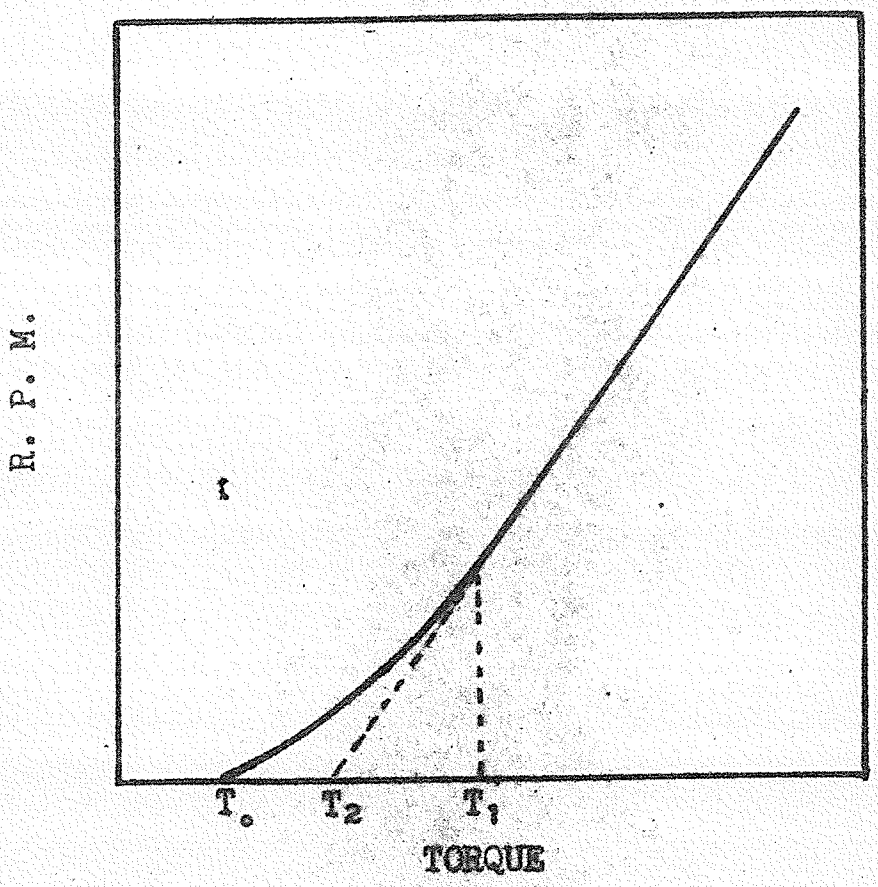

Consistency curve of a Bingham Body made with a Rotational Viscometer.

FIGURE 1

cedure to calibrate the wire with a Newtonian liquid of known viscosity. Examples of such liquids are glycerol, sugar solutions and various standard oils. The equation for K is

$$K = \frac{\eta \omega}{\theta S} \qquad \text{----(15)}$$

and

$$T = K \theta \qquad \text{----(16)}$$

where θ is the deflection. This method is practical enough if the calibrating liquid is not too high in viscosity and if the rate of shear is not maintained above that critical value where the material ceases to act as a Newtonian (17).

The design of the constructed cell used in our investigation enabled the wire constant to be obtained directly without recourse to a standard calibrating liquid. This is a decided advantage because the rate of shear at which the viscosity determination is made is rarely available to the purchaser of such a standard material. Consequently, the figure given for the viscosity coefficient would be just as useless as it would be if the temperature at which the determination was made was omitted.

In 1906 Einstein (22) developed his equation relating the viscosity of a solution or suspension to the solute concentration and to the viscosity of the vehicle. The equation is

$$\eta = \eta_0 \quad (1 + k \ \phi) \qquad \text{----(17)}$$

or

$$\eta / \eta_0 = 1 + k \phi \qquad \text{----(18)}$$

where η is the viscosity of the suspension, η_0 is the viscosity of the continuous phase, ϕ the concentration of the dispersed phase (volume

per cent) and k is a constant which depends on the shape of the particles. For spherical particles k = 2.5.

A graph of η/η_0 versus ϕ yields a straight line of slope = 2.5. From Equation (18) it can be seen that the viscosity is independent of the size of the particles, depending only on the per cent volume of the suspension that they occupy. Einstein developed this equation for streamline flow; the type occuring in a rotational viscometer. Modification of the Einstein equation has been presented to cover various other conditions not included in his work.

THIXOTROPY

The word "thixotropy" means to change by touch. The thing that is "changed" is the structure of the material. It breaks down when shaken or stirred. Thixotropic structure, however has an attribute that distinguishes it from all other types of structures--in the course of time the broken thixotropic structure will rebuild itself, if not prevented from doing so by externally applied forces.

It should be noted that the complete reaction -- unbroken to broken, and back again to the rebuilt structure -- takes place isothermally. There are types of structures that will not rebuild when broken. These structures are associated with aging and must not be confused with thixotropy. Technologists in the paint and printing ink industry associate aging with a chemical reaction between the pigment and vehicle or with changes in the state of dispersion or of flocculation arising from surface adsorption. Such changes are nonreversible and differ in that respect from thixotropy.

Green (15) uses the hysteresis loop as a criterion of thixotropy. If a material is run in a rotational viscometer and the curves of in-

creasing rpm and decreasing rpm versus torque (the upcurve and downcurve respectively) do not coincide but form a loop, then the material is thixotropic.

There are many ways by which the thixotropic structure can be explained. However, the exact nature of the mechanism of thixotropy is still unknown. Microscopic examination reveals the fact that thixotropic materials of the pigment-vehicle-type are flocculated. There are also flocculation pigment systems that are not thixotropic, and as a result no definite conclusion can be drawn from microscopical observations.

One plausible explanation of thixotropy is as follows: Assume first that the thixotropic phenomenon arises from structure and second, that this structure possesses rigidity. Then to produce flow, the structure must be broken, at least temporarily. As long as flow continues, the broken structure will not reform even in part, unless the rate of shear is lessened. The applied shearing force used in a viscometric measurement will in this case be divided. That part of the force used in breaking the thixotropic bond does not produce flow; hence, it will appear as a point on the force axis, that is, where flow equals zero. This point is called the yield value intercept. A good model of thixotropy must show how bonds of different strength become possible. This can be accomplished by having bonds of different cross-sectional areas. In FIGURE (2), two particles are bonded with three different degrees of strength. This is done with contact areas of three different sizes. Obviously bond (1) will be the weakest and bond (3) the strongest.

Thixotropy is not produced instantaneously, but requires a finite time, especially for a complete rebuilding of the structure. A satisfactory model of thixotropy must show what causes this time lag, and it must also show why the buildup is continuously progressive (i.e.)

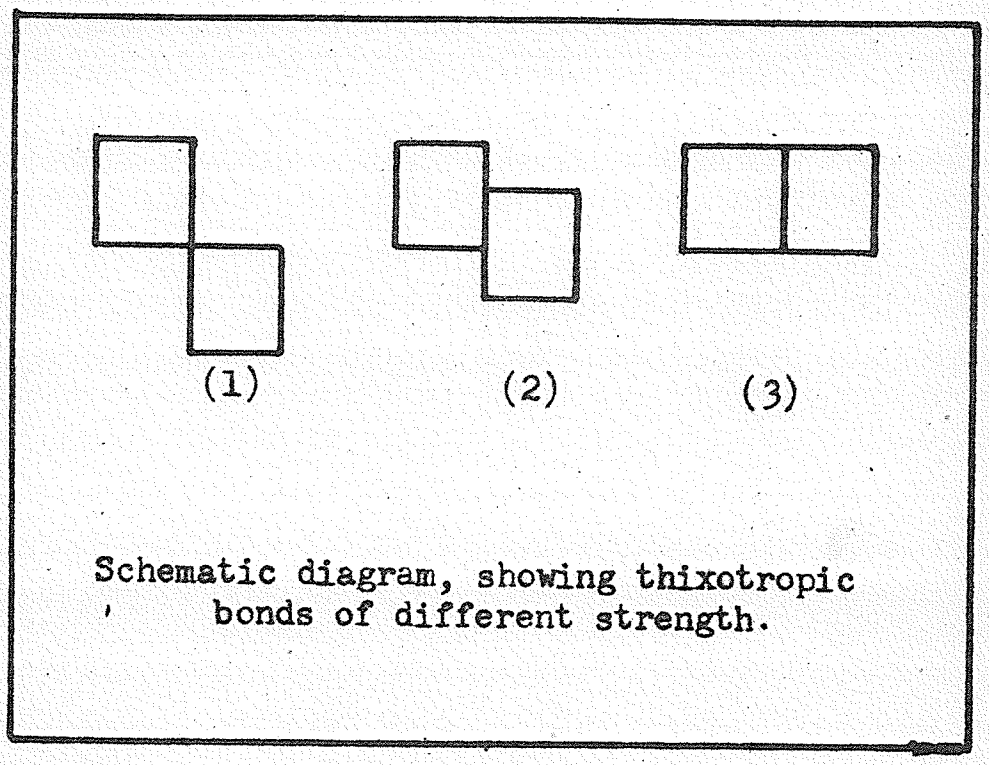

Schematic diagram, showing thixotropic bonds of different strength.

FIGURE 2

why the time intervals are not all equal in the same material. This can be accomplished by assuming the thixotropic structure to be an arrested one. This would be the case if each particle acted like a magnet, or polar molecule each possessing a north and a south pole. Structure would form only when unlike poles came in contact. Because some particles will always be nearer to a north-and-south pole alignment than others, the duration of the time lag will vary from particle to particle. As a result the buildup will not be instantaneous, as it probably is in the case of oriented flocculation, but, instead, is continuously progressive until the process is completed.

There is another type of thixotropic structure where rigidity in the ordinary sense plays no part. This is the type of thixotropic breakdown shown by oils under high rates of shear as described by Weltmann (17). Such materials as heavy-bodied linseed oils behave under low rates of shear like Newtonian's. When subjected to sufficiently high rates, they produce a hysteresis loop indicating that a temporary structural breakdown has taken place. This can be accounted for in the following manner. Under low shear rates the molecules remain in a disorderly and tangled condition. At high rates of shear the molecules are straightened out and aligned. This reduces the viscous resistance between adjacent layers. As the shearing rate is decreased, the molecules require an appreciable time to regain their former state of entanglement. Hence, the time lag that is characteristic of thixotropic buildup is produced, and a hysteresis loop results. The above phenomenon can also be explained purely in the orientation of long molecules.

When, in the study of thixotropy, materials such as paints, printing inks, emulsions or dispersions in general are measured, only a

rotational viscometer can be used. Thixotropic hysteresis loops can be formed only with the rotational type of instrument. Since it is only with this type of instrument that the rate of shear can be increased and then decreased without discontinuity. A loop forms because it consists of measurements made on a material that is being continuously broken down until the point of highest shearing rate is obtained. This is the top of the curve (see FIGURE 3). When the down curve is run (immediately after the completion of the up curve), no further breakdown occurs, and this curve, therefore, is linear (except at lower end). As a consequence, the two curves cannot coincide, and a loop is created. In an instrument of the capillary type, the material under test is extruded, and cannot be remeasured in its broken-down state. This means that the up and the down curves are each made at the same thixotropic level, that is, in the same state of breakdown. Hence, the curves will coincide, and no evidence of thixotropy, so far as the hysteresis loop is concerned, will be evident.

Green and Weltmann (19) showed experimentally that the area of the hysteresis loop is proportional to the square of the top angular velocity ω. (The relation between ω and rpm is $\omega = \text{rpm}/9.55$). Hence

$$\text{area } A = Q(\text{rpm})^2 \qquad \text{----(19)}$$

where rpm is the top rpm and Q is the proportionality constant. The same investigation also showed when u was plotted against $\ln 1/(\text{rpm})^2$, Δ T remaining constant, that a linear relation was obtained (19) (21). Then if m is the slope of the resulting curve

$$m = \frac{d \ln \frac{1}{(\text{rpm})^2}}{d u} \qquad \text{----(20)}$$

Calling the constant of integration ln k (for it must be dimensionless) gives

$$e^{mu} = \frac{k}{(rpm)^2} \text{ or } \frac{k}{\omega^2} \qquad \text{----(21)}$$

Both Equations 20 and 21 were derived theoretically (19).

The following is Weltmann's method of making a hysteresis loop. The viscometer is first adjusted for its lowest practical rpm. The loop is started at that point; assume that it is 10 rpm in this case. The degree deflection on the torque scale is noted but not recorded. The rpm is next increased, say, to 20. The first scale reading is now written down. During the time required to do this, the bob has reached its next point. This new scale reading is noted, but again it is not recorded. The rpm is now advanced to 30. The second point is written in during this interval. This process is repeated, the rpm being increased by the same number at each step. The time interval between each two steps must be as nearly constant as the operation is able to make it.

After a sufficient number of points have been recorded to arrive at the desired top rpm, the down curve is commenced immediately. It is assumed that the test material is thixotropic and so no time must be lost. Descent on this curve is made by using the same intervals in rpm and in timing that were previously employed against the torque-scale reading, and a loop as shown in FIGURE 3 will result. The straight part of the down curve, extrapolated to the torque axis yields the intercept T_2, which when multiplied by the instrumental constant C (Equation 12) gives the yield value in dynes per sq. cm. The most customary procedure is to plot the scale deflect instead of the torque and then multiply the intercept by the wire constant K to convert to torque. This also holds for any point T in calculating the plastic viscosity from the Equation, $\mu = (T-T_2)\ S/\omega$.

When a thixotropic material is subjected to a constant shearing

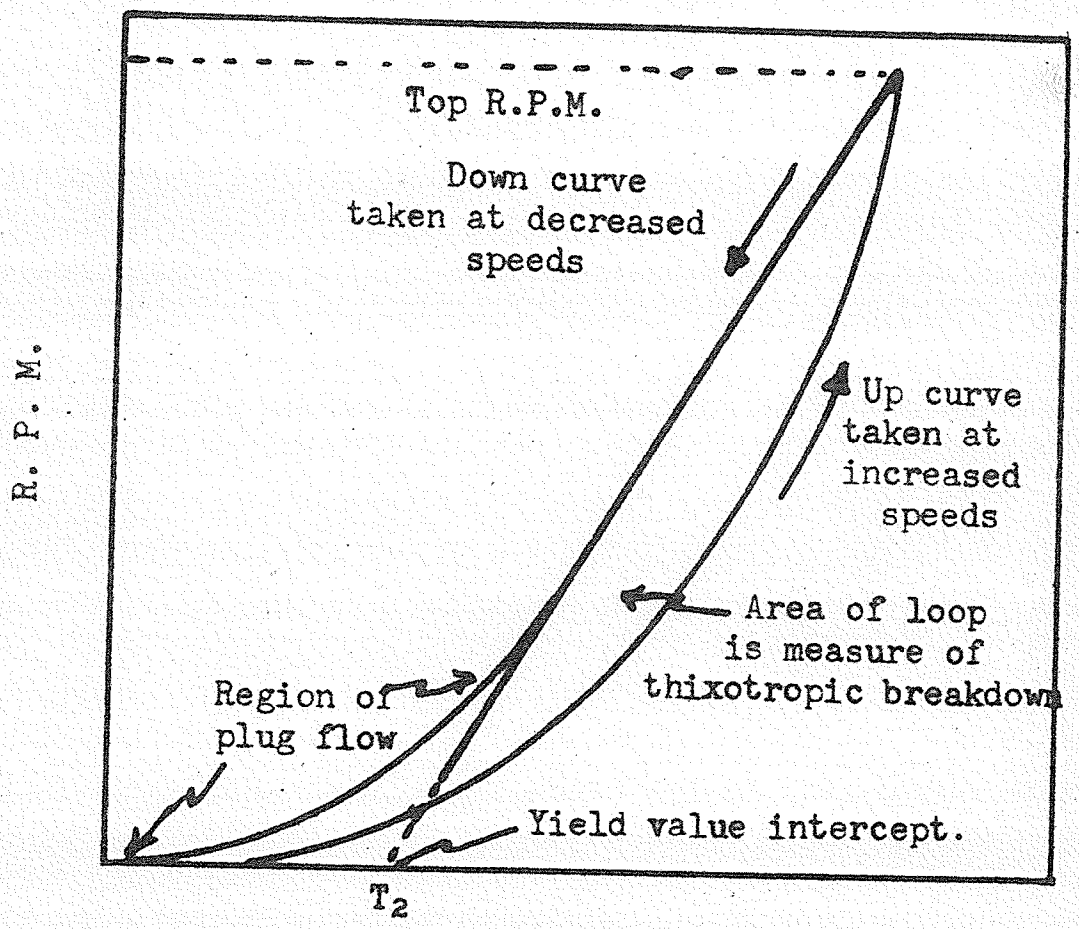

Generalized curve showing thixotropic flow and loop as measured on a Rotational Viscometer.

FIGURE 3

rate over a period of time, it breaks down rapidly at first, and then more slowly, until finally it reaches an equilibrium point where the rate of build up equals the rate of breakdown. T his procedure is called "breakdown with time." If further breakdown is now desired, it can be induced only by increasing the rate of energy input, which is accomplished by raising the rpm. This is called "breakdown with rate of shear". Whether or not an equilibrium point exists in this case when no further breakdown can be obtained is not known.

When the time interval T is increased, the number of points N and the top rpm remaining constant, the upcurve is displaced toward the rpm axis (19), (see FIGURE 4). If no breakdown took place, the upcurve would be straight (except at lower end) and represented by the line T_2A. If the material is thixotropic, it will continuously break down during the running of the upcurve. If it is assumed that the up curve could be run in zero time, there would still be breakdown on account of the increasing rate of shear. The curve would, therefore, meet the top rpm at some point, At_o, which would have a smaller torque than that of A, but greater than a torque for a real curve run in finite time. In practice, the time cannot be zero; hence, the curve will fall to the left of At_o and meet the top rpm at a point A_t. If continued rotation is allowed at this point without changing the speed, the material will continue to break down with time until the equilibrium point is reached at A_{tE}.

After equilibrium is established with a constant rate of shear, further breakdown can be had only by increasing the rate of energy input, or power. It should be noted that the product, torque times rpm, has the dimensions of power. Therefore, the area of the rectangle OGAF, FIGURE 5, is a measure of the power necessary to altar the state

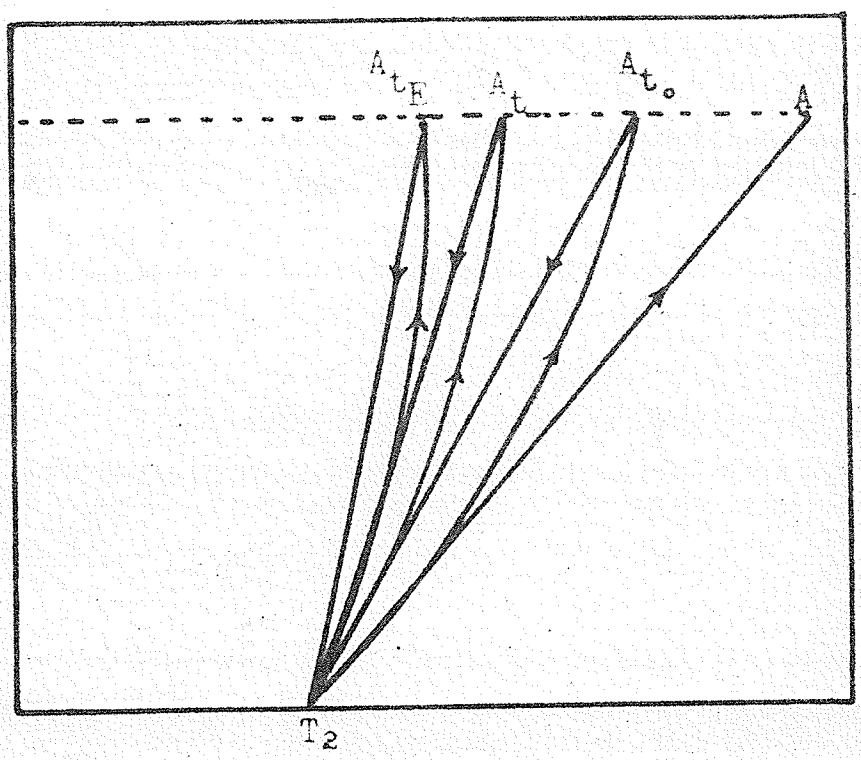

Thixotropic Breakdown Under Constant Shear

FIGURE 4

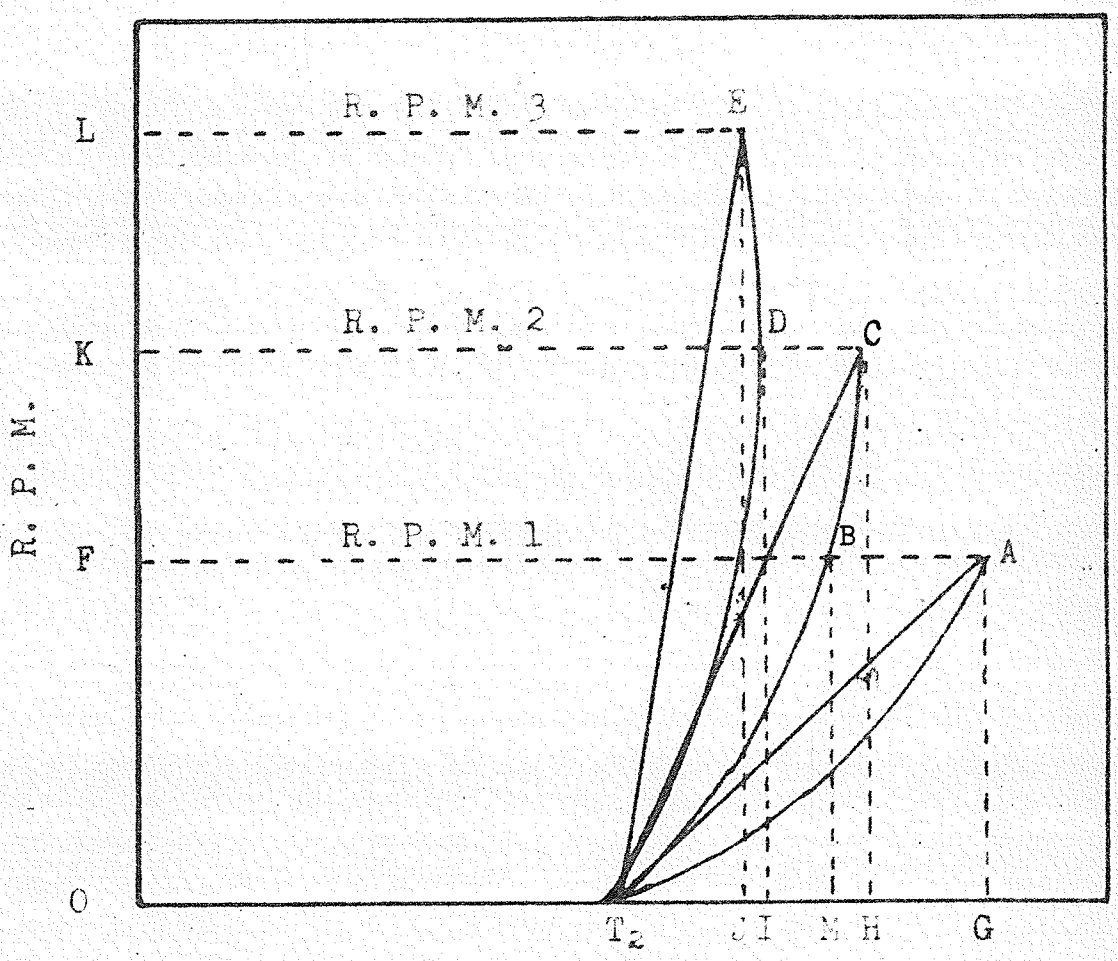

Thixotropic Breakdown with Increasing Rate of Shear.

FIGURE 5

of breakdown at A and the rate of shear for rpm. If rpm is maintained until equilibrium is reached, the torque at A drops to the torque at B. The power has also fallen and is now equal to the area OFBM. To increase the size of the power rectangle, it is necessary to increase the rpm to, say, rpm_2. This causes further breakdown as can be seen by the shift in the down curve from position BT_2 to CT_2. Again, if rpm_2 is maintained over a sufficient period, C moves to the equilibrium position D, and further breakdown can be had only by another increase in the power.

The up curve is the experimental record of increasing breakdown. If no breakdown should take place, the curve would be straight. Its bow shape indicates that the structure is breaking and so cannot induce a torque sufficient to give a linear relationship with the rpm. Because no action can take place in zero time, the breakdown is the combined result of an increasing rate of shear and its time of application. When the rate of shear is decreased, no further breakdown from rate of shear can take place. A ny further breakdown would now be the result of time of application. However, this possibility is nullified by the fact that build up can also take place under the decreased rpm.

The down curve remains linear (if made within a reasonably short period of time) until it reaches the lower end where plug flow commences. Whatever the cause is for the linearity of the down curve, it seems reasonable to assume that it is an indication that the thixotropic structure is neither breaking down nor building up. The down curve represents a condition of temporary stability and is referred to as a "thixotropic level". It is possible to have an infinite number of such levels for any thixotropic material.

In the development of the theoretical equation of the loop, Green and Weltmann (19) made the basic assumption that the loss in torque

due to breakdown is proportional to the rate of shear. The second coefficient of thixotropic breakdown M is the loss in shearing force per unit area per unit increase in rate of shear. It is expressed in dyne-seconds/sq. cm. By use of Equation (21) and two points u, ω, and u_2 ω_2, M is given by the equation

$$M = \frac{2(u_1 - u_2)}{\ln \frac{\omega_2^2}{\omega_1^2}} \qquad \text{----(22)}$$

where u_1 and u_2 are the plastic viscosities respectively and ω_1 and ω_2 are the corresponding angular velocities measured at the lower and higher rpm.

A third coefficient of thixotropic breakdown is derived by Green (15).

$$V = \frac{f_2 - f_1}{u_1 - u_2} \qquad \text{----(23)}$$

where V is the increase in yield value per unit decrease in plastic viscosity.

PART II

EXPERIMENTAL SECTION

The problem under investigation required a series of emulsions of the water-oil type. It was desirable to have the dispersed phase conducting and to this end .5N sodium hydroxide solution was used. Our system then is one which is composed of conducting particles in a non-conducting medium. In the preparation of such a system it is necessary to have a third substance called the emulsifying agent. For the water-oil type emulsion this agent is almost invariably soluble in the continuous phase. Various theories have been put forth with regards to the action of the emulsifier. Few well substantiated theories of emulsifier action exist as shown by the great variety of agents used, and the random way in which they are normally selected. The generally accepted mechanism of emulsifier action is contained in many tests on colloids, e.g. Alexander and Johnson (23).

PREPARATION OF EMULSIONS

The problem of preparing a series of stable emulsions in the range 3 to 50 per cent (by volume of the dispersed phase) was first attacked by the trial and error method. The first emulsifying agents used were products of the Armour Chemical Company. These included the following agents, Ethomeen $T/_{15}$, Ethomeen 18/15, Ethomid 18/15, Ethomid H $T/_{15}$, and Ethofat 60/15. Little success was had with these agents.

After a search of the available literature it was concluded that there was very little information existing on emulsions of the water-oil type. The main concern seemed to be the oil-water type. As a consequence of this search, however, it was decided to try some of the older standard ensifying agents (24) (25). Of these Zinc oleate,

calcium oleate and magnesium oleate were used. Here again difficulty was encountered. It should be mentioned, however, that these agents were not entirely unsuccessful but neither a series of stable emulsions nor emulsions with the proper desirable characteristics could be prepared. Of the numerous other agents which were tried, the ones which looked most promising were the following: Span 62, Span 80, arlacel C, Tween 65, Tween 81, Tween (85), all of the Atlas Powder Company, Brantford, Ontario.

These Spans and Tweens were selected by the "H L B" system. The term "H L B" indicates the size and strength of the hydrophilic and lipophilic groups that form the molecule of the surface active agent. For water-oil type emulsions agents with H L B values in the range 3.5 - 6.0 were best suited. By combining the above agents in various proportions their H L B values can be made to fall in the required range. An example of such a calculation is as follows:

	H L B		Proportion	
Span 80 ----------	4.3	x	85%	----- 3.6
Tween 81 ----------	10.0	x	15%	----- 1.5
			H L B of combination	----- 5.1

Antorox B-100 a product of Standard Chemical Company was also tried. The agent which was finally used to prepare the series of stable emulsions was anhydrous lanolin.

The following technique was used in the preparation of the emulsions. Heavy mineral oil (Imperial oil stanolax) of specific gravity .878 was measured out from a 500 cc. burett. To this oil in a beaker heated lanolin, measured in a graduate, was added while stirring. When these two components were thoroughly agitated the correct amount of the dispersed phase was added from a buret. The dispersed phase was added

while the stirrer was in motion and was a mixture of .5N sodium hydroxide mixed with 95% ethyl alcohol to a specific gravity of .878. The resulting emulsion was stirred for 20 minutes. A heavy piece of cardboard was fitted over the mouth of the beaker while stirring was done. This minimized the evaporation of the alcohol. The emulsion was stirred in a multiple stirring apparatus. In this way six emulsions could be prepared at the same time. After stirring, the emulsion was put into a hand-operated type of homogenizer. (See PLATE II). The handle of this homogenizer was connected through a speed reducer (30: 1) to a motor (1/10 h.p.) so as to permit continuous homogenization. The nozzle of the homogenizer was fitted with a small copper tube which emptied back into the homogenizer bowl. In this manner the cycle was completed. This relatively inexpensive apparatus replaced a more expensive type of equipment like the ball mill or roller mill. The emulsion was left in the homogenizer over a period of one-half an hour. This enabled the emulsion to pass through approximately one hundred times.

At various intervals the action of the homogenizer was observed by viewing a sample under a microscope. Before homogenization, the dispersed particles although spherical, were large and of various sizes and could be viewed with a relatively low power line. After homogenization, however, the particles of the dispersed phase were broken up to such an extent that an oil immersion lens (1.9 mms) was required to detect them. The action of the homogenizer could also be detected by visual observation since the emulsion acquired a creamy consistency after continuous homogenization. It was when this creamy consistency was acquired that the dispersed particles were observed under a microscope to be so small.

The emulsions were kept in ground glass stoppered bottles to

PLATE I. Old bob (on left) and new bob (on right) with the filling gun in the foreground.

PLATE II. Apparatus used for homogenizing the emulsions.

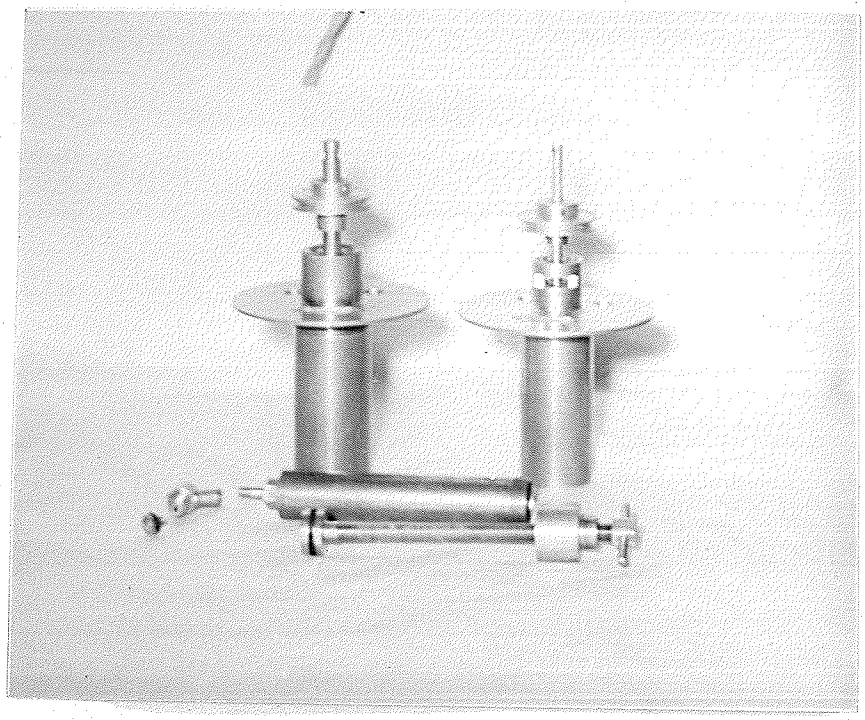

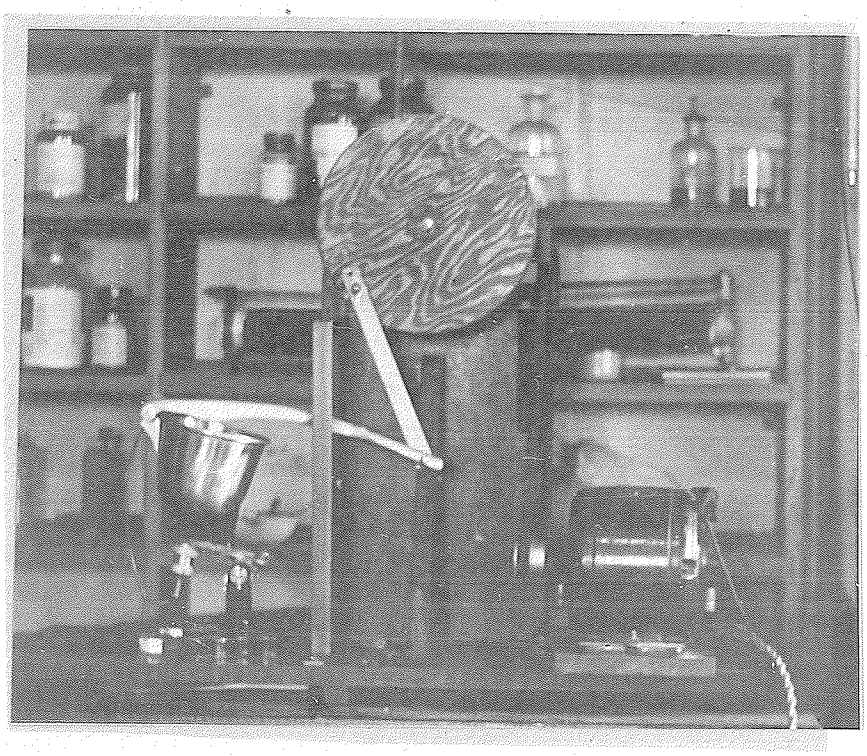

prevent evaporation of the alcohol. 100 c.c.'s of emulsion were prepared at each time. Emulsions from 2% to 50% by volume of the dispersed phase (NaOH - alcohol) were prepared in this manner. These varied in their stability from 2 to 30 days. The stability was measured by their conductance. Examples of the formulae used are as follows:

Formula 1. 3% EMULSION		Formula 5. 25% EMULSION	
Stanolax oil	93 cc	.....	65 cc
Anhydrous lanolin	4 cc	.....	10 cc
(.5 NaOH - 95% alcohol).	3 cc	.....	25 cc

It should be noted that emulsions using .5N sodium hydroxide as the dispersed phase were prepared in the required concentration range. However, these proved to have a conductance not measurable on the bridge network used.

Testing of the emulsions was done in the 150 ml. beakers in which they were prepared. Two copper strips 3 inches long and 3/4 inch wide separated by a bakelite top was inserted in the beaker. The distance between the two strips was approximately 1 3/4 inches. Resistance of the emulsion was measured by a Simpson Resistance meter. This measurement was very rough but a more accurate one was not required. From the resistance reading it was possible to determine (roughly) the stability of the emulsion also whether or not the emulsion could be measured on the bridge network. A stable measurable emulsion had a very high resistance, (of the order of 2-Megohoms) or a very low conductance.

Rotary Cell

The requirements that must be considered in the design of the cell are:

(1) Cell must be a concentric cylinder rotating condenser.

(2) Simultaneous readings of capacity and viscosity must be possible.

(3) Capacity of cell must be between 100 and 200 $\mu\mu f$ to insure maximum precision on the reading of the Schering bridge.

(4) Outer cylinder or cup must be the rotating one.

(5) Cell must be easy to clean and fill.

(6) Cell must be thermostated.

(7) Cell must have proper range of shear gradients.

(8) The stationary plate or bob must be easily replaced so as to enable to change the volume of the cell and hence the shear gradient.

The practical cylindrical rotating viscometer is derived from the design of Couette (9) in which the outer cylinder is rotated and the torque on the inner measured. The simple theory for this instrument was given some years earlier by Barr (10). The requirements for a practical viscometer of the rotating cup type have also been described by Weltmann (11). This design is desirable since it allows rapid changes in the speed of the cup but the constant temperature bath complicates the construction. The rotating bob instrument permits simple and precise means for controlling temperature. Taylor (12) showed that the outer cylinder arrangement is considerably superior to that in which the inner cylinder rotates, in that stream line flow occurs up to much higher speeds. For quantitative work therefore, the former arrangement is preferable. However the difference between the two types diminishes as the gap width between the cylinders decreases and for high speeds and small gaps a rotating inner cylinder is often used, since mechanical construction is simpler.

To calculate the unknown dimensions namely the radii and length

one can use for a rough estimation the equation for a parallel plate condenser.

$$C = \frac{.0886 \times \text{area of plates (sq.cms)}}{\text{distance between plates}} = \mu\mu f \qquad \text{----(24)}$$

$$C = \frac{.0886 \times \epsilon \times 2\pi rh}{d} = \mu\mu f \qquad \text{----(25)}$$

where r = mean radius in cms.

ϵ = dielectric constant of medium

l = length of plates in cms.

d = distance between plates in cms.

For a cylindrical condenser the following equation is used:

$$C = \frac{l}{4.15 \log_{10} \frac{r_c}{r_b}} \mu\mu f \qquad \text{----(26)}$$

where l = length of plate in cms.

r_c = radius of outer cylinder (cup)

r_b = radius of inner cylinder (bob)

Equation 26 in another form becomes

$$C = \frac{.2416 \; l \epsilon}{\log_{10} \frac{r_c}{r_b}} \qquad \text{----(27)}$$

From stream line flow the velocity gradient in the liquid at a distance r from the axis of the system is

$$G = \frac{dv}{dr} \quad \frac{2\omega \frac{1}{r^2}}{1/r_b^2 - \frac{1}{r_c^2}} \qquad \text{----(28)}$$

where ω is the angular velocity of the outer rotating cylinder ($\omega = 2\pi$ frequency $= \frac{2\pi R.P.M.}{60}$) and r_b and r_c are the radii of inner and outer cylinders respectively. Derivation of this equation is given by Hatschek (9). Stream line flow in this type of apparatus involves the orderly motion of liquid in circular paths concentric with the cylinder,

with velocities increasing from zero at the surface of the inner cylinder to a maximum of the outer one. From Equation (28), it is clear that the velocity varies across the gap between the cylinder but since r_b and r_c do not differ much, in general the variation is small compared with that occurring in capillary viscometers.

With a decrease in the width of the gap the possible variation in velocity gradient decreases and if

$d = r_c - r_b \ll r_b$ then it becomes effectively constant at the value

$$\frac{dv}{dr} \approx \frac{r_b \omega}{d} \left(\approx \frac{r_c \omega}{d} \right) \qquad \text{----(29)}$$

For stream line motion between the cylinder and negligible end effects, the torque on the inner stationary cylinder caused by the rotation of the outer is given by

$$T = C\theta = \frac{4\pi l \eta \omega}{\frac{1}{r_b^2} - \frac{1}{r_c^2}} \qquad \text{----(30)}$$

where θ = angular deflection of the cylinder

C = torsional constant of the wire

l = length of inner cylinder which is covered by liquid

η = viscosity of liquid between plates

ω = angular velocity.

Equation (12) can be rearranged to give

$$\theta = \frac{\eta}{C} \frac{4\pi}{\left(\frac{1}{r_b^2} - \frac{1}{r_c^2} \right)} l\omega = K \eta l \omega$$

where constant $K = \frac{4\pi}{C\left(\frac{1}{r_b^2} - r_c^2 \right)}$ depends upon the torsion wire and the dimensions of the apparatus.

For a liquid whose viscosity coefficient is independent of

rate of shear (or velocity gradient), the plot of α vs. ω should be a straight line passing through the origin and whose slope has the value $K\eta^{-1}$.

The condition for turbulent flow in a coaxial cylindrical system of the type used is given by the equation: (For verification of this formula see Taylor (12) (13). (This gives the critical value for turbulence)

$$\frac{\omega_c^2}{(\eta/\rho)^2} = \pi^4 \frac{r_b + r_c}{2 P d^3 r_b^2} \qquad \text{----(31)}$$

where ω_c = critical angular velocity for turbulence

η = viscosity of liquid between plates

ρ = density of liquid between plates

η/ρ = kinematic viscosity

r_b = radius of bob or inner cylinder

r_c = radius of cup or outer cylinder

P = numerical factor given by

$$P = .0571 \left(1 - .652 \frac{d}{r_b} + \frac{.00056}{1-.652 \frac{d}{r_b}}\right) \qquad \text{----(32)}$$

If the gap between plates is small (i.e.) if $r_b \approx r_c$ then

$$\frac{\omega_c^2}{(\eta/\rho)^2} \frac{\pi^4}{2Pd^3 r_b} \qquad \text{----(33)}$$

$$\omega_c \propto \frac{\eta}{\rho d^{3/2}} r^{\frac{1}{2}} \qquad \text{----(34)}$$

That is, the critical angular velocity varies approximately as the inverse $\frac{3}{2}$ power of the distance between plates and the inverse $\frac{1}{2}$ power of the radius. Hence, the critical angular velocity gradient must vary as the inverse $\frac{5}{2}$ power of the gaps. The critical angular velocity is also directly proportional to the viscosity of the liquid. Concerning possible limitations of formula (31) see Buckheim (14).

To calibrate the cell it is necessary to have a standard liquid of known dielectric constant ϵ_B. If we denote the geometric capacitance by C_g, the stray capacitance by C_s, the leads capacitance by C_L, the capacitance of the empty cell by C_1 and that of the cell filled with the standard liquid by C_2 we have

$$C_1 = C_g + (C_s + C_L) \qquad \text{----(35)}$$

$$C_2 = \epsilon_B C_g + (C_s + C_L) \qquad \text{----(36)}$$

and subtracting (18) from (17) we have

$$C_2 - C_1 = (\epsilon_B - 1) C_g \qquad \text{----(37)}$$

from which $$C_g = \frac{C_2 - C_1}{(\epsilon_B - 1)} \qquad \text{----(38)}$$

The first cell which was machined (FIGURE 6) had $R_b = 2.3317$ and $R_c = 2.4079$ where R_b and R_c are the radii of the bob and cup (in centimeters) respectively. With these values the geometric capacitance was calculated with the use of Equation (27), and found to be 176.2 $\mu\mu f$. This agreed fairly well with the value 201.8 $\mu\mu f$ which was obtained experimentally from the calibration of the cell.

The velocity gradient was calculated using Equation (28). For unit angular velocity the velocity gradient was found to vary from 3.362 sec^{-1} at the surface of the inner cylinder to 3.153 sec^{-1} at the surface of the outer cylinder making the average velocity gradient 3.257 sec^{-1}. Using Equation (31) the critical rate of rotation for turbulence was evaluated as $(rpm)_c = 1.49 \times 10^5 \eta/\rho$.

CALIBRATION OF THE CELL

The capacitance of the empty cell was measured and found to be 398.1 $\mu\mu f$ at 28.6°C. The cell was then filled with dried analytical reagent grade benzene and the capacitance again measured at the same

temperature and found to be 654.6 $\mu\mu f$. (In filling the cell with benzene a different procedure had to be used due to the high fluidity of the benzene. The cell was filled from the top. Several readings of the cell were taken both when empty and when full). The dielectric constant for benzene at the temperature of 28.6 C is 2.271. Using Equation (38) the geometric capacitance was found to be 201.8 $\mu\mu f$. The capacitance of the leads was 126.7 $\mu\mu f$ and hence stray capacitance was 69.6 $\mu\mu f$.

The first cell was machined entirely of brass with the exception of the bakelite fittings used to insulate the stationary bob from the rotating cup. The diameters of the inner and outer plates were 1.836 inches and 1.896 inches respectively giving a spacing of .060 inches. The lengths of the bob and cup were 3.637 inches and 4.000 inches respectively. The volume of the cell was calculated to be 22.95 cubic centimeters. The overall length of the cell was 6 inches (not including the legs).

DESCRIPTION OF CELL

With reference to FIGURE 6, the following is a detailed description of the cell. The outer plate or cup, (B) is held in position by two bearings, M and F, so that it is free to rotate. The inner plate or bob (A) is held in position by two bearings D and D' which are insulated from their brass housing by a shim of bakelite E. A collar (G) on the $\frac{1}{2}$" shaft (S) keeps the bob from resting on the bottom of the cup. By moving this collar up or down it is possible to vary the distance between the bottom of the bob and cup. The top of the cup (C) has a hole in it large enough to permit passage of the shaft. This hole was press fitted with a bakelite fitting E' through which the shaft passed.

FIGURE 6 - Cross section of condenser-viscometer cell.

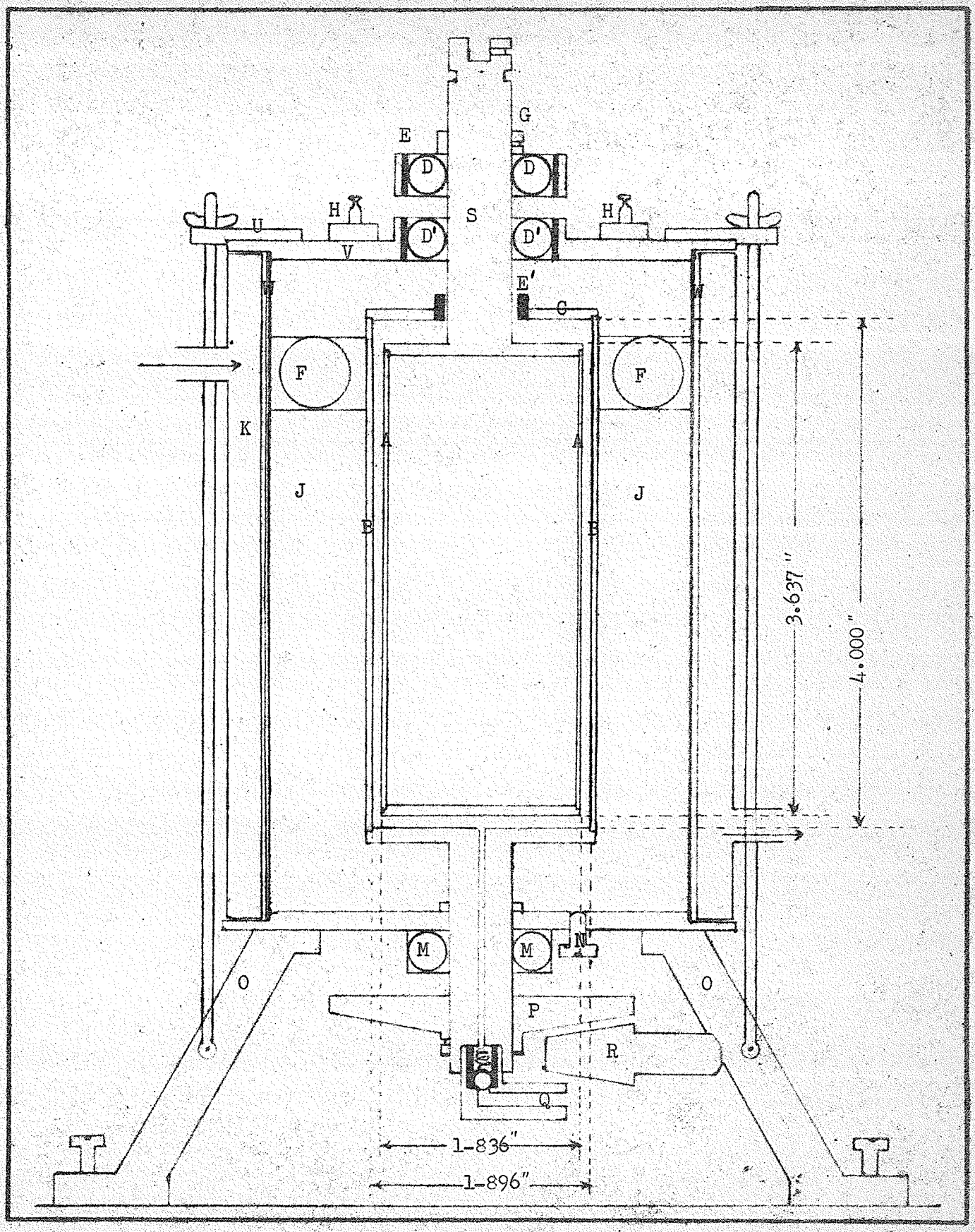

FIGURE 6

The cap itself was machine fitted on the cup and could be pressed into position by applying a force through the holes (H) in the top of the cell. These holes were fitted with removable plastic plugs.

T he cell in general can be considered to be composed of two sections, the top and the bottom. The top section consists of the bob, the cap for the cup, the shaft, and the two bearings with their housing. The bottom consists of the cup, large bearing, small bearing, outside wall, and water jacket. These two sections can be viewed in PLATE I. The top part of the cell (V) was made of $\frac{1}{4}$" brass and was machine fitted onto the outer wall (W) which holds the large bearing (F) in place. The centering of the bob depended upon the precision of this fitting until a centering device was constructed. This consisted of a circular ring (U) (See PLATE III) (beside motor on the wooden platform) of brass $\frac{3}{4}$ of and inch wide with three slatted projections which extended beyond the dimensions of the top of the cell and through which $\frac{1}{4}$" brass rods could pass. The bottoms of these rods were hinged to the brass legs (O), the tops were threaded and fitted with wing nuts. By adjusting the tension on these wing nuts the bob could be centered quite accurately. The effect of the tension applied was noted on the detector screen.

The water jacket (K) was a separate unit and could be fitted over the outside cylinder wall (W) when the top of the cell was removed from position.

The space (J) between the outside wall and the cup was filled (with oil) through the plug (N). This prevented a dead air space and thus assisted in the thermostating of the cell. The cell was filled through the bottom of the shaft at Q. The hole through this shaft was 1/32". The bottom of this shaft was fitted with the filling device which consisted of a ball bearing type of grease nipple to which a grease gun

could be attached. Also on this shaft was a bevelled gear (P), held in place by a set screw. The mate (R) of this gear was fitted on shaft of the speed unit which was a $\frac{1}{4}$ h.p. Leland variable speed/motor (800 - 2400 rpm). The gear ratio was 3:1. The whole cell was fitted with three cast brass legs, 4" high which were fastened to a wooden platform.

Electrical contact was made through the torsion wire. The cup was grounded. A $\frac{1}{8}$" hole was drilled in the top of the shaft (S) into which one end of the torsion was fitted. It was held in place by a set screw. The other end of the torsion wire had a similar fitting which fitted into a slot in a brass fitting. This brass fitting was insulated with bakelite from the bar into which it was set. This bar was 12" long, $\frac{3}{4}$" wide and $\frac{1}{4}$" thick. It was supported above the cell on two angle iron supports. The bar could be raised or lowered by set screws. See PLATE IV for view of the set up.

A mirror was soldered to the torsion wire $4\frac{1}{2}$" from the top of the wire. A telescope with a centimeter scale was mounted on the angle iron frame. The height of the telescope could be adjusted by a screw which raised or lowered the angle of the mounting. The distance from the mirror to the scale was 56 cms. The torsion wires were nickel-steel drill rods. Torsion wire or couple Number 1 had a diameter of .0466" and was $5\frac{7}{8}$" long while couple Number 3 had a diameter of .0625" and was 6" long.

To calibrate the torsion wires a pulley of diameter 4.38 centimeters was machined to fit the shaft (S). Another similar pulley was arranged at right angles to this one between the angle iron supports (See PLATE IV and V.) The top of this pulley was in line with the pulley on the shaft. A small hole was drilled close to the edge of the pulley on the shaft and a pin machined to fit it. A nylon fish line was attached

PLATE III. View of cell dismanteled showing the cup and bob.

PLATE IV. Shows pulleys and weighing pan in position to calibrate couples.

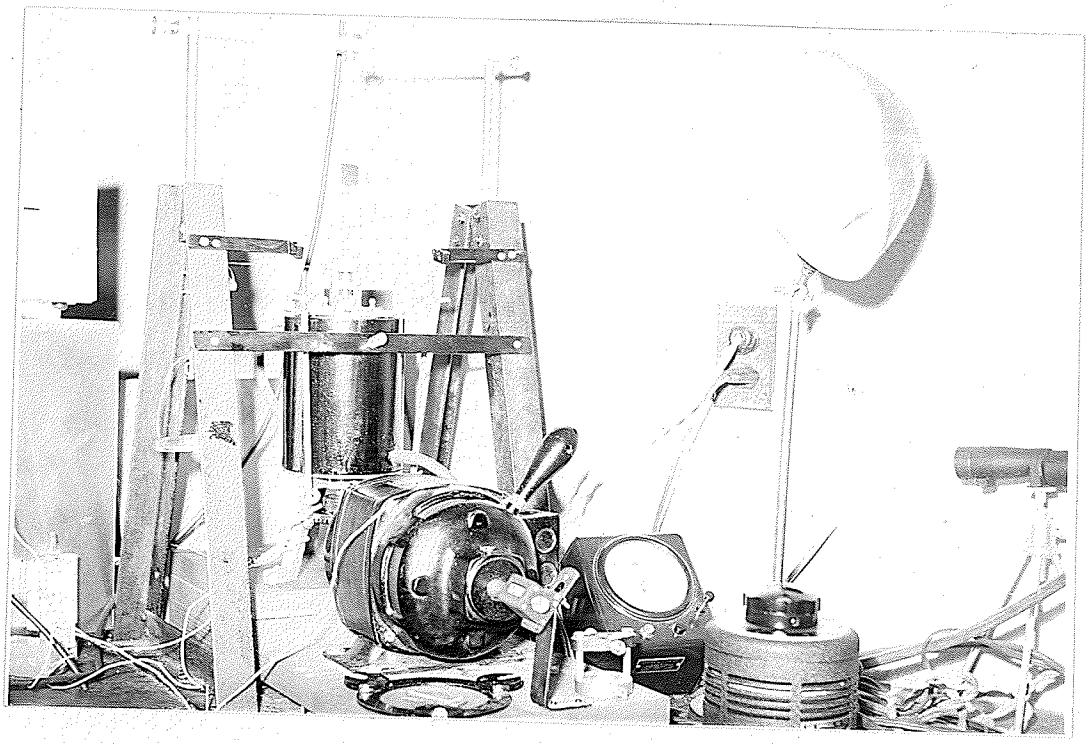

to this pin, wrapped around the pulley and then drawn over to the other pulley. At this end a pan was attached on to which weights could be placed. PLATE V shows pan in position. A fixed weight on the pan gave a certain deflection on the scale. Table XIII of the results section gives the calibration data for the torsion wires used.

PLATE VI shows the complete apparatus with auxillary equipment as set up in the lab.). Left to right on the top of the bench are the following pieces of equipment; oscilloscope, schering bridge with oscillator sitting on top of it, cell with angle iron supports for the torsion wire, motor, (Leland Variability), variac for controlling motor speeds, thermostat, (28.6 C), electronic relay control. Below the thermostat is a water pump. The constant voltage supply is on the left of the water pump and the amplifiers are to the left of this. The veeder root rpm counter (5 figures) can be seen in PLATE V, connected directly to the shaft of the motor.

The electrical apparatus required to measure the capacitance consisted of a commercial capacitance bridge Type 716C (General Radio Company). This is a schering type bridge which has a direct capacity reading over the frequency range 30 cycles per second to 300,000 cycles per second. The oscillator selected was a Model 200 C Audio Oscillator (Hewlett Packard Company). Its frequency range is 20 cycles/second to 200,000 cycles/second. A stabilized constant voltage supply (FIGURE 7) was built. This gave a constant voltage output of 175 to 300 volts D.C .

A two stage amplifier with a frequency range 30 cycles/second to 3000,000 cycles/second was built (FIGURE 8). An oscillograph was used as a null detector. This was supplemented by head phones (10,000 ohms impeadance). All connections were made with microphone cable and

banana clips. The metallic casing of the cable was grounded in each connection. Low loss coaxial connectors were used on the amplifier to minimise the effects of stray capacitance.

The above apparatus was set up as follows: the oscillator was connected directly to the capacitance bridge, the amplifier between the bridge and the oscillograph and the head phones across the positive and negative terminals of the vertical plates of the oscillograph. The constant voltage of the power supply was fed into the amplifier. Each piece of apparatus was grounded.

To investigate the sensitivity of the above circuit a standard capacitance (500 $\mu\mu f$) Type 505E General Radio Company was used. This was plugged in across the "unknown direct" terminals. The sensitivity was tested at the frequencies 100 cycles and 1, 10 and 100 kilocycles per second. All runs were done at the fixed frequency of 10 kilocycles at which the sensitivity was $\pm$ .1 $\mu\mu f$. Various modifications of amplification were tested but the final arrangement consisted of the amplifier in Figure 8 with one succeeding similar stage.

Difficulties arising from preliminary runs necessitated the machining of a new top to the cell. The most serious objection to the old top was the difficulty in cleaning and oiling the bearings. This affected the deflection reading at low rpm. PLATE II shows both tops. The one on the right hand side is the new one. The cutaway sections of the bearing housing can be seen in this photo. The pulleys used in calibration of the couples are in position on the shafts. The filling gun with its attachments is also in the photo. Since it was necessary to machine a new cell top it was decided that the new top should have a bob of smaller diameter. This was necessary for investigation at higher rates of shear.

PLATE V. Side view of cell showing telescope mounted in position.

PLATE VI. General set up of the apparatus.

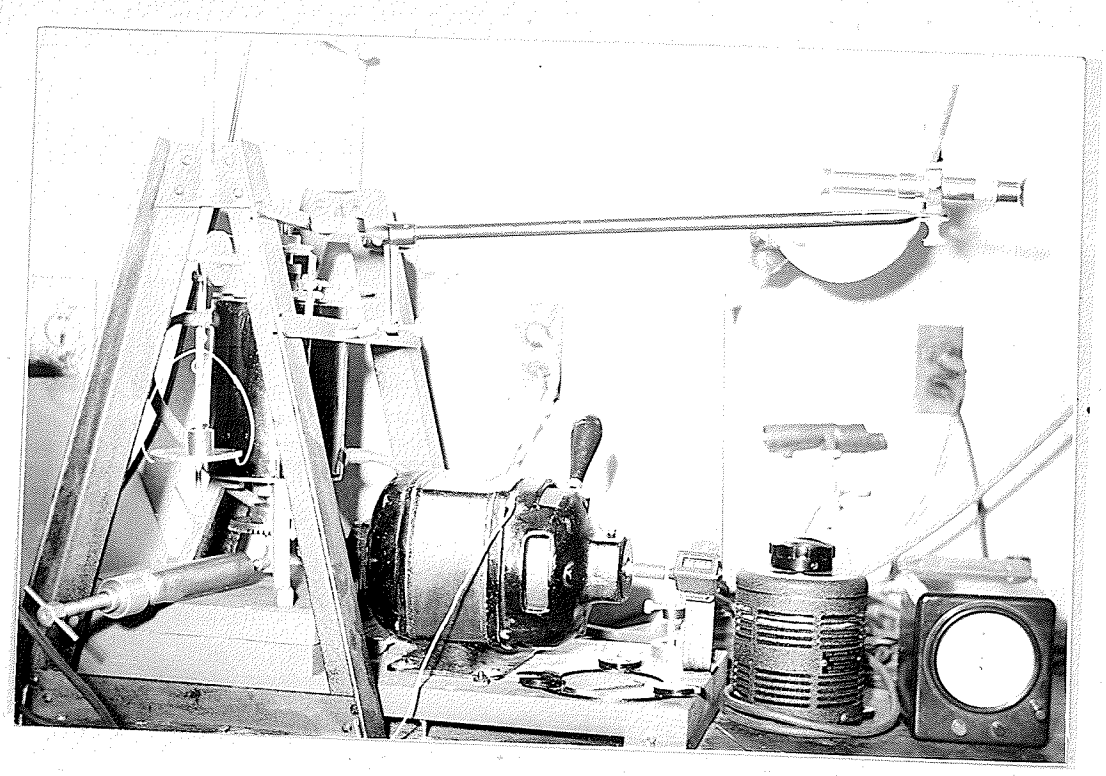

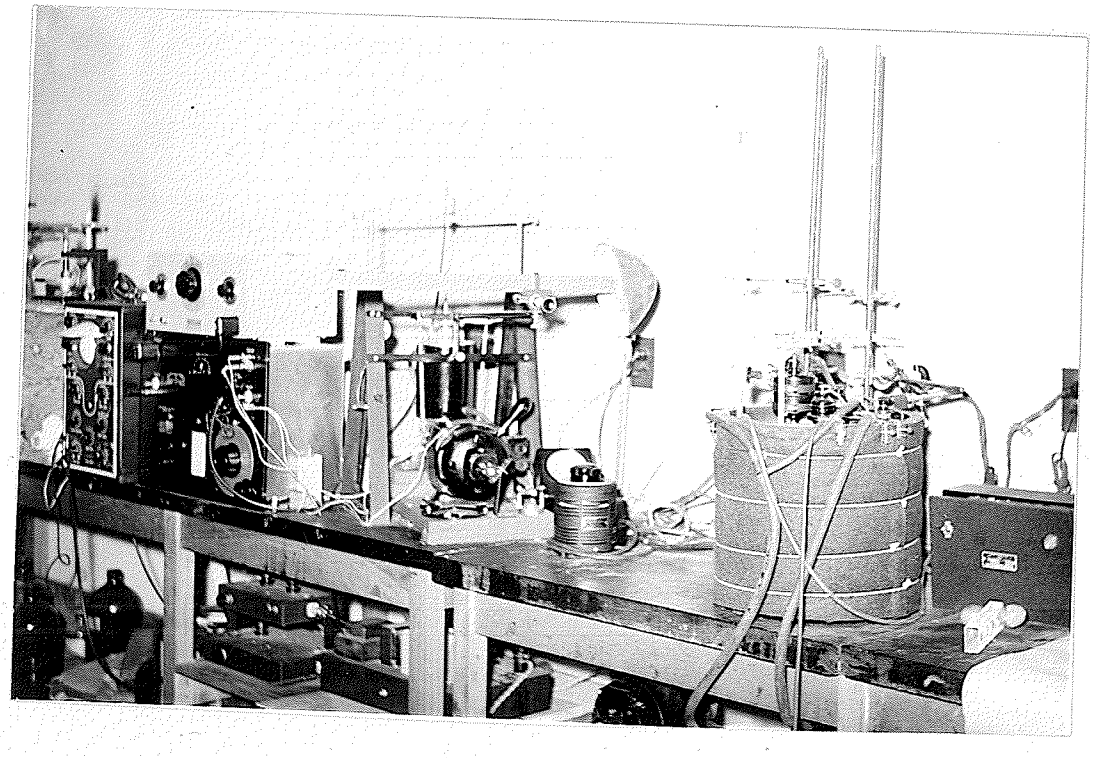

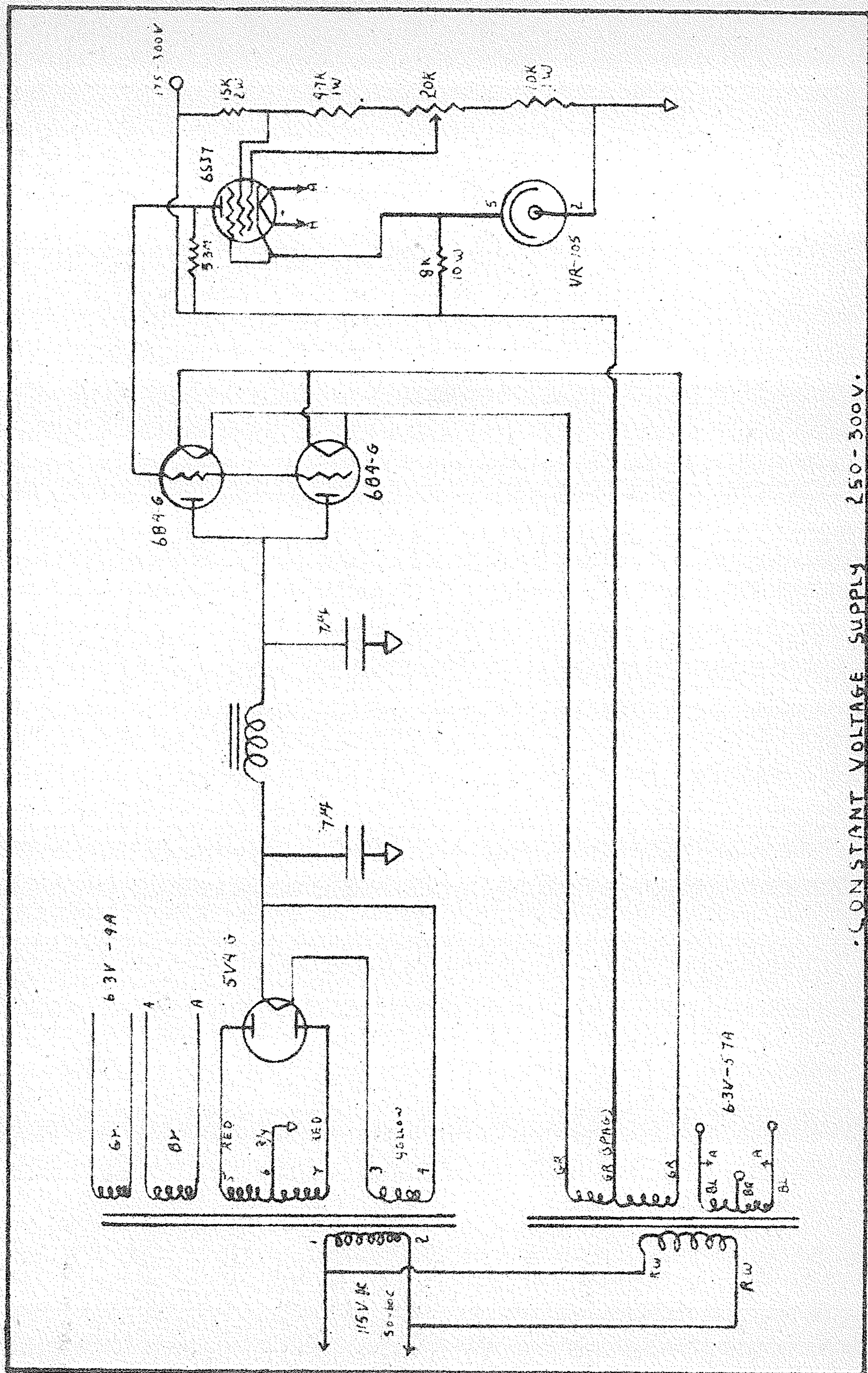
CONSTANT VOLTAGE SUPPLY 250-300V.
6SJ7
6B4-G
6B4-G
5V4G
VR-105
15K 2W
47K 1W
20K
10K 1W
8K 10W
6.3V - 4A
6.3V - 5A
RED
YELLOW
RW

- FIGURE 7 -

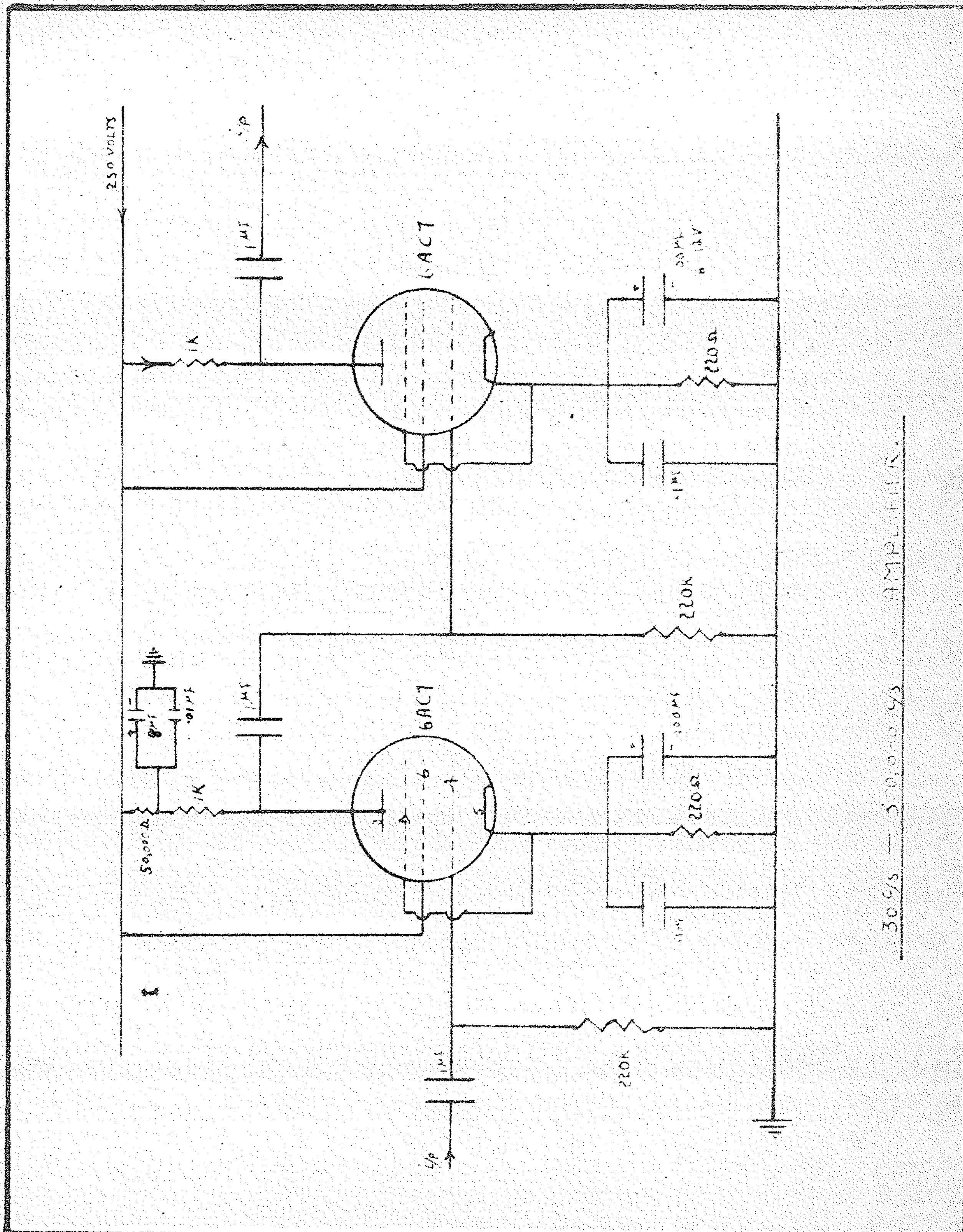
250 VOLTS
6ACT
6ACT
1K
1K
220K
220K
220Ω
220Ω
50,000Ω
AMPLIFIER.

- FIGURE 8 -

The new top had the following changes:

(1) radius of the bob was .8685", giving a spacing between cup and bob of .159".

(2) shaft diameter of .2756" (7 mms.) compared with the old one of .4724" (12 mms.).

(3) diameter of pulley used in calibration of the couples was 4.30 cms.

(4) calibration of the cell with analytical reagent grade benzene yielded a geometric capacitance of 65.53 $\mu\mu f$. This compared very well with 64.55; the calculated value of Cg. Total extraneous capacitance (ie) leads and stray) was 215.9 $\mu\mu f$.

(5) The volume of the new cell was found to be 42.57 cc.

(6) The velocity gradient calculated with the use of Equation (28) for unit angular velocity was found to vary from 1.303 sec^{-1} at the surface of the inner cylinder to 1.093 sec^{-1} at the outer cylinder. The average velocity gradient is 1.198 sec^{-1}. At 100 rpm the velocity gradient is 119.8 sec^{-1}.

The new top increased the sensitivity of measurement of deflection, and as a result the couples were recalibrated. Data is given in Table I of results section.

General procedure for taking a run was as follows: The power supply, amplifiers and oscillograph were allowed a warm up time of 30 minutes. The emulsion was prepared and kept in the constant temperature bath until the temperature of the thermostat was reached. During this interval the cell was cleaned and assembled. Thermostated water at 28.6 C was pumped through the cell jacket via rubber hose connection at a rate of 4 liters per minute. The capacitance of the empty cell at rest was recorded at

time of assembly and after 20 minutes of thermostating. The empty cell was then rotated and any off centering which was viewed on the oscillograph screen was corrected by adjusting the three wing nuts, till a null point was found.

The deflection scale was set at zero. This was accomplished by loosening the set screw which held the top of the torsion wire in position and rotating the shaft till the mirror (which was on the wire) was in line with the telescope. The set screw was then tightened and finer adjustment was made by moving the scale to the left or right till zero coincided with the cross hairs on the telescope. The cell was now ready for filling.

The emulsion was sucked into the gun by drawing the piston out. The cap of the gun was then turned on and the piston screwed in while the gun was held with the nozzel upwards until emulsion was forced out. T his procedure eliminated any air which may have been drawn in during the filling of the gun. The gun was then fitted to its attachment on the cell and the piston slowly turned in. The emulsion was forced into the cell and generally the cap of the cup was raised from position when the cell was full. At this point the gun was removed and a screw fitted in its place to prevent any possible leakage. (This procedure was followed even though the fitting on the cell was constructed with a ball bearing held by a spring which permitted flow in and prevented flow out). The cap was then forced back into position through the three openings in the top of the cell. The excess emulsion was forced out between the shaft and the bakelite collar of the cap.

The capacitance of the filled cell was recorded at the time of filling and at various intervals up to 30 minutes. A fter this time

the temperature of the cell and emulsion was assumed to be that of the thermostat.

The reversible motor was set at its maximum speed throughout the experiments and the rpm was controlled by a powerstat into which the motor was connected directly. The lowest starting setting on the powerstat was 20 volts. Even at this setting the motor had to be rotated by hand to start it. While the motor was on, the veeder root counter was set to 88880 and when it read 88910 the setting was turned (by hand) to 99910. On continued rotation the counter read 99920, 99921, etc., till 99990 was reached and at this point the counter was watched closely until 99999 appeared whence the electric stop watch was started. This gave the necessary time required to start the watch and hence the counter read 00000 at zero time. It should be noted that when slow speeds were used, the counter was set directly at 99990 and when 99999 appeared, the stop watch was started. At higher speeds the former procedure had to be used as it permitted time to find a capacity balance on the bridge. The capacitance change during the measured time (1 min) was followed on the bridge up to 55 seconds. This capacity was recorded with the rpm which was read from the counter. It should be mentioned that conductances were automatically recorded with the bridge readings. The deflection was noted immediately at the 60 second mark. The powerstat was then increased to 22 volts and the above procedure repeated. The total time required for one setting of the powerstat was one and a half minutes. When the top rpm was reached, decreasing speed was immediately begun, the same interval being used whenever possible.

The above procedure for making a run was used (with some exceptions explained in results section) in obtaining the data recorded in Table III of the results section from which Figures 12 to 18 and Figures 19 to 23

were plotted.

The capacitance readings used in calculation of the dielectric constant were not corrected for any end effects. However corrections for dissipation factor weremade. These were of real significance only when the dissipation factor, D, was greater than .1. An example of such a calculation is as follows:

Direct capacitance reading ..... 642.0 $\mu\mu f$

Dissipatiom factor D ..... .135

$(1+D^2) = 1.018$, $(1+D\ D_o) =$ 1.035

where $D_o = .026 \times \frac{f}{f_o}$, f = frequency of oscillator

f_o = frequency setting on range selector of the bridge.

For most runs $\frac{f}{f_o} = 1$ and hence $D_o = .026$. However for the runs made with 40% and 50% emulsions $D_o = .26$ since $\frac{f}{f_o} = \frac{10}{1}$.

Further $(1+0^2)\ (1+D\ D_o) = 1.054$. Corrected capacitance $= \frac{642.0}{1.054} = 609.2$

correcting for stray capacitance $609.2 - 215.9 = 393.3$.

Dielectric constant $= \frac{\text{corrected capacitance}}{\text{geometric capacitance}} = \frac{393.3}{65.5} = 5.99$.

A correction factor can be applied for the end effects and can be determined in a number of ways (26) (27).

PART III

RESULTS SECTION

Datum which was obtained with the first cell, was believed to be inferior to succeeding datum and hence was not used in any calculations.

Calibration data for couples 1 and 3 (FIGURE 9 and 10) in the new cell is given in Table I. A run with pure oil was also taken and data is shown in Table II (FIGURE 11).

Table III gives data for the dispersions in the range 3% to 50% as obtained in the new cell. FIGURES 12 to 18 inclusive show plots of deflection versus rpm for 8%, 15%, 30%, 35%, 40% (Trial I), 40% (Trial II) and 50% (Trial) respectively. FIGURES 19 to 23 inclusive show plots of dielectric constant versus rpm for 30% (Trial I), 35% (Trial II), 40% (Trial I), 40% (Trial II), and 50% (Trial II) respectively. Table IV shows a sample of the corrections made on the bridge reading in the calculation of the dielectric constant.

Table V shows the change in dielectric constant with shear (see FIGURES 24 and 25). The shear values were obtained from graphs of the dielectric constant versus rpm (in FIGURES 19 to 23). It should be noted that in some cases two or three values are given. This is due to the steps which were obtained in the graphs.

Using Equation 4 of the introduction section and FIGURE 24, the form factor was found to be 1.7. With this value of, f, the agglomeration factor A_v was calculated for the various dispersions. Values are given in Table VI. A graph, etc. (p.66).

A graph (FIGURE 26) of the agglomeration factor versus concentration of the dispersed phase was plotted. Also in Table VI are the rest values of the capacitance as calculated with the Bruggeman equation.

These figures should be compared with the shear values of Table V.

The variation of the agglomeration factor with time was calculated for several emulsions and the data is compiled in Table VII. See FIGURES 21 and 28.

Rheological data is tabulated in Table VIII and IX. Table VIII shows the viscosity as calculated at various rpm. A more accurate calculation was compiled in Table IX. All the data for the following graphs was taken from this Table. FIGURE 29 shows graph of viscosity versus concentration, FIGURE 30 shows η / η_0 versus concentration, and FIGURE 31 shows $\eta_s \rho / \phi$ versus ϕ, where ϕ is the concentration of the dispersed phase. FIGURE 30 is a test of the Einstein equation (Equation 18). The slope of the straight line was found to be 5.1.

The viscosity in poise was calculated using the equation

$$\eta = \frac{F}{AG} \qquad \text{----(39)}$$

where F is the force

A = area of the plates

G = velocity gradient,

but, we that

$$F = \frac{m\ g\ r}{R_b} \qquad \text{----(40)}$$

where m = mass in grams required to give a certain deflection

g = acceleration of gravity

r = radius of pulley on bob shaft

R_b = radius of bob

and substituting this value of F into Equation (39) and rearranging, we get

$$\eta = \frac{mgr}{\pi R_b^3\ h\ G\ rpm} \quad \text{poise} \qquad \text{----(41)}$$

Since g, r, π, R_b, h, and G are constants and equal to 980 cm/sec^2, 2.15 cm, 3.14, 2.20599, 9.2227 and 1.198 respectively, this equation becomes

$$\eta = \frac{m}{rpm} \times 5.68 \text{ poise} \qquad \text{----(42)}$$

The yield values for the dispersions were calculated and data is shown in Table VIII.

The wire constant K was calculated for couples No. 1 and 3 using the equation

$$K = \frac{\omega \times g \times r}{\theta} \qquad \text{----(43)}$$

where ω = weight in grams to give deflection θ

g = acceleration of gravity

r = radius of pulley

for couple No. 1 (FIGURE 9)

$$K = \frac{100 \times 980 \times 2.15}{16.5} = 12800$$

for couple No. 3 (FIGURE 10)

$$K = \frac{200 \times 980 \times 2.15}{9.7} = 43500$$

The constants S and C were also calculated using Equations(11)and (12)

$$S = \frac{\frac{1}{(R_b)^2} - \frac{1}{(R_c)^2}}{4\pi h} = 2.85 \times 10^{-4}$$

R_b and R_c are radii of bob and cup respectively and h is height of the bob.

$$C = \frac{S}{2.303 \log \frac{R_c}{R_b}} = 3.25 \times 10^{-3}$$

Several calculations were made on the 50% dispersion. Applying the Green theory on the rheological data the plastic viscosity U_1 and U_2 for both loop was calculated using Equation (14)

$$U_1 = \frac{(T - T_2)\ 9.55\ SK}{rpm} \quad \text{poise}$$

(the factor 9.55 converts rpm to ω) K converts the deflection to torque.

In the present case rpm, = 382

deflection T, = 14.15 (taken from straight line of down curve see FIGURE 21.

K = 43500

S = 2.85×10^{-4}

T_2 = 1.3(see Table XX)

$$U_1 = \frac{(14.15 - 1.3)\ 9.55 \times 2.85 \times 10^{-4} \times 43500}{382} = 4.01 \text{ poise}$$

rpm_2 = 680

deflection = 18.0

T_2 = 2.5

$$U_2 = \frac{(18.0 - 2.5)\ 9.55 \times 2.85 \times 10^{-4} \times 43500}{680} = 2.71 \text{ poise}$$

The second coefficient of thixotropic breakdown M (the loss in shearing force per unit are increased in rate of shear) was calculated using Equation (22).

$$M = \frac{2(U_1 - U_2)}{\ln \frac{\omega_1^2}{\omega_2^2}}$$

$$M = \frac{2(4.01 - 2.71)}{\ln \frac{(758)^2}{(408)^2}} = 2.10 \text{ dynes/sq cm/} \frac{dv}{dr}$$

The increase in yield value per unit decrease in plastic viscosity, V, was also calculated using Equation (23).

$$V = \frac{F_2 - F_1}{U_1 - U_2}$$

$$V = \frac{353 - 183}{4.01 - 2.71} = 130.2 \text{ dynes/sq cm/poise.}$$

TABLE I (New Cell)

COUPLE NO. 1

WT. IN GRAMS	DEFLECTION
10	1.5
20	3.6
30	4.85
40	6.3
50	7.85
60	9.7
70	10.6
80	13.0
90	14.7
100	16.4
120	20.15
130	22.1

COUPLE NO. 3

WT. IN GRAMS	DEFLECTION
50	2.0
100	4.6
150	6.6
200	9.3
250	12.2
300	14.6
350	17.0
400	19.9
450	22.7
500	24.8

TABLE II (Oil in New Cell)

COUPLE NO. 1

RPM of CELL	DEFLECTION
0	0
103	2.9
135	4.0
215	6.4
256	7.8
346	10.35
450	14.2
523	16.2
610	18.6
660	19.85
600	18.4
493	14.9
370	10.9
330	10.15
183	5.4
92	3.25
42	1.65
0	0

COUPLE NO. 3

RPM of CELL	DEFLECTION
0	0
58	.45
146	1.1
225	1.85
315	2.75
393	3.6
433	3.8
513	4.4
596	5.05
626	5.3
683	5.75
800	6.2?
646	5.5
586	5.05
463	4.0
300	2.65
120	1.05
46	.5
31	.3
0	0

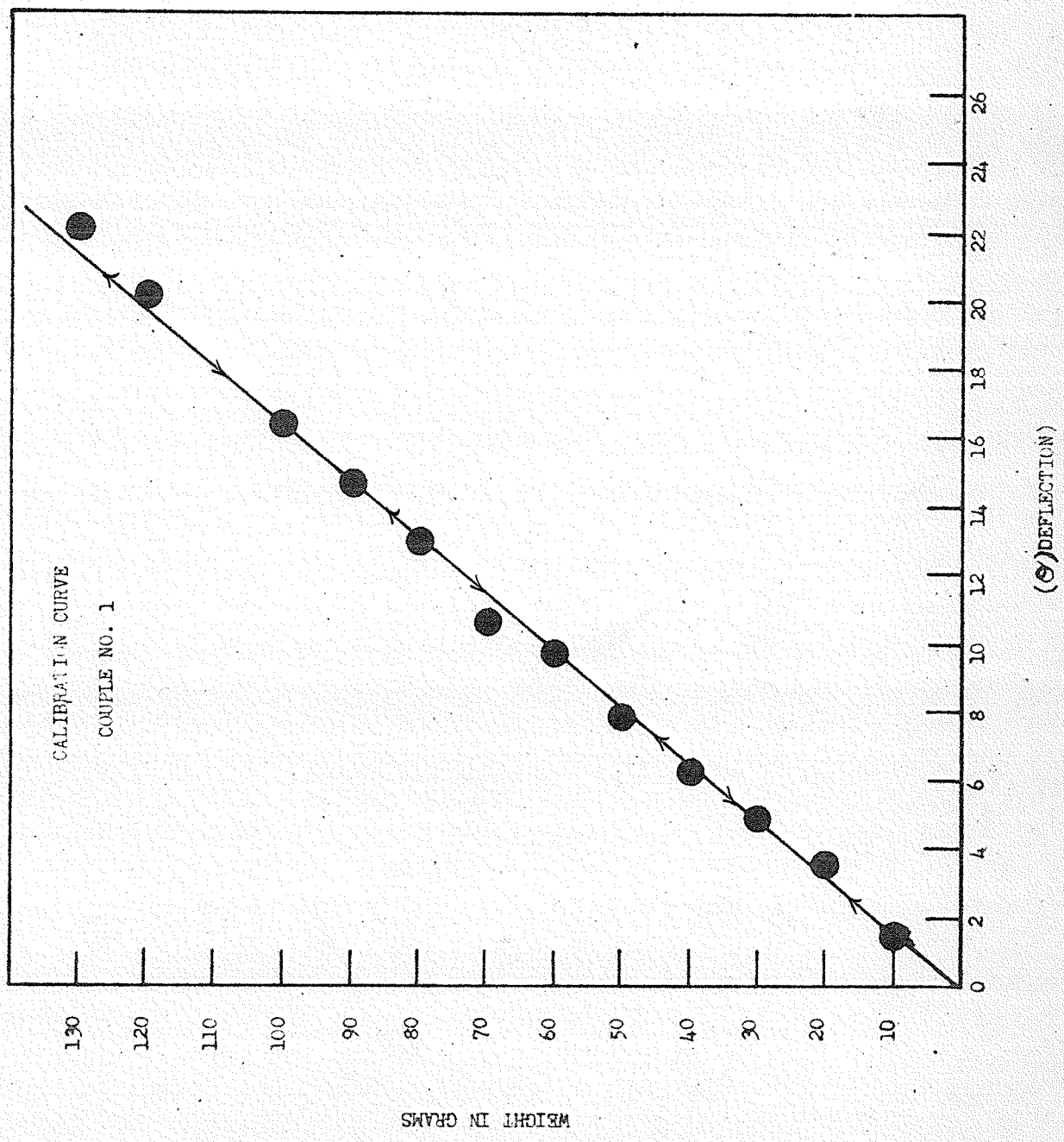
CALIBRATION CURVE
COUPLE NO. 1
WEIGHT IN GRAMS
130
120
110
100
90
80
70
60
50
40
30
20
10
0
2
4
6
8
10
12
14
16
18
20
22
24
26
(θ) DEFLECTION)

- FIGURE 9 -

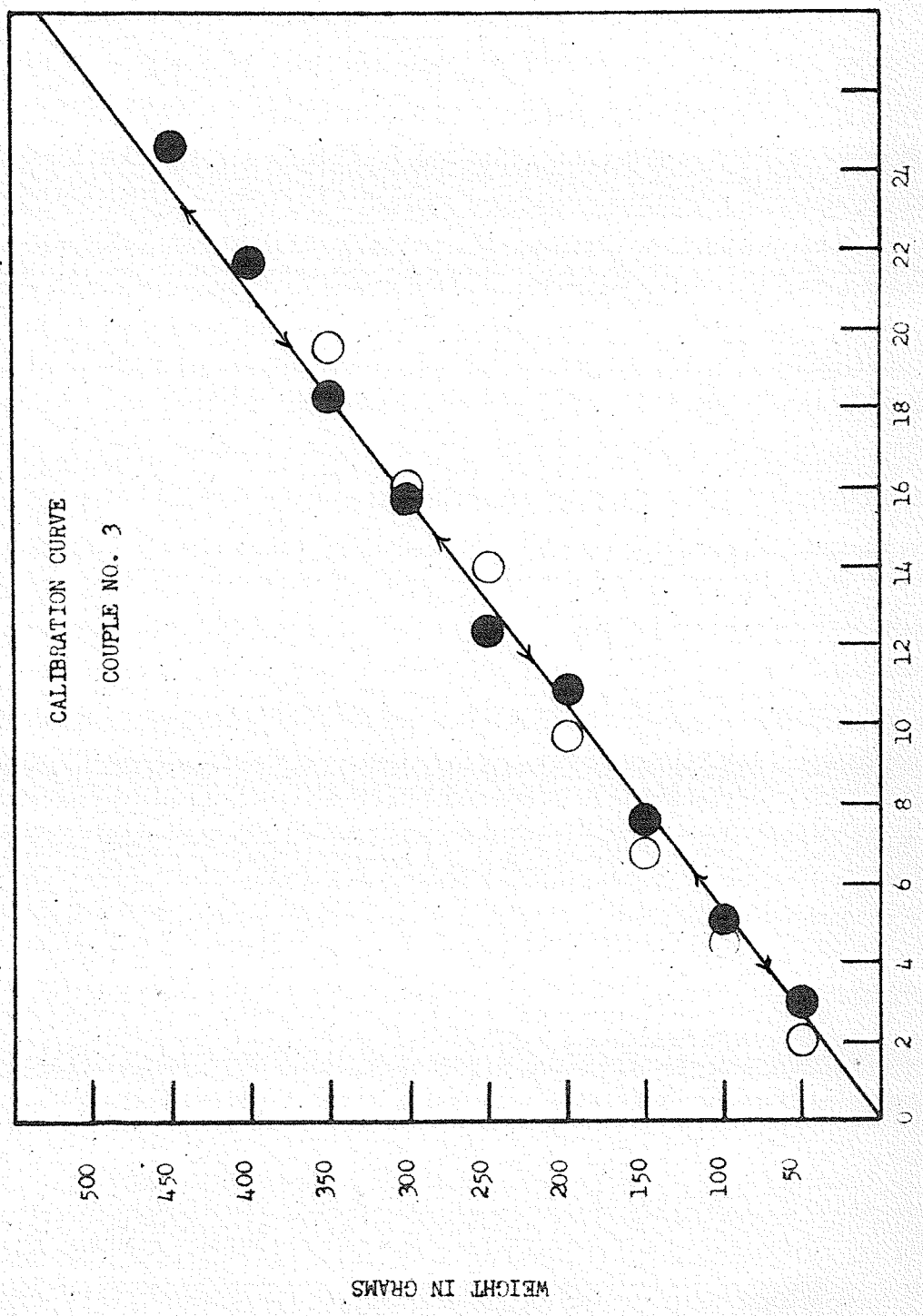
CALIBRATION CURVE
COUPLE NO. 3
WEIGHT IN GRAMS
500
450
400
350
300
250
200
150
100
50
0
2
4
6
8
10
12
14
16
18
20
22
24
(DEFLECTION)

- FIGURE 10 -

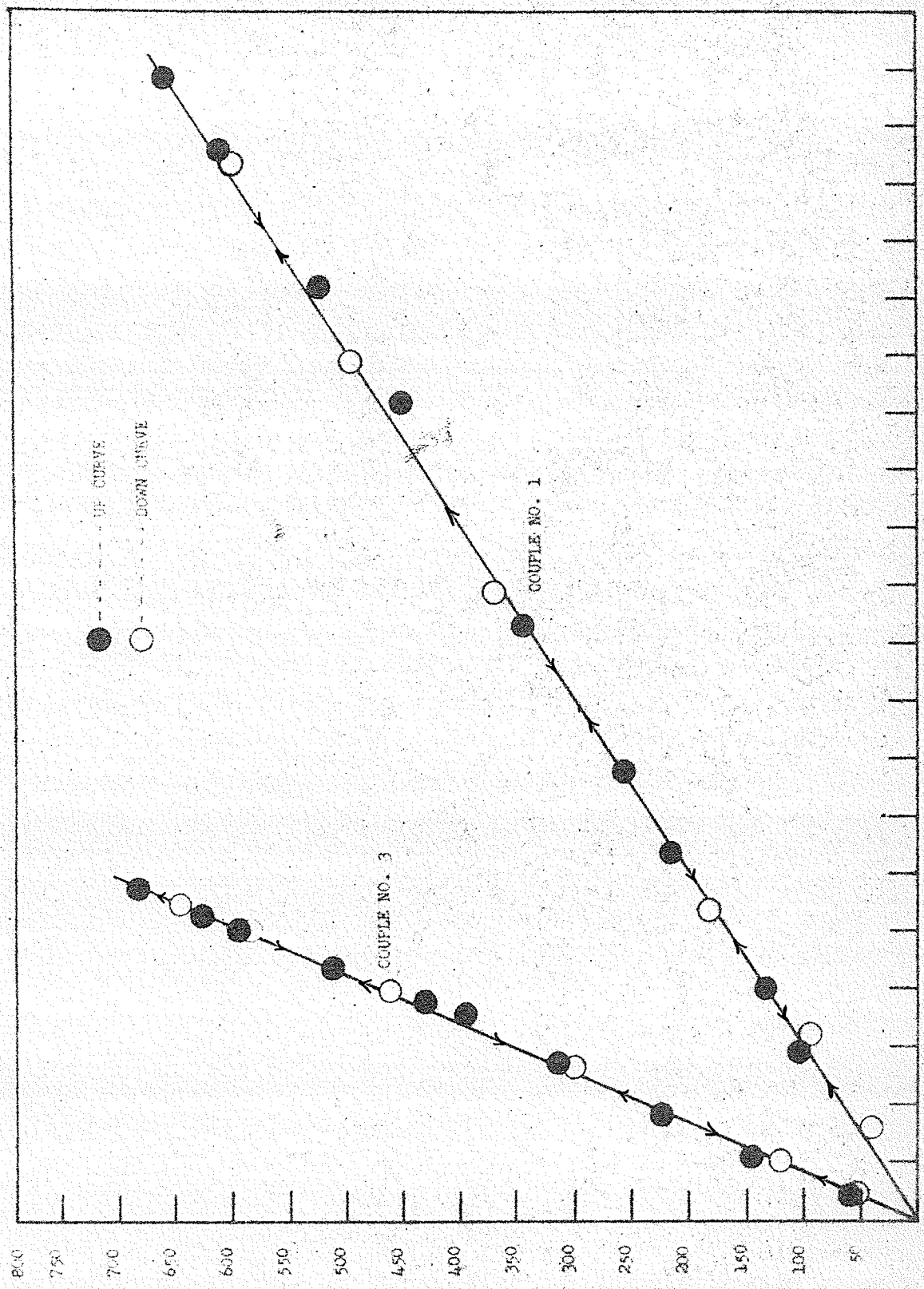
UP CURVE
DOWN CURVE
COUPLE NO. 1
COUPLE NO. 3
(DEFLESTION)
R P M OF CHAL

- FIGURE 11 -

TABLE III

TRIAL I

3%	RPM of CELL	DEFLECTION	DIELECTRIC CONSTANT
Couple 1	0	0	2.64
	0	0	2.63
	33	.5	2.62
	71	1.2	2.61
	115	2.6	2.60
	165	4.7	2.57
	260	7.6	2.61
	370	12.4	2.19
	447	14.5	2.20
	528	17.0	2.17
	612	19.15	2.16
	627	19.75	2.14
	660	20.65	2.14
	700	22.25	2.11
	733	23.0	2.11
	690	22.0	2.11
	633	19.9	2.12
	537	16.2	2.59
	380	10.9	2.59
	270	8.0	2.59
	125	4.15	2.59
	78	2.15	2.60
	32	1.1	2.60
	0	0	2.60
	1	0	2.61
	11	0	2.61
	20	0	2.61
	36	0	2.61

TRIAL II

3%	RPM of CELL	DEFLECTION	DIELECTRIC CONSTANT
Couple 1	0	0	2.60
	102	2.15	2.59
	173	4.80	2.59
	270	8.20	2.59
	373	12.40	2.60
	457	14.60	2.60
	533	17.30	2.60
	617	19.60	2.60
	660	21.2	2.11
	727	23.2	2.11
	697	22.4	2.10
	630	20.1	2.11
	610	18.85	2.10
	560	16.25	2.58
	445	13.4	2.58
	360	10.4	2.58
	257	7.9	2.59
	155	4.8	2.59
	76	2.1	2.59
	36	1.1	2.60
	0 Mins.	0	2.55

TRIAL II - Continued

3%	RPM of CELL	DEFLECTION	DIELECTRIC CONSTANT
Couple 1	.5	0	2.60
	1	0	2.60

TRIAL I

8%	RPM of CELL	DEFLECTION	DIELECTRIC CONSTANT
Couple 1	0	0	3.09
	0	0	3.10
	0	0	3.11
	23	1.0	3.07
	85	3.95	3.06
	143	6.0	3.05
	160	6.4	3.01
	208	8.6	3.02
	293	13.3	3.01
	403	17.7	3.03
	473	20.35	2.54
	547	23.2	2.49
	567	23.6	2.47
	617	25.3	2.45
	520	21.4	2.46
	387	15.5	2.51
	307	12.4	2.51
	223	9.1	3.02
	150	6.35	3.01
	91	4.35	3.02
	43	2.3	3.02
	0 Mins.	--	3.03
	2	--	3.05
	7	--	3.06
	55	--	3.05

TRIAL II

8%	RPM of CELL	DEFLECTION	DIELECTRIC CONSTANT
Couple 1	0	0	3.05
	69	2.7	3.02
	89	3.8	3.01
	127	5.35	3.01
	177	7.1	3.01
	253	10.4	3.01
	363	15.6	2.53
	423	18.3	2.45
	503	21.6	2.39
	560	23.6	2.36
	617	25.7	2.35
	407	21.8	2.43
	327	16.4	2.46
	237	13.2	3.02
	193	9.25	3.02

-continued

TABLE III - Continued

TRIAL II - continued

8%	RPM of CELL	DEFLECTION	DIELECTRIC CONSTANT
Couple 1	107	7.6	3.01
	57	4.7	3.01
	40	2.9	3.02
	0	1.9	3.02
	3	0	3.03
	18	0	3.03
	30	0	3.05

TRIAL I

15%	RPM of CELL	DEFLECTION	DIELECTRIC CONSTANT
Couple 1	0	0	3.91
	0	0	3.98
	0 15 Min	0	4.02
	0 30 Min	0	4.09
	0 50 Min	0	4.15
	34	1.1	3.99
	54	1.65	3.95
	95	3.80	3.92
	142	5.65	3.88
	180	6.95	3.64
	247	10.3	3.73
	290	12.9	3.70
	350	15.5	3.71
	387	17.3	3.71
	452	19.2	3.79
	513	22.3	3.70
	580	24.8	3.69
	520	22.7	3.71
	457	20.0	3.64
	387	16.6	3.65
	312	14.3	3.69
	227	10.2	3.68
	170	7.5	3.80
	105	4.9	3.85
	58	3.15	3.88
	31	1.65	3.91
	0	0	3.90
	1	---	3.91
	3	---	3.92
	7	---	3.96
	15	---	4.00
	23	---	4.03

TRIAL II

15%	RPM of CELL	DEFLECTION	DIELECTRIC CONSTANT
couple 1	0	0	4.03
	80	3.2	3.82
	150	6.25	3.77
	243	10.3	3.74
	360	16.2	3.73
	450	20.15	3.73
	520	23.4	3.74
	493	21.9	3.77
	417	18.4	3.73
	327	14.7	3.74
	253	11.2	3.80
	132	6.0	3.85
	89	4.5	3.88
	0 Mins.	0	3.93
	6	0	3.96
	7	0	3.97

TRIAL I

20%	RPM of CELL	DEFLECTION	DIELECTRIC CONSTANT
Couple 1	0	0	4.65
	0	0	4.83
	0	0	4.88
	0	0	4.88
	0	0	4.88
	20	.55	4.78
	41	1.35	4.73
	70	2.80	4.67
	95	4.2	4.67
	144	7.1	4.66
	198	10.5	4.66
	253	13.3	4.66
	292	15.8	4.61
	343	18.2	4.58
	400	21.7	4.40
	447	24.3	3.77
	427	22.6	3.77
	393	21.5	3.79
	340	18.8	3.80
	317	17.45	3.83
	275	15.1	4.69
	248	14.0	4.66
	196	10.8	4.68
	128	6.75	4.71
	90	5.35	4.71
	69	4.2	4.73
	43	2.65	4.78
	29	1.85	4.79

- continued

TABLE III - Continued

TRIAL I - continued

20%	RPM of CELL	DEFLECTION	DIELECTRIC CONSTANT
Couple 1	.5 Mins	0	4.74
	2 Mins	0	4.70
	3 Mins	0	4.73
	5 Mins	0	4.73
	10 Mins	0	4.74
	15 Mins	0	4.75
	20 Mins	0	4.76
	26 Mins	0	4.77
	30 Mins	0	4.78

TRIAL II

20%	RPM of CELL	DEFLECTION	DIELECTRIC CONSTANT
Couple 1	0	0	4.74
	0	0	4.80
	0	0	4.82
	0	0	5.78
	53	2.1	5.12
	67	2.8	5.08
	93	4.4	5.05
	132	6.8	5.06
	183	10.0	4.80
	245	13.75	4.87
	295	16.5	4.90
	330	19.1	4.90
	360	21.0	4.88
	397	22.5	4.88
	463	25.7	4.80
	507	27.8	4.84
	563	31.25	4.82
	623	33.8	4.70
	653	35.2	4.71
	697	36.8	4.72
	633	33.8	4.77
	580	30.4	4.74
	433	22.3	4.75
	366	19.0	4.77
	255	13.6	4.88
	182	9.6	4.91
	118	6.6	4.95
	73	4	5.02
	49	3	5.08
	0 Mins	0	5.33
	10 Mins	--	5.56
	15 Mins	--	5.56
	40 Mins	--	5.68

TRIAL I

25%	RPM of CELL	DEFLECTION	DIELECTRIC CONSTANT
Couple 3	0	.0	5.77
	0	.0	5.79
	0	.0	5.84
	0	.0	5.99
	28	.4	5.95
	0	.0	6.08
	36	.5	5.93
	56	.8	5.81
	110	1.75	5.64
	155	2.65	5.57
	206	3.65	5.52
	262	4.70	5.46
	313	5.5	5.20
	343	6.0	5.20
	382	6.7	5.03
	433	7.15	5.02
	473	7.75	
	337	6.15	5.14
	247	4.75	5.31
	98	2.0	5.44
	41	1.15	5.56
	19	.85	5.72
	0	.0	5.94
	69	1.20	5.51
	165	2.65	5.32
	267	4.80	5.29
	390	6.80	5.25
	473	8.25	5.28
	543	9.0	5.21
	596	9.5	5.20
	637	10.0	5.20
	667	10.3	5.20
	690	10.6	5.20
	723	10.85	5.20
	710	10.5	5.20
	670	10.2	5.23
	655	9.85	5.23
	627	9.5	5.28
	585	9.0	5.28
	530	8.3	5.28
	440	7.25	5.28
	346	6.00	5.31
	275	4.85	5.32
	123	2.45	5.74
	54	1.35	6.03
	54	1.35	6.25
	1 Min	.0	6.14
	3	--	5.83
	4	--	5.81
	7	--	5.71
	11	--	5.73

TABLE III - Continued

TRIAL II

25%	RPM of CELL	DEFLECTION	DIELECTRIC CONSTANT
Couple 3	0	0	5.60
	0	0	5.60
	0	0	5.61
	0	0	5.63
	1	0	5.94
	73	1.25	5.53
	105	1.75	5.53
	142	2.45	5.50
	188	3.5	5.48
	248	4.35	5.45
	267	4.75	5.39
	333	6.25	5.33
	367	6.50	5.25
	428	7.50	5.25
	332	6.25	5.25
	233	4.65	5.25
	98	2.25	5.50
	62	1.25	5.60
	0	0	5.50
	0	0	5.53
	83	1.5	5.45
	170	2.9	5.30
	268	4.55	5.28
	396	7.15	5.22
	456	8.0	5.21
	543	9.2	5.20
	600	10.0	5.21
	630	10.35	5.20
	667	10.55	5.20
	700	10.85	5.18
	733	11.25	5.20
	716	11.0	5.20
	693	10.5	5.21
	660	10.15	5.21
	630	9.65	5.20
	603	9.25	5.20
	543	8.5	5.20
	456	7.5	5.20
	367	6.3	5.16
	257	4.65	5.24
	123	2.55	5.40
	61	1.45	5.50
	0 Mins	0	5.56
	1	0	5.57

TRIAL III

25%	RPM of CELL	DEFLECTION	DIELECTRIC CONSTANT
Couple 1	0	0	5.35
	0	0	5.63
	0	0	5.68
	82	4.3	5.34
	116	6.4	5.34
	150	8.4	5.34
	207	12.25	5.33
	243	14.6	5.32
	273	16.7	5.32
	310	18.7	5.25
	347	21.25	5.20
	380	23.7	5.20
	417	26.5	5.20
	393	24.8	5.21
	330	20.5	5.19
	230	15.0	5.35
	176	12.25	5.36
	102	6.7	5.42
	59	4.3	5.51
	46	3.25	5.41
	0 Mins	0	5.59
	1 Mins	0	5.67
	2 Mins	0	5.70
	4 Mins	0	5.75
	5 Mins	0	5.76

TRIAL IV

25%	RPM of CELL	DEFLECTION	DIELECTRIC CONSTANT
Couple 1	0	0	8.17
	0	0	8.20
	0	0	8.32
	25	2.7	6.64
	53	3.9	6.22
	89	5.8	6.05
	125	8.25	6.00
	162	10.8	5.90
	216	14.5	5.76
	280	18.7	5.57
	312	21.0	5.61
	356	23.0	5.43
	417	27.0	5.42
	367	24.2	5.54
	295	19.8	5.67
	175	12.9	5.77
	99	7.4	5.89
	48	3.9	6.08
	27	2.75	6.28

- continued

TABLE III - Continued

TRIAL IV - Continued

25%	RPM of CELL	DEFLECTION	DIELECTRIC CONSTANT
Couple 1	20	2.30	5.71
	0 Mins	0	6.40
	1	0	6.44
	2	0	6.49
	3	0	6.53
	4	0	6.60
	5	0	6.64
	10	0	6.80
	15	0	6.91
	90	0	5.79
	0	0	6.35

TRIAL I

30%	RPM of CELL	DEFLECTION	DIELECTRIC CONSTANT
Couple 3	0	0	7.78
	0	0	7.89
	0	0	7.97
	22	.5	6.94
	49	1.2	6.81
U	123	2.6	6.79
P	133	2.95	6.78
	206	4.6	6.71
C	212	4.7	6.71
U	277	6.0	6.61
R	320	7.4	6.67
V	370	7.9	6.67
E	410	8.9	6.67
	433	9.2	6.65
	483	10.2	6.70
	516	10.6	6.62
	553	11.4	6.61
	603	12.15	6.59
	633	12.5	6.58
	683	12.6	6.55
	690	12.7	6.55
	640	11.85	6.50
D	613	11.5	6.49
O	600	11.1	6.50
W	543	9.9	6.49
N	463	8.85	6.47
	420	8.1	6.45
C	366	7.1	6.47
U	333	6.55	6.47
R	275	5.60	6.47
V	213	4.55	6.49
E	160	3.4	6.52
	152	3.5	6.52
	63	2.0	6.87
	35	1.3	6.93
	0 Mins.	0	7.60
R	2.5	--	7.80
E	3	--	7.80
C -			

TRIAL I - Continued

30%	RPM of CELL	DEFLECTION	DIELECTRIC CONSTANT
Couple 3	4	--	7.83
	5	--	7.83
- O T	6	--	7.84
V I	7	--	7.91
E M	87	--	7.91
R E	114	--	7.94
Y			

TRIAL II

30%	RPM of CELL	DEFLECTION	DIELECTRIC CONSTANT
Couple 3	0	0	7.94
	91	2.1	6.63
	207	4.2	6.55
U	245	4.9	6.53
P	300	6.2	6.50
	348	7.0	6.53
C	383	8.0	6.52
U	430	8.6	6.49
R	483	9.8	6.46
V	533	10.65	6.46
E	566	11.2	6.48
	600	11.6	6.46
	563	10.8	6.44
D	536	10.3	6.46
O	488	9.4	6.47
W	456	8.75	6.47
N	413	8.15	6.46
	373	7.3	6.47
C	316	6.4	6.50
U	275	5.65	6.47
R	208	4.5	6.50
V	132	3.2	6.55
E	76	2.25	6.81
	0	0	7.42
R	1		7.59
E	2		7.76
C T	3		7.70
O I	4		7.68
V M	7		7.58
E E	9		7.55
R	11		7.49
Y	15		7.46

TABLE III - Continued

TRIAL III

30%	RPM of CELL	DEFLECTION	DIELECTRIC CONSTANT
	0	0	
	343	7.1	6.58
	406	8.25	6.49
	296	6.4	6.50
	222	4.8	6.50
	148	3.55	6.53
	66	1.8	6.65
	33	1.25	6.88
	0	0	7.23
	1		7.62
	2		7.72
	3		7.78
	5		7.75
	10		7.66
	24 hrs.		7.54
	48 "		7.86

TRIAL IV

30%	RPM of CELL	DEFLECTION	DIELECTRIC CONSTANT
	0	0	7.55
U	0	0	7.60
P	0	0	7.63
	83	2.25	7.39
C	126	3.2	7.05
U	148	3.65	6.79
R	195	3.95	6.76
V	213	5.1	6.75
E	270	6.4	6.96
	315	7.25	6.82
DOWN	145	3.75	6.94
CURVE	39	1.5	7.46
	0	0	8.10
	315	7.25	6.61
U	360	7.95	6.46
P	406	8.9	6.38
	433	9.75	6.43
C	458	10.05	6.41
U	492	10.35	6.46
R	508	10.65	6.43
V	586	12.25	6.44
E	610	12.35	6.39
	633	12.45	6.39
	636	12.45	6.38
	653	12.45	6.39
	716	12.85	6.41
	766	13.0	6.40
	800	13.25	6.36

TRIAL IV - Continued

30%	RPM of CELL	DEFLECTION	DIELECTRIC CONSTANT
	650	11.8	6.35
D	616	11.4	6.43
O	593	11.1	6.44
W	536	10.0	6.39
N	443	8.5	6.39
	360	7.15	6.49
C	288	5.96	6.55
U	243	5.25	6.65
R	142	3.35	6.84
V	136	3.30	
E	0	0	7.87
	75 mins.	--	7.97

TRIAL I

35%	RPM of CELL	DEFLECTION	DIELECTRIC CONSTANT
	0	0	9.60
Couple 3	0	0	10.10
	0	0	10.26
	80	2.0	8.21
U	135	3.35	8.09
P	158	4.0	8.01
	210	5.4	7.91
C	246	6.1	7.87
U	265	6.4	7.86
R	322	7.75	7.86
V	393	9.0	7.83
E			
	276	6.7	7.83
D	245	6.1	7.86
O	176	4.6	7.86
W	166	4.5	7.89
N	96	2.9	8.07
	66	2.2	8.15
C	46	1.6	8.35
U	17	.8	8.62
R			
V			
E			
	0 Mins	0	9.37
R	1	--	9.54
E	2	--	9.64
C	3	--	9.71
O	4	--	9.78
V	5	--	9.84
E	6	--	9.92
R	10		10.18
Y	11		10.22

-Continued

TABLE III - Continued

TRIAL I - continued

35%	RPM of CELL	DEFLECTION	DIELECTRIC CONSTANT
U	398	9.3	7.83
P	436	9.75	7.81
	466	10.4	7.87
C	533	11.2	7.86
U	570	11.7	7.81
R	620	12.15	7.43
V	603	12.0	7.52
E	670	12.25	7.77
	666	12.3	7.52
	693	12.5	7.52
	800	12.85	7.43
D	683	12.1	7.43
O	633	11.35	7.42
W	560	10.4	7.43
N	490	9.25	7.54
	373	7.1	7.62
C	276	5.8	7.62
U	182	4.4	7.71
RVE	79	2.15	7.98
	0 Mins.	0	8.94
R	1		9.13
E	2		9.16
C	4		9.22
O	5		9.28
V	7		9.48
E	10		9.75
R	14		10.19
Y			

TRIAL II

35%	RPM of CELL	DEFLECTION	DIELECTRIC CONSTANT
Couple 3	0	0	11.38
	46	1.5	8.76
	90	2.4	8.36
U	126	3.35	8.76
P	176	4.7	8.61
	210	5.45	8.30
C	255	6.35	8.26
U	278	6.95	8.06
R	326	7.9	7.98
V	390	9.0	8.04
E			
	273	6.65	8.07
D	192	5.3	8.12
O	139	3.95	8.29
W	93	2.8	8.62
N	36	1.45	9.52
CURVE	13	1.15	9.90

- continued

TRIAL II - Continued

35%	RPM of CELL	DEFLECTION	DIELECTRIC CONSTANT
Couple 3	1	0 Mins	11.14
RE-	2.5	--	11.48
COVERY	3	--	11.52
	5	--	11.81
	112	3.1	8.61
	246	6.35	5.33
U	326	7.95	5.33
P	373	9.0	5.42
	396	9.3	5.42
C	463	10.65	5.37
U	510	11.05	5.11
R	543	11.8	5.14
V	583	12.2	5.16
E	613	12.35	5.13
	633	12.5	5.10
	660	12.7	5.08
	690	12.9	5.08
D	633	12.0	5.17
O	576	10.9	5.17
W	488	9.35	5.20
N	348	6.7	5.33
	256	5.6	5.27
C	145	3.65	5.94
U	72	2.35	8.29
RVE	43	1.6	8.64
	0 Mins.	0	10.15
R	2	--	10.61
E	3	--	10.80
C	4		10.88
O	5		11.94
V	7		11.05
E	18		11.37
R			
Y			

- continued

TABLE III - Continued

TRIAL I

40%	RPM of CELL	DEFLECTION	DIELECTRIC CONSTANT
Couple 3	0	0	17.85
	0	0	18.52
	0	0	18.73
	0	0	18.90
U	21	.5	13.05
P	57	1.65	12.86
	93	2.90	12.60
C	132	4.20	12.44
U	169	5.4	12.27
R	208	6.5	12.12
V	225	7.0	12.04
E	286	8.7	11.84
	323	9.5	11.70
	380	11.0	11.55
D	270	8.05	11.64
O	230	7.0	11.63
W	143	4.7	11.81
N	63	2.35	12.31
CURVE	21	1.10	12.97
	0 Mins	0 Mins	15.26
R	1	--	16.25
E	2	--	16.76
C	3	--	16.79
O	4		16.97
very	5		17.11
U	380	10.9	7.08
P	420	11.65	7.14
	486	12.3	7.14
C	496	12.9	7.09
U	530	13.6	7.16
R	586	14.4	7.14
V	616	14.6	7.12
E	650	14.8	7.16
	680	15.2	7.19
D	623	14.0	7.17
O	610	13.5	7.19
W	566	12.7?	7.19
N	500	11.25	7.16
	413	9.5	7.16
C	346	8.25	7.14
U	213	5.6	10.83
R	132	3.8	11.12
V	76	2.65	11.43
E	42	1.8	12.03
	24	1.2	12.47
R	0 Mins	0	14.30
E	1	--	14.71
C	2	--	15.29
O	3		15.35
V	4		15.52
E	5		15.72
R	6		15.92
Y	13		17.06
	15		17.29

-continued

TRIAL I - continued

40%	RPM of CELL	DEFLECTION	DIELECTRIC CONSTANT
Couple 3	17		17.58
	18		17.69
	22		18.09
	25		18.36
	30		18.69

TRIAL II

40%	RPM of CELL	DEFLECTION	DIELECTRIC CONSTANT
	0	0	18.76
U	52	1.45	12.32
P	75	2.25	11.98
	123	4.0	11.90
C	155	4.7	11.52
U	192	6.3	11.25
R	253	7.3	11.28
V	303	8.4	11.23
E	330	9.15	11.17
	363	9.9	11.08
	396	10.5	10.96
D	315	8.65	11.08
O	260	7.2	11.08
W	178	5.3	11.14
N	72	2.7	11.58
	46	2.0	11.78
CURVE	22	1.15	12.51
	0 Mins	0	14.19
R	1 Mins	--	14.86
E	2 Mins	--	15.12
C	3 Mins	--	15.29
O	4 "	--	15.43
V	5 "	--	15.57
E	6 "	--	15.69
R	7 "		15.78
Y	10 "		16.07
	12 "		16.22
	15 "		16.45
	20 "		16.74
	21 "		16.80
	24 "		16.95
	25 "		16.99
	342	9.4	11.19
U	406	10.5	10.99
P	426	11.25	10.91
	493	12.5	10.91
C	546	13.15	10.71
U	596	14.1	10.71
R	630	14.4	10.91
V	663	14.6	10.61
E	683	14.9	10.56
	716	15.2	10.47
	800	15.2	10.44

- continued

TABLE III - Continued

TRIAL II - continued

40%	RPM of CELL	DEFLECTION	DIELECTRIC CONSTANT
	700	13.8	10.35
D	630	12.8	10.41
O	600	12.1	10.39
W	540	11.05	10.39
N	466	9.8	10.44
	373	8.0	10.59
C	260	6.0	11.06
U	182	4.5	11.14
R	110	3.1	11.22
V	49	1.6	11.67
E	32	1.1	11.89
	0 Mins		13.44
R	1 Mins		13.87
E	2 Mins		14.04
C	5 Mins		14.22
O	10 Mins		14.56
V	19 Mins		15.15
E	23 Mins		15.38
RY			

TRIAL III - continued

40%	RPM of CELL	DEFLECTION	DIELECTRIC CONSTANT
D	683	15.1	4.59
O	630	14.15	4.67
W	600	13.6	4.61
N	533	12.2	4.70
C	462	11.0	4.96
U	385	9.4	5.08
RVE	282	7.3	10.44
	140	4.4	10.87
	85	3.3	11.13
	58	2.6	11.26
	43	2.25	11.51
R	0	0	12.74
E	1	--	12.67
C	3		12.64
O	12	--	12.71
V	18	--	12.76
ERY	35	--	12.82

TRIAL III

40%	RPM of CELL	DEFLECTION	DIELECTRIC CONSTANT
	0	0	14.04
	59	2.2	12.16
U	93	3.35	11.98
P	141	4.8	11.71
	176	5.95	11.46
C	226	7.3	11.34
U	272	8.7	11.29
R	333	10.5	6.35
V	392	12.0	6.38
E	446	12.9	6.36
	358	10.6	6.71
D	233	7.6	11.06
O	223	7.2	11.05
W	100	3.85	11.37
N	48	2.42	11.86
CURVE	25	1.62	12.23
	0 Mins	0	13.81
	2 Mins	--	13.66
RECOVERY	4 Mins	--	13.69
	366	11.6	6.00
	430	12.65	5.57
	483	13.65	5.23
	550	14.2	5.16
	563	14.3	5.16
	606	15.15	4.94
	636	15.4	5.04
	663	15.65	4.95
	690	16.0	4.67
	730	16.12	4.70

- continued

TRIAL I

50%	RPM of CELL	DEFLECTION	DIELECTRIC CONSTANT
	0	0	33.59
	0	0	37.82
	0	0	33.30
U	43	.9	21.98
P	95	2.2	20.97
	144	3.4	19.93
C	179	4.2	19.34
U	216	5.0	18.85
R	249	5.8	18.54
V	273	7.0	17.72
E	322	8.4	17.35
	356	9.7	17.12
	410	11.4	15.90
	412	12.2	--
D	323	10.0	16.37
O	156	6.5	16.86
W	135	4.85	16.37
N	70	3.15	16.66
	29	1.75	18.02
CURVE	328	11.1	16.28
	403	12.8	11.29
U	443	12.7 ?	9.81
P	486	14.6	8.65
	503	14.6	8.50
C	520	14.8	7.95
U	583	16.25	7.45
R	623	16.8	7.10
V	650	17.05	6.88
E	696	17.4	6.76
	723	17.7	6.75

-continued

TABLE III - Continued

TRIAL I - continued

50%	RPM	of CELL	DEFLECTION	DIELECTRIC CONSTANT
D	663		16.5	6.79
O	625		15.3	7.20
W	596		14.5	7.07
N	506		12.65	7.26
	400		11.0	7.26
C	333		9.45	14.99
U	215		6.65	15.03
R	128		4.5	15.63
VE	67		2.9	16.54
1 Mins	36		2.05	17.84
2 Mins	36		2.05	18.02
3 Mins	36		2.05	18.11
5 Mins	35		2.0	18.54
6 Mins	35		1.9	17.85
0 Mins			0	24.34
1			--	25.77
2			--	26.61
170				35.79

TRIAL II

50%	RPM	of CELL	DEFLECTION	DIELECTRIC CONSTANT
	0		0	24.95
	0		0	26.06
	0		0	27.09
	0		0	27.35
U	24		1.15	17.28
P	42		1.8	15.76
	72		3.0	15.11
C	110		4.6	14.62
U	151		6.3	14.24
R	178		7.75	13.96
V	225		9.45	13.77
E	267		11.1	7.36
	333		13.0	7.16
	360		14.0	7.16
	408		15.3	6.76
	380		14.15	6.88
	356		13.4	6.67
	316		12.2	6.58
D	286		11.2	6.67
O	258		10.0	6.15
W	222		8.85	13.43
N	159		7.0	13.55
	105		4.90	14.19
C	72		3.65	14.79
U	40		3.40	15.73
RVE	33		1.90	16.21

- continued

TRIAL II - continued

50%	RPM	of CELL	DEFLECTION	DIELECTRIC CONSTANT
R	0		--	17.02
E	1		--	16.95
C	4		--	17.41
O	17		--	19.30
VERY	20		--	19.69
	69		2.65	7.84
UP	252		10.0	8.59
C	406		15.2	6.12
U	473		17.0	6.06
R	493		17.2	6.18
V	570		19.1	6.12
E	616		19.75	6.12
	686		20.0	5.43
	720		20.15	5.17
	758		20.25	5.16
	700		18.85	5.19
	683		18.0	5.16
	656		17.25	5.16
	613		16.50	5.16
	570		15.0	5.39
	516		14.0	5.86
	490		13.5	5.42
	458		13.	5.46
	423		12.4	5.45
	376		11.1	5.59
	333		10.0	5.97
	278		8.8	6.17
	226		7.65	13.26
	212		7.2	13.14
	150		5.2	13.48
	89		3.75	13.90
	54		2.50	14.45
	41		2.10	14.68
	0		0	15.76
	1		0	15.63
	3		0	15.69

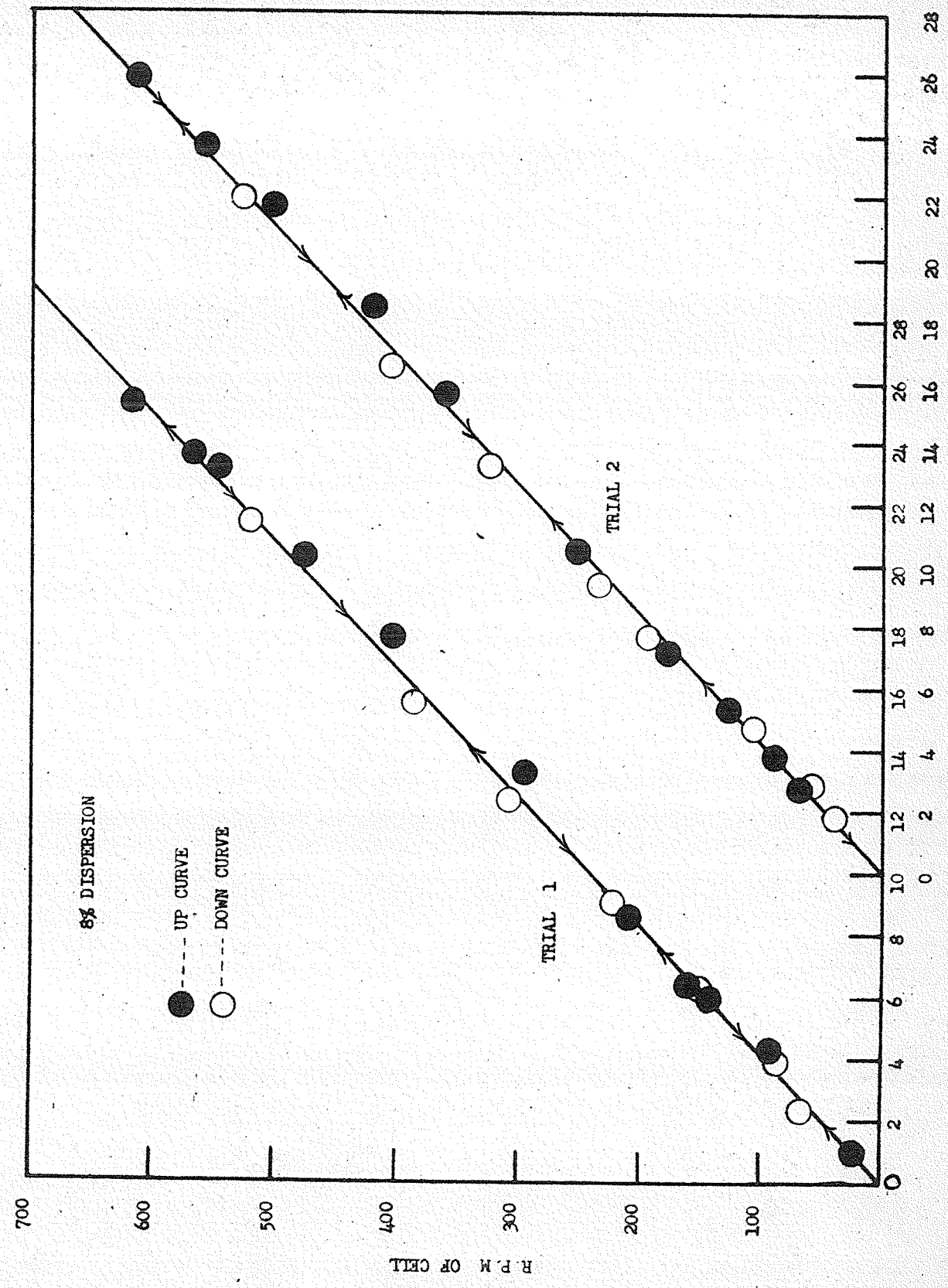
8% DISPERSION
UP CURVE
DOWN CURVE
TRIAL 1
TRIAL 2
R.P.M OF CELL
(DEFLECTION)
700
600
500
400
300
200
100
0
2
4
6
8
10
12
14
16
18
20
22
24
26
28

- FIGURE 12 -

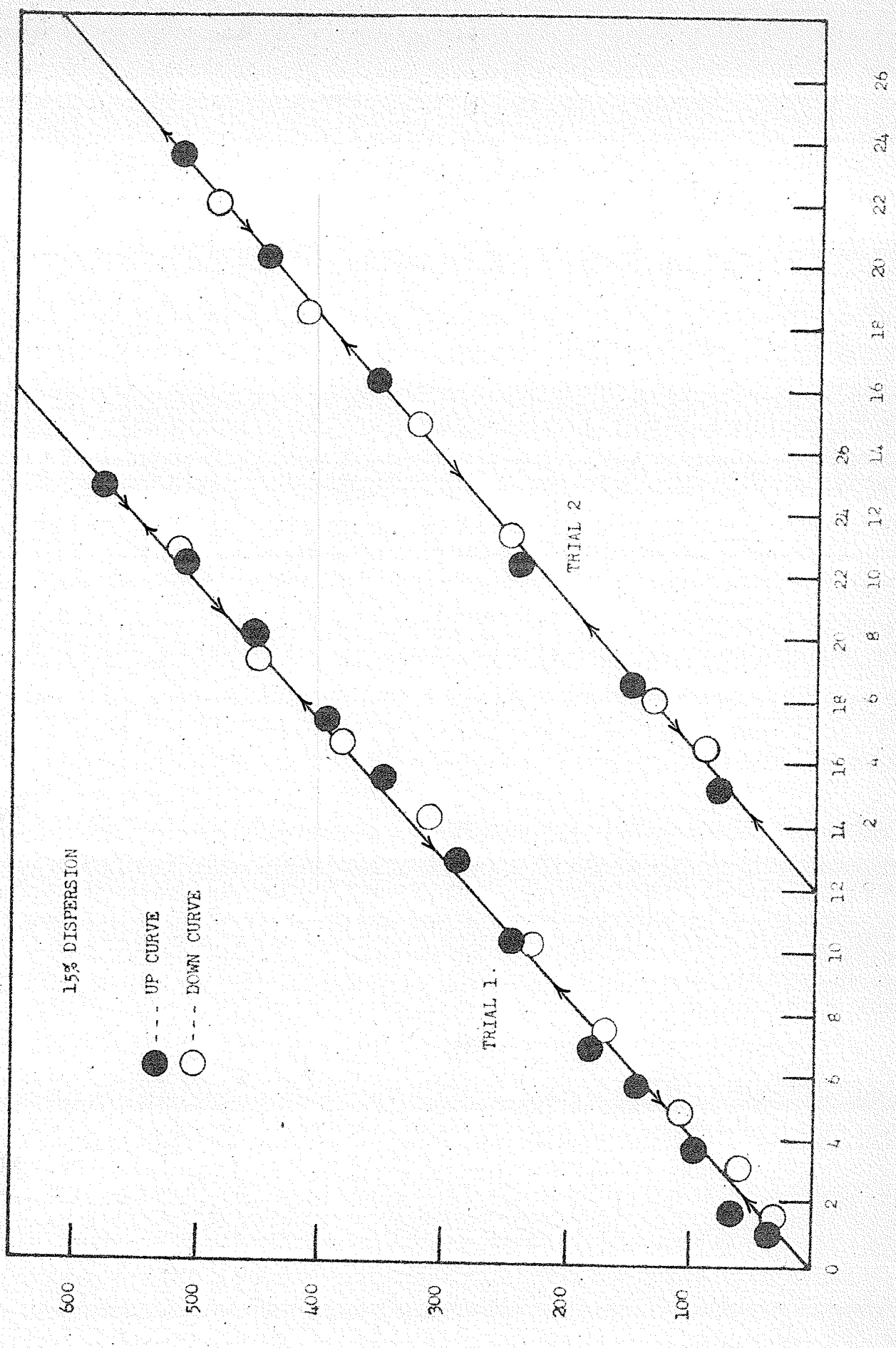
15% DISPERSION
- - - UP CURVE
- - - DOWN CURVE
TRIAL 1.
TRIAL 2
R.P.M OF CELL
(DEFLECTION)
600
500
400
300
200
100
0
2
4
6
8
10
12
14
16
18
20
22
24
26

- FIGURE 13 -

30% DISPERSION
UP CURVE
DOWN CURVE
R.P.M. OF CELL
700
650
600
550
500
450
400
350
300
250
200
150
100
50
0
1
2
3
4
5
6
7
8
9
10
11
12
(DEFLECTION)

- FIGURE 14 -

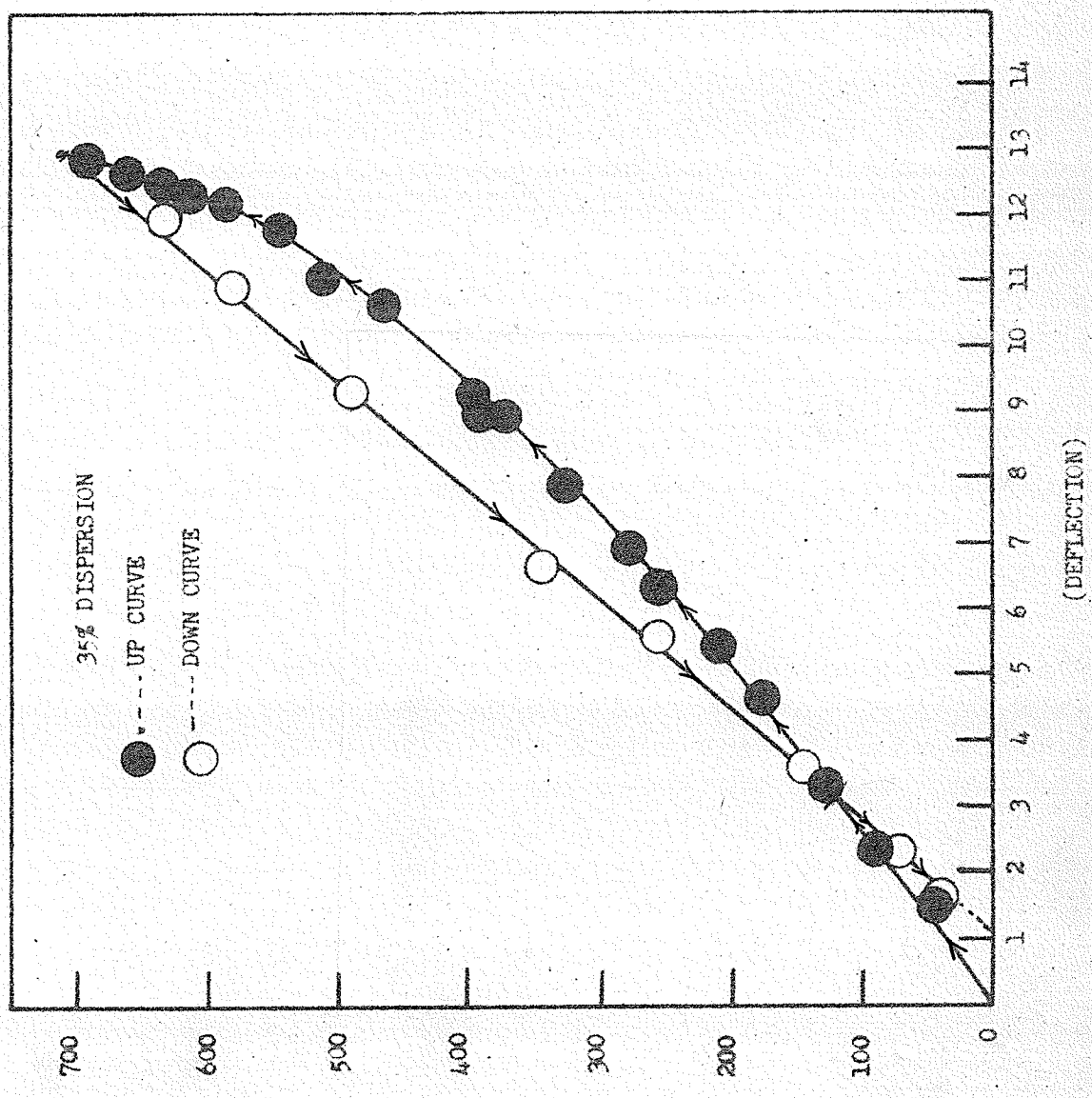
35% DISPERSION
UP CURVE
DOWN CURVE
R.P.M. OF CELL
700
600
500
400
300
200
100
0
1
2
3
4
5
6
7
8
9
10
11
12
13
14
(DEFLECTION)

- FIGURE 15 -

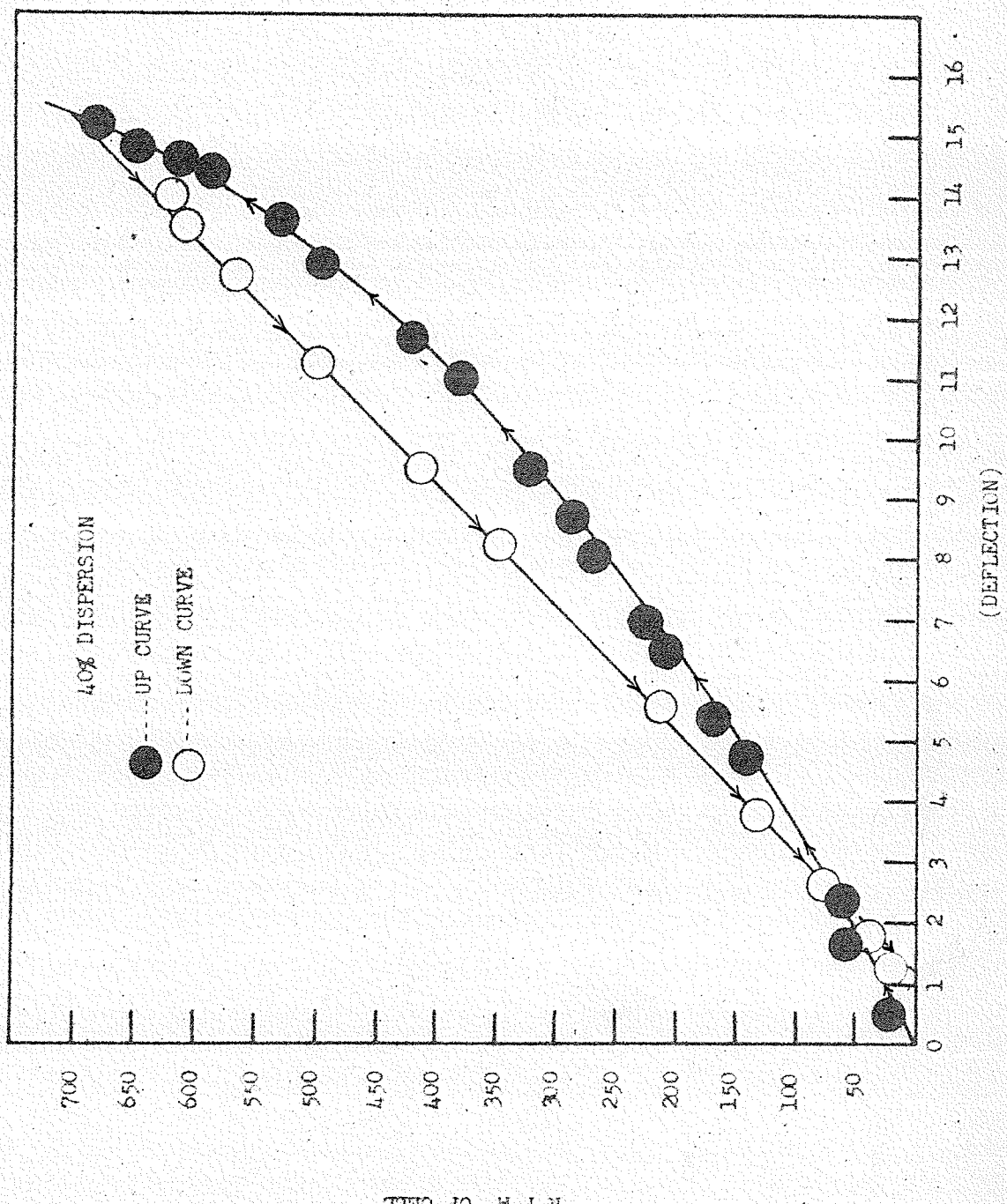
40% DISPERSION
UP CURVE
DOWN CURVE
(DEFLECTION)
R P M OF CHIL
0
1
2
3
4
5
6
7
8
9
10
11
12
13
14
15
16
50
100
150
200
250
300
350
400
450
500
550
600
650
700

- FIGURE 16 -

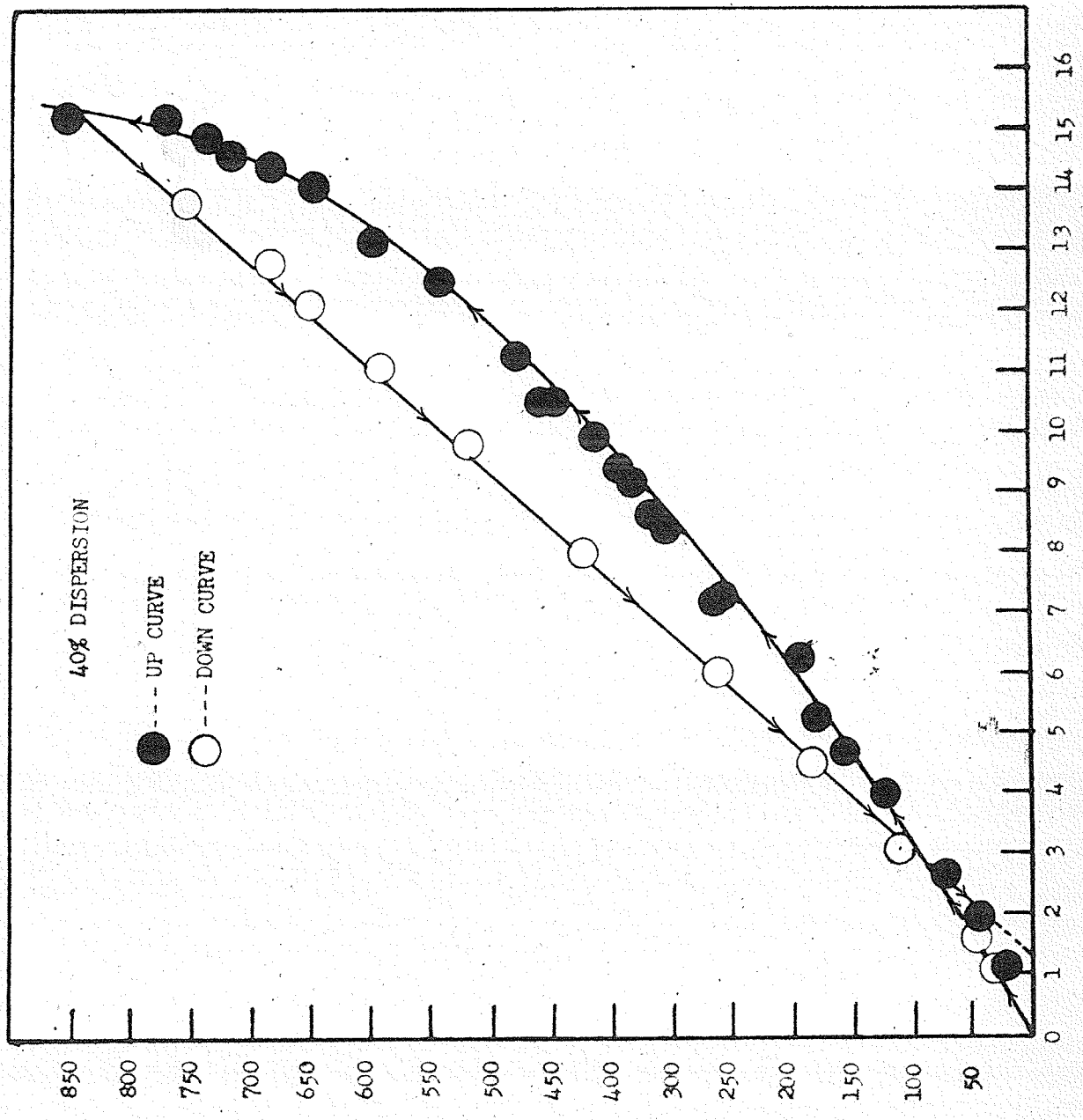
40% DISPERSION
--- UP CURVE
--- DOWN CURVE
R P M OF CELL
(DEFLECTION)
850
800
750
700
650
600
550
500
450
400
300
250
200
150
100
50
0
1
2
3
4
5
6
7
8
9
10
11
12
13
14
15
16

- FIGURE 17 -

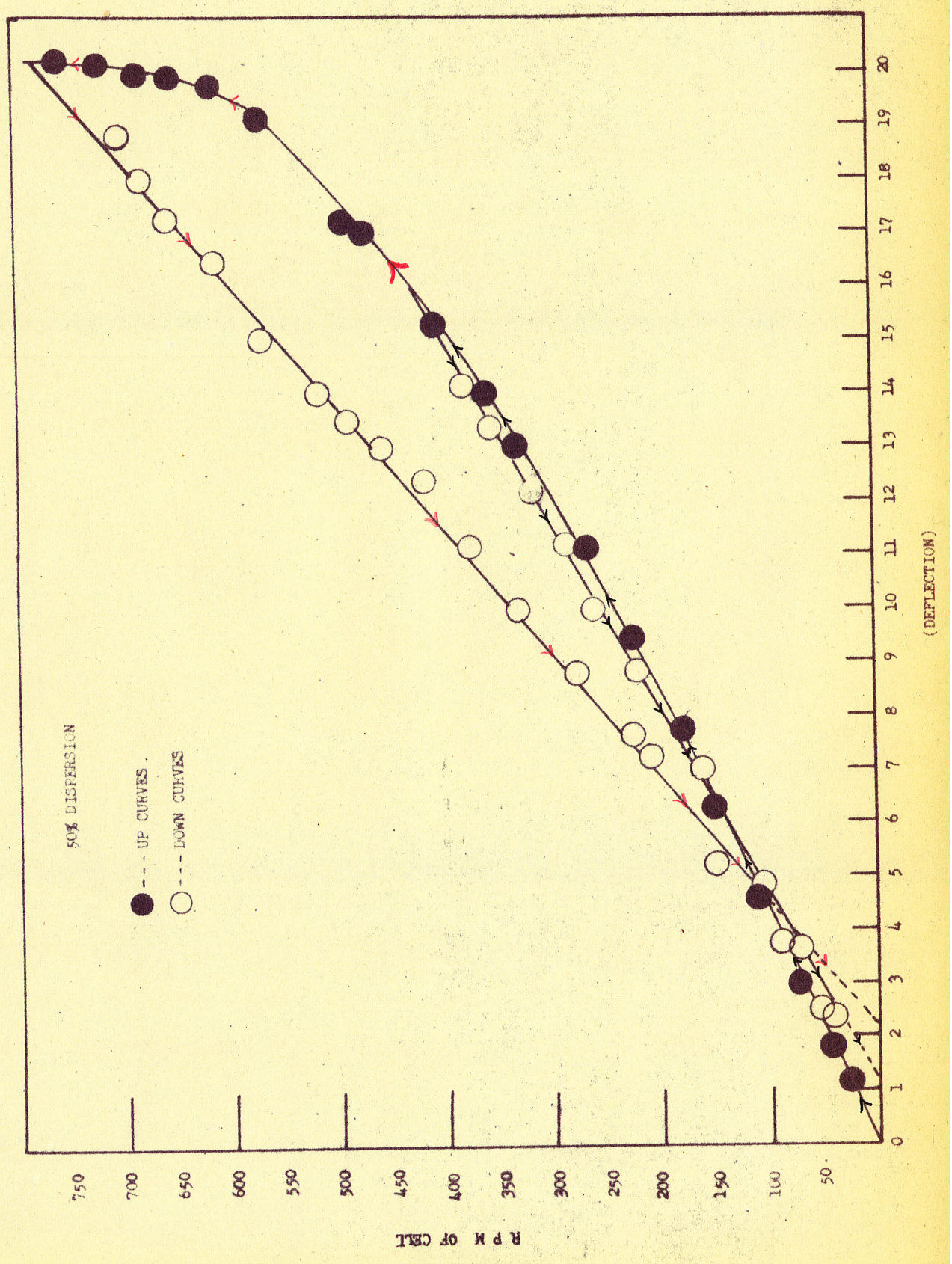
50% DISPERSION
--- UP CURVES.
--- DOWN CURVES
R P M OF CELL
750
700
650
600
550
500
450
400
350
300
250
200
150
100
50
0
1
2
3
4
5
6
7
8
9
10
11
12
13
14
15
16
17
18
19
20
(DEFLECTION)

- FIGURE 18 -

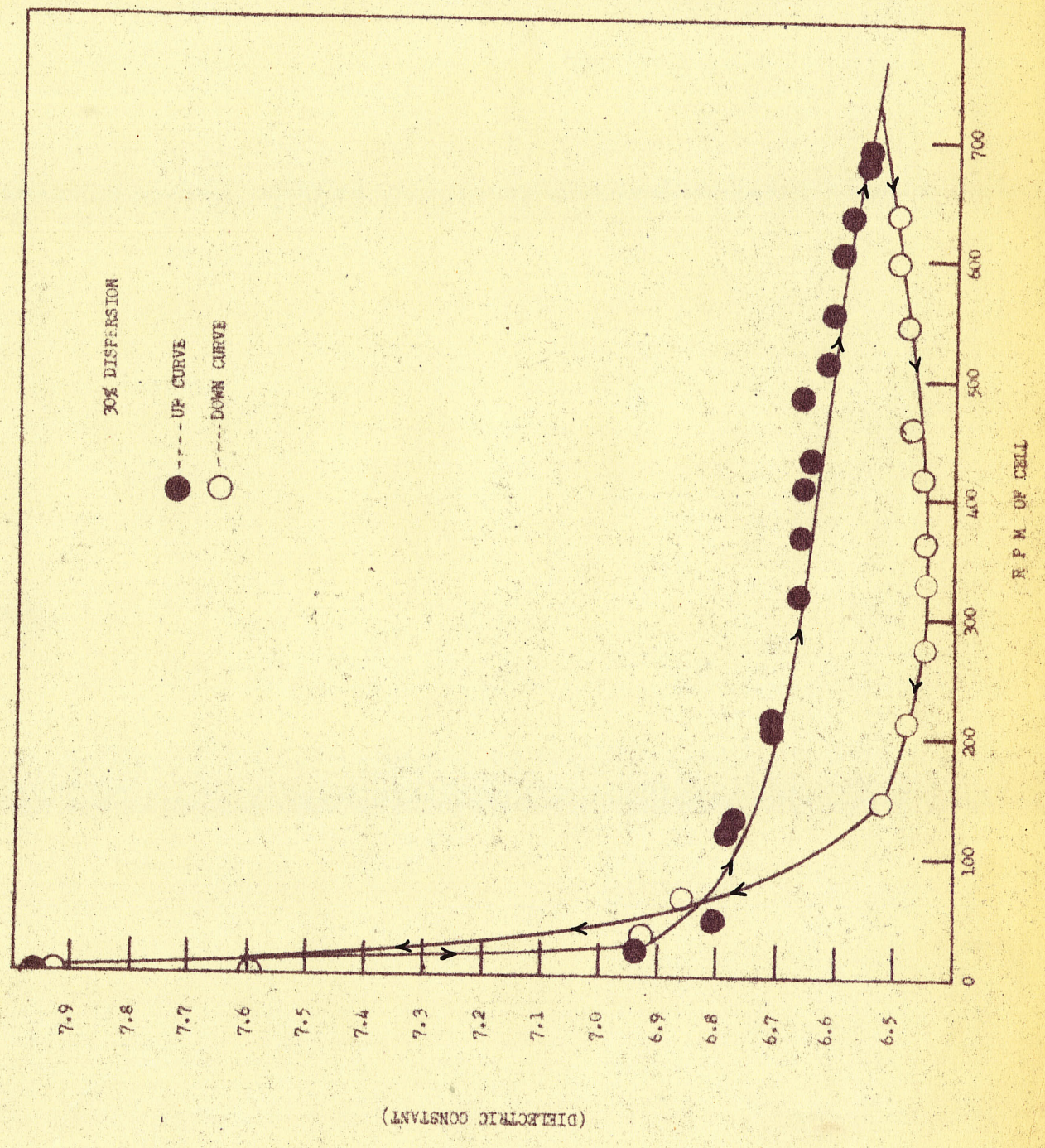
30% DISPERSION
UP CURVE
DOWN CURVE
R P M OF CELL
0
100
200
300
400
500
600
700
7.9
7.8
7.7
7.6
7.5
7.4
7.3
7.2
7.1
7.0
6.9
6.8
6.7
6.6
6.5
(DIELECTRIC CONSTANT)

- FIGURE 19 -

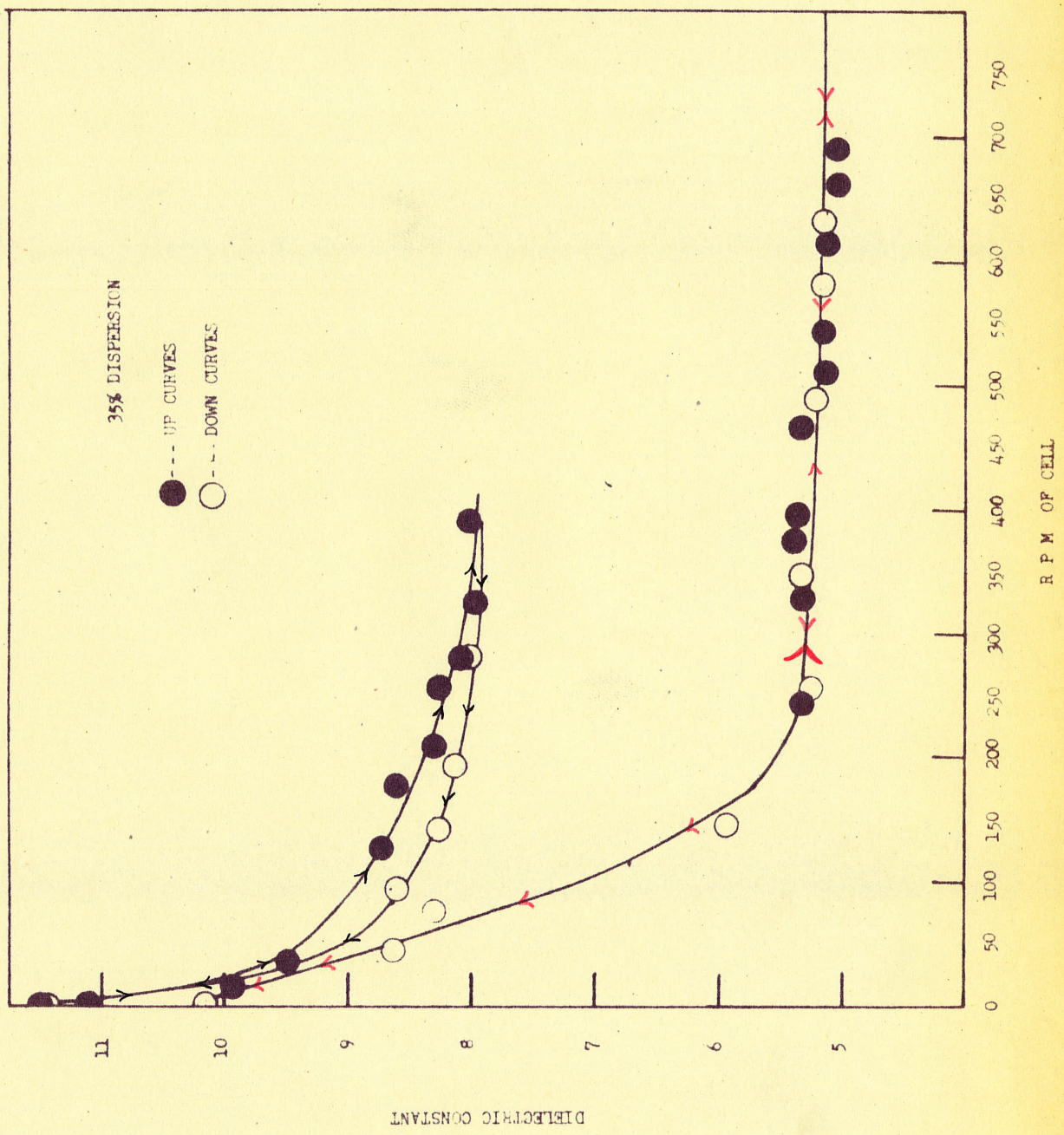
35% DISPERSION
--- UP CURVES
- - - DOWN CURVES
DIELECTRIC CONSTANT
11
10
9
8
7
6
5
0
50
100
150
200
250
300
350
400
450
500
550
600
650
700
750
R P M OF CELL

- FIGURE 20 -

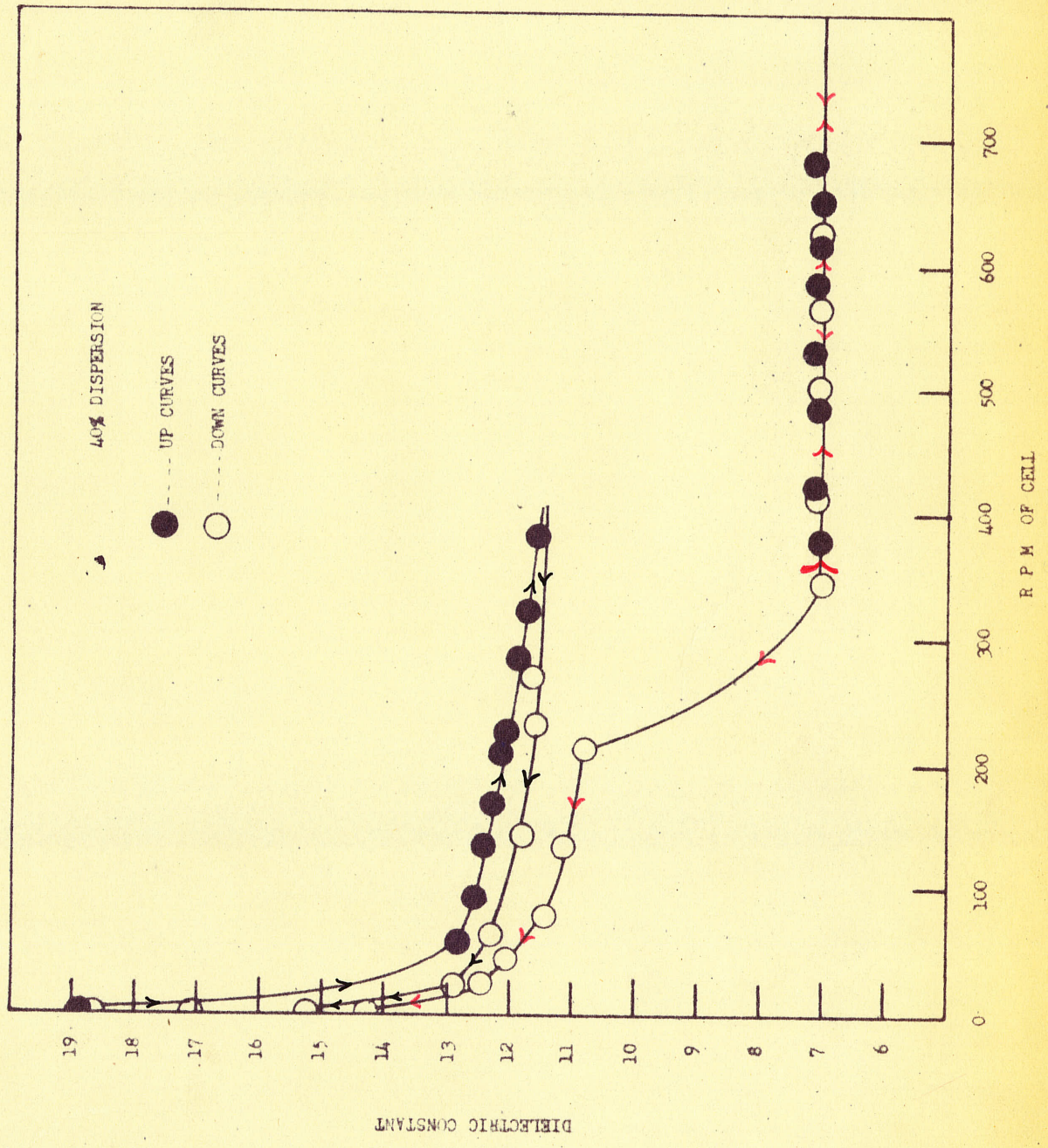
40% DISPERSION
UP CURVES
DOWN CURVES
DIELECTRIC CONSTANT
19
18
17
16
15
14
13
12
11
10
9
8
7
6
0
100
200
300
400
500
600
700
R P M OF CELL

- FIGURE 21 -

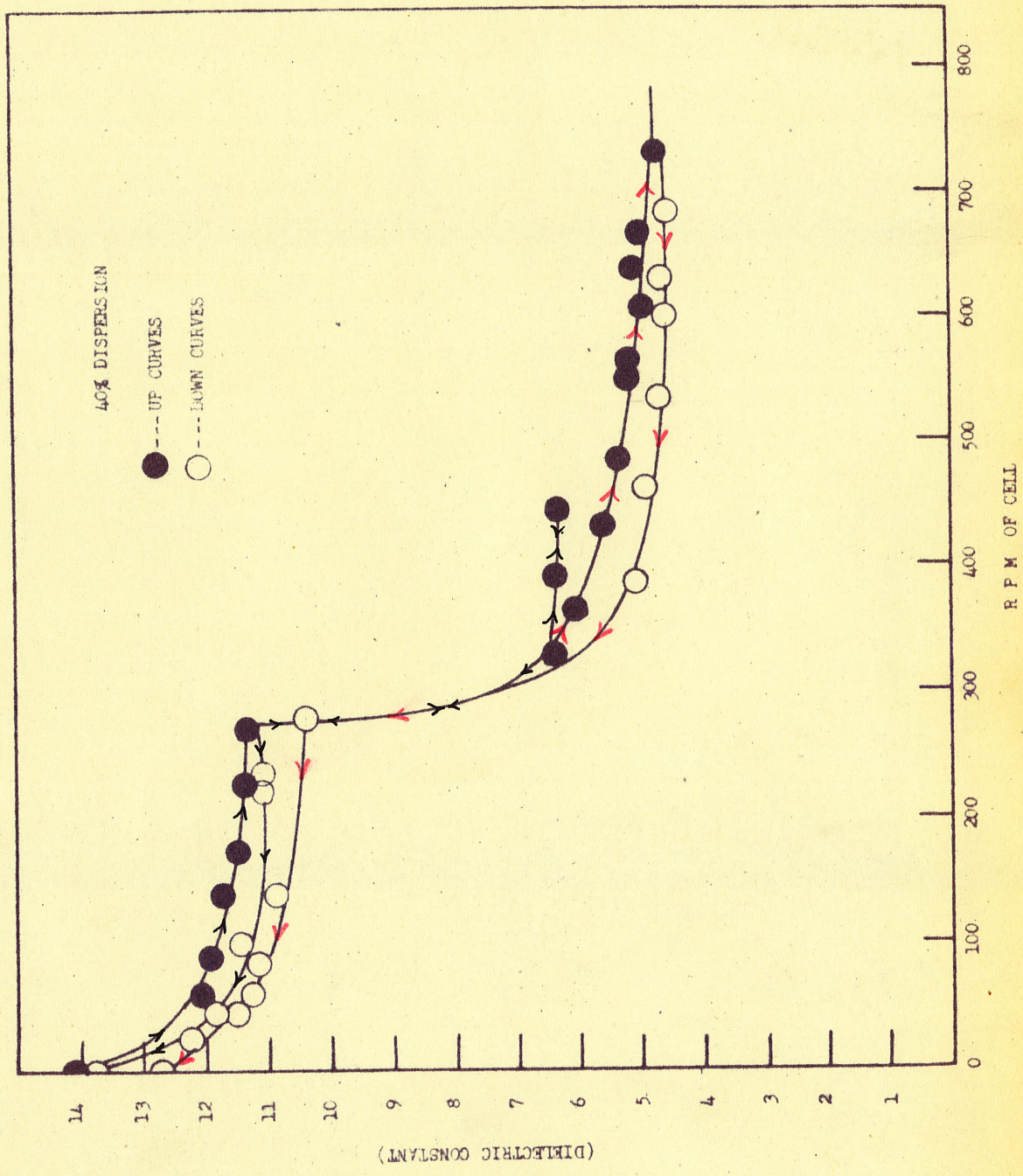
40% DISPERSION
--- UP CURVES
--- DOWN CURVES
(DIELECTRIC CONSTANT)
14
13
12
11
10
9
8
7
6
5
4
3
2
1
0
100
200
300
400
500
600
700
800
R P M OF CELL

- FIGURE 22 -

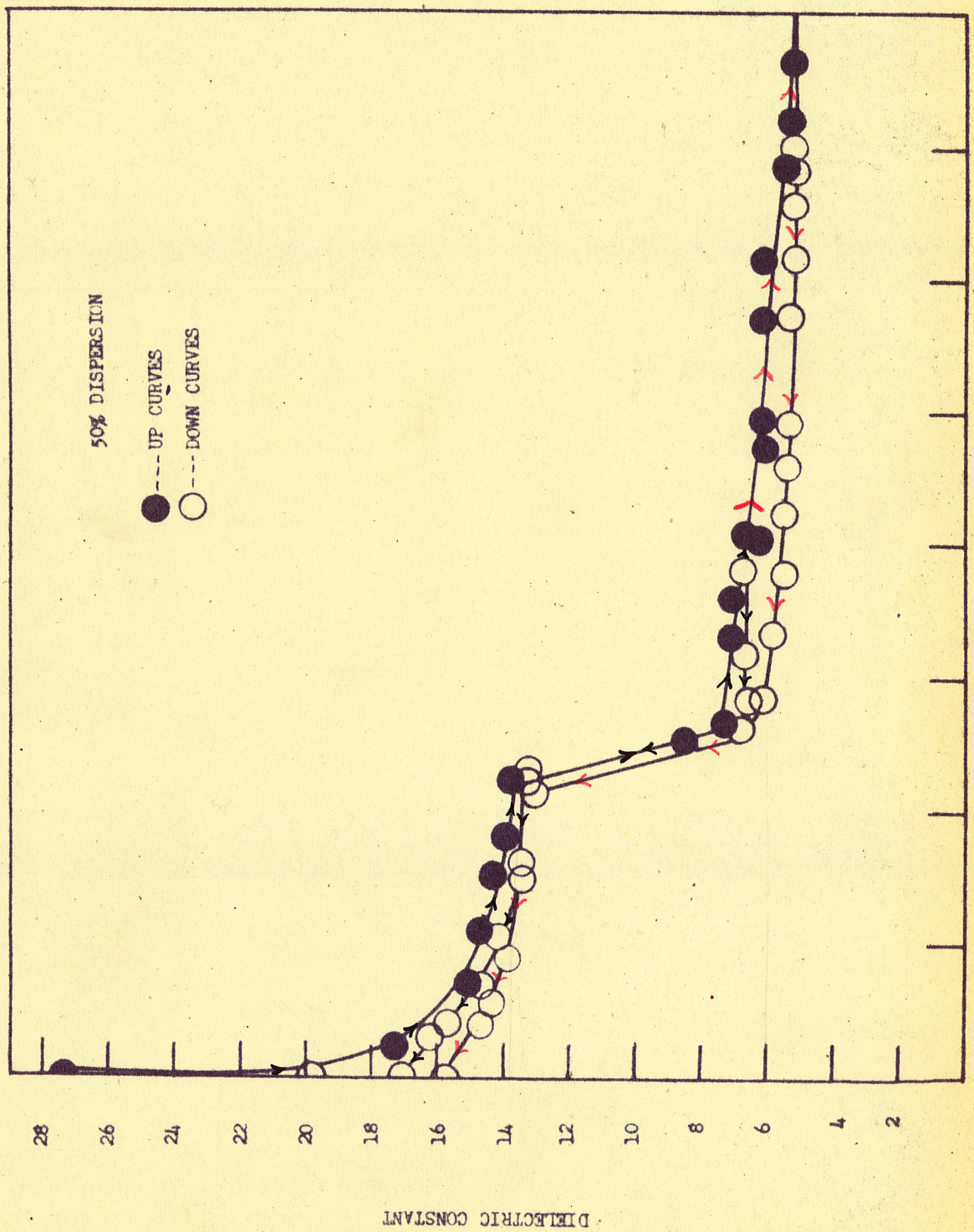
50% DISPERSION
---UP CURVES
---DOWN CURVES
DIELECTRIC CONSTANT
28
26
24
22
20
18
16
14
12
10
8
6
4
2
0
100
200
300
400
500
600
700
R P M OF CELL

- FIGURE 23 -

30% Trial 1

TABLE IV

RPM	DIRECT (C_x) CAPACITANCE READING	DISSIPATION FACTOR D_o	DEFLECTION	$(1+D^2)$	D_o=.026 $(1+DD_o)$	$(1+D^2)$	$1+DD_o$	$\frac{C_x}{(1+D^2)(1+DD_o)}$	C_x corrected for stray	DIELECTRIC= $\frac{C_x}{G_g}$ CONSTANT
0	728.0	.0425	0	1.0016	1.0011	1.0027		726.	510.	7.78
0	734.7	.042	0	1.0016	1.0011	1.0027		732.7	517.	7.89
0	740.0	.0385	0	1.0014	1.0010	1.0024		738	522.	7.97
22	672.2	.0345	.5	1.0012	1.0009	1.0021		670.7	455.	6.94
49	663.3	.0365	1.2	1.0013	1.0009	1.0023		661.7	446.	6.81
123	662.5	.0345	2.6	1.0012	1.0009	1.0021		661.7	445.	6.79
133	661.8	.035	2.9	1.0013	1.0009	1.0023		660.2	444.	6.78
206	657.6	.0352	4.6	1.0013	1.0009	1.0023		656.	440.	6.71
212	657.6	.0355	4.7	1.0013	1.0009	1.0023		656.	440.	6.71
377	656.1	.0375	6.0	1.0014	1.0010	1.0024		648.5	433	6.61
320	654.8	.039	7.4	1.0015	1.0010	1.0025		653	437	6.67
370	654.8	.039	7.9	1.0015	1.0010	1.0025		653	437	6.67
410	654.3	.040	8.9	1.0016	1.0010	1.0026		652.6	437	6.67
433	654.2	.039	9.2	1.0015	1.0010	1.0025		692.5	436	6.65
483	653.6	.040	10.2	1.0016	1.001	1.0026		655.8	439	6.70
516	651.8	.0415	10.6	1.0018	1.0011	1.0029		649.9	434	6.62
553	650.2	.0405	11.4	1.0016	1.0011	1.0026		648.5	433	6.61
603	649.2	.039	12.15	1.0015	1.0010	1.0026		647.5	432	6.59
683	648.5	.038	12.5	1.0013	1.001	1.0023		647	431	6.58
690	646.5	.038	12.6	1.0013	1.001	1.0023		645	429	6.55
640	643.8	.038	12.7	1.0013	1.0011	1.0023		645	429	6.55
613	643.1	.041	11.85	1.0016	1.0012	1.0026		642	426	6.50
600	644.3	.046	11.5	1.0020	1.0012	1.0032		641	425	6.49
543	643.0	.0465	11.15	1.0021	1.0010	1.0032		642	426	6.50
463	642.1	.0395	9.9	1.0016	1.0011	1.0026		641	425	6.49
420	641.1	.0415	8.05	1.0018	1.0010	1.0024		640	424	6.47
366	641.3	.0395	8.1	1.0016	1.0010	1.0026		639.4	423	6.46
333	641.1	.0345	7.1	1.0016	1.0010	1.0026		639.6	424	6.47
275	641.9	.039	6.55	1.0015	1.0010	1.0025		639.5	424	6.47
213	642.3	.0385	5.60	1.0014	1.0010	1.0024		640	424	6.47
160	644.1	.037	4.55	1.0013	1.0010	1.0023		640.7	425	6.49
152	643.0	.037	3.40	1.0013	1.0010	1.0023		642.6	427	6.52
63	668.5	.0368	3.50	1.0012	1.0015	1.0021		641.6	427	6.52
35	673.4	.056	2.0	1.0028	1.0016	1.0043		665.6	450	6.87
0	717.2	.062	1.3	1.0038	1.0014	1.0054		669.7	454	6.93
2.5	730.8	.052	0	1.0027	1.0016	1.0041		714.2	498	7.60
M		.0618	0	1.0038		1.0054		726.8	511	7.80
1			0							
N										
S.										

TABLE V

CONCENTRATION (Vol %)	DIELECTRIC CONSTANT (Rest Value)	DIELECTRIC CONSTANT with shear (taken from graph of ϵ vs. RPM		Δ DIELECTRIC CONSTANT	
		STEP I	STEP II		
3	2.60 2.63	2.59 2.52		.01 .11	
8	3.11 3.05	3.01 3.01	2.48 2.45	.66	
15	4.03 4.15	3.73 3.70		.43	
20	5.78 4.88	4.25 4.65		.23	
25	5.68 5.60	5.2 5.2		.48 .74	
30	7.96 7.93	6.41 6.45		1.48	
35	11.38 10.28	8.0 7.8	5.1 7.4	3.28 2.86	6.28 --
40	14.15 18.76 18.9	11.3 11.2 11.6	4.90 10.45 7.1	2.85 6.56 7.31	9.25 8.31 11.8
50	27.35 33.30	13.6 16.4	5.4 15.0 6.6	13.75 16.9	21.95 26.7

TABLE VI

Conc. Vol %	rest	(Av Calc) $\rho_{rest} = \rho_{oil}(1+3A_V/V)$	$\rho_{rest} = \frac{\rho_{oil}}{(1-V)^3}$
3%	2.63	.943	2.52
8%	3.11	.863	2.94
15%	4.15	1.05	3.76
20%	4.88	1.10	4.50
25%	6.08 5.94 5.68	1.61 1.29 1.24	5.49
30%	7.96 7.93	1.61 1.60	6.72
35%	10.26 11.38	1.94 2.21	8.39
40%	18.9 18.76 14.15	3.55 3.53 2.53	10.65
50%	33.3 27.35	5.3 4.32	18.4

TABLE VII

	TIME Mins	DIELECTRIC CONSTANT	Av Calc.using 1.7
15%	0	3.90	.908
	1	3.91	.914
	3	3.92	.935
	7	3.96	.946
	15	4.00	.970
	23	4.03	.982
30%	0	7.60	1.50
	2.5	7.80	1.56
	3.	7.80	1.56
	4.	7.83	1.57
	5.	7.83	1.57
	6.	7.84	1.58
	7.	7.91	1.59
	87	7.91	1.59
	114	7.94	1.60
35%	0	9.37	1.71
	1	9.54	1.77
	2	9.64	1.79
	3	9.71	1.81
	4	9.78	1.83
	5	9.84	1.84
	6	9.92	1.86
	10	10.18	1.92
	11	10.22	1.94
	0	8.94	1.62
	1	9.13	1.67
	2	9.16	1.68
	4	9.22	1.69
	5	9.28	1.70
	7	9.48	1.75
	10	9.75	1.82
	14	10.19	1.93

	TIME	DIELECTRIC CONSTANT	Av Calc.using 1.7
40%	0	14.3	2.56
	1	14.7	2.65
	2	15.3	2.77
	3	15.4	2.79
	4	15.5	2.82
	5	15.7	2.86
	6	15.9	2.91
	13	17.1	3.15
	15	17.3	3.20
	17	17.6	3.27
	18	17.7	3.29
	22	18.1	3.38
	25	18.4	3.43
	30	18.7	3.50
50%	0	21.0	3.03
	1	22.0	3.20
	2	22.6	3.81
	3	23.7	3.98
	5	23.7	3.99
	6	23.9	4.03

TABLE VIII

CONCENTRATION %	VISCOSITY η (POISE)	COUPLE USED	$\eta/\eta_0 = \eta_r$	$\eta r^{-1} = \eta_{sp}$	ϕ	η_{sp}/ϕ	INTERCEPT (TORQUE) FROM GRAPHS	INTERCEPT X K = TORQUE	TORQUE X C $= f_c$ YIELD VALUE. dynes/sq cm.	COMMENT ON FLOW TYPE
3	1.11 1.099	1 1	1.025 1.015	.025 .015	.03	.835 .502	0 0	--	--	Newtonian
8	1.55 1.47 1.42	1 1 1	1.44 1.36 1.315	.44 .36 .315	.08	5.5 4.5 3.94	0 0 0	--	--	Newtonian
15	1.435 1.54	1 1	1.329 1.423	.329 .423	.15	2.19 2.83	0 0	--	--	Newtonian
20	1.82 1.985	1 1	1.69 1.835	.69 .838	.20	3.45 4.17	.4 .4	5,125	17.12	non Newtonian
25	2.07 2.11	3 1	1.915 1.955	.915 .955	.25	3.66 3.82	1.0	12,800	41.8	non Newtonian
30	2.40 2.478 2.27	3 3 3	2.22 2.29 2.105	1.22 1.29 1.105	.30	4.07 4.31 3.70	.9 .9 1.1	38,100 38,100 47,900	123.5 123.5 155.1	non Newtonian
35	2.69 2.71 2.42	3 3 3	2.49 2.51 2.24	1.49 1.51 1.24	.35	4.27 4.32 3.55	1.5 1.4	65,250 60,990	211.8 197.5	non Newtonian
40	3.42 2.69 3.12 2.65	3 3 3 3	3.17 2.49 2.88 2.45	2.17 1.49 1.88 1.45	.40	5.43 3.74 4.70 3.63	1.45 1.5 2.0	63,000 65,250 87,000	204 211.8 282.5	non Newtonian
50	3.20 3.13 4.55 4.18	3 3 3 3	2.96 2.90 4.22 3.87	1.96 1.90 3.22 2.87	.50	3.93 3.81 6.44 5.74	(1) 2.2 (2) $2.5=T_2$ $1.3=T_1$	95,750 108,500 56,500	311.0 353.0 183.0	non Newtonian
Oil	1.08	1					0			Newtonian

TABLE IX

TRIAL	CONCENTRATION (Volume %)	DEFLECTION (Read from Graph)		MASS (gms) (Read from Graph)		MASS/RPM		VISCOSITY (η) (POISE)	
		at 200 rpm	at 400 rpm	at 200 rpm	at 400 rpm	at 200 rpm	at 400 rpm	at 200 rpm	at 400 rpm
	0	Couple No.1	14.2 at 450 rpm	--	85.5	--	.190	---	1.08
	0	Couple No.3	3.8 at 433 rpm	--	82.5	--	.191	---	1.08
2	3	6.35	15.95 at 500 rpm	38.7	96.5	.193	.194	1.10	1.10
1	8	8.40	16.75	51.0	101.5	.255	.254	1.45	1.45
2	15	8.90	17.9	54.0	108.0	.270	.270	1.54	1.54
1	20	10.85	21.7	65.7	130.5	.328	.326	1.86	1.85
3	25	12.25	24.5	74.0	147.5	.370	.369	2.10	2.09
4	25	13.1	26.0	79.5	--	.397	--	2.25	--

TRIAL	CONCENTRATION	at 200 rpm		at 600 rpm		at 200 rpm		at 600 rpm		at 200 rpm		at 600 rpm		at 200 rpm		at 600 rpm	
		down Curve	up Curve	down Curve	up Curve	down Curve	up Curve	down Curve	up Curve	down Curve	up Curve	down Curve	up Curve	down Curve	up Curve	down Curve	up Curve
1	30	4.25	4.5	--	--	92	98	--	--	.460	.490	--	--	2.62	2.78	--	--
2	30	--	--	11.25	11.6	--	--	231	238	--	--	.385	.397	--	--	2.19	2.26
1	35	4.65	5.30	10.9	11.95	102	113	225	245	.510	.565	.373	.409	2.90	3.21	2.13	2.32
2	35	4.60	5.50	11.35	12.30	100	117	233	253	.500	.585	.388	.422	2.84	3.32	2.20	2.39
1	40	5.35	6.75	13.5	14.4	114	140	276	295	.570	.70	.460	.492	3.24	3.98	2.62	2.80
1	50	--	--	15.1	16.5	--	--	305	337	--	--	.507	.562	--	--	2.88	3.19
2	50	7.0	8.5	16.2	19.3	147	177	330	393	.735	.885	.550	.655	4.17	5.03	3.12	3.72

TABLE IX - (Continued)

TRIAL	ø	VISCOSITY (η)(POISE)		$\eta / \eta_0 = \eta_r$		$\eta_r - 1 = \eta_{sp}$		$\eta_{sp} / ø$	
		at 200 rpm	at 400 rpm	at 200 rpm	at 400 rpm	at 200 rpm	at 400 rpm	at 200 rpm	at 400 rpm
--	0	--	1.08	--	1.00	--	0	--	0
--	0	--	1.08	--	1.00	--	0	--	0
2	.03	1.10	1.10	1.02	1.02	.02	.02	.67	.67
1	.08	1.45	1.45	1.34	1.34	.34	.34	4.25 ?	4.25?
2	.15	1.54	1.54	1.42	1.42	.42	.42	2.79	2.79
1	.20	1.86	1.85	1.72	1.71	.72	.71	3.60	3.55
3	.25	2.10	2.09	1.95	1.94	.95	.94	3.78	3.74
4	.25	2.25	--	2.08	--	1.08	--	4.32	--

TRIAL	CONCENTRATION	at 200 rpm		at 600 rpm		at 200 rpm		at 600 rpm		at 200 rpm		at 600 rpm		at 200 rpm		at 600 rpm	
		down curve	up curve	down curve	up curve	down curve	up curve	down Curve	up Curve					down curve	up curve	down curve	up curve
1	.30	2.62	2.78	--	--	2.42	2.58	--	--	1.42	1.58	--	--	4.74	5.25	--	--
2	.30	--	--	2.19	2.26	--	--	2.03	2.09	--	--	1.03	1.09	--	--	3.44	3.65
1	.35	2.90	3.21	2.13	2.32	2.69	2.97	--	2.15	1.69	1.97	--	1.15	4.82	5.62	--	3.29
2	.35	2.84	3.32	2.20	2.39	--	3.08	2.04	--	--	2.08	1.04	--	--	5.95	2.97	--
1	.40	3.24	3.98	2.62	2.80	3.00	3.68	2.42	2.59	2.00	2.68	1.42	1.59	5.00	6.70	3.55	3.98
1	.50	--	--	2.88	3.19	--	--	2.67	2.96	--	--	1.67	1.96	--	--	3.34	3.91
2	.50	4.17	5.03	3.12	3.72	3.86	4.66	2.89	3.44	2.86	3.66	1.89	2.44	5.72	7.32	3.78	4.88

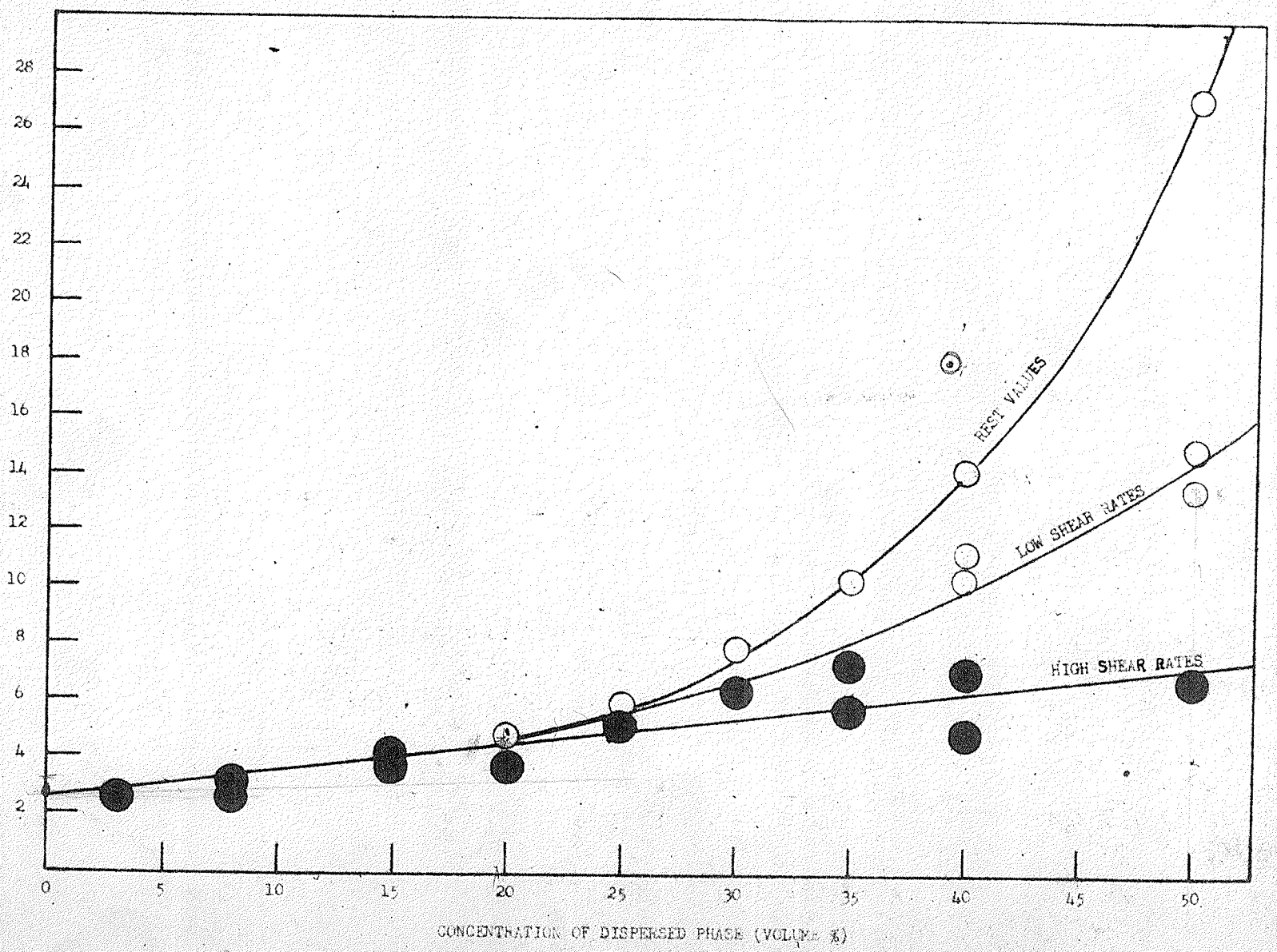
DIELECTRIC CONSTANT
28
26
24
22
20
18
16
14
12
10
8
6
4
2
0
5
10
15
20
25
30
35
40
45
50
CONCENTRATION OF DISPERSED PHASE (VOLUME %)
REST VALUES
LOW SHEAR RATES
HIGH SHEAR RATES

- FIGURE 24 -

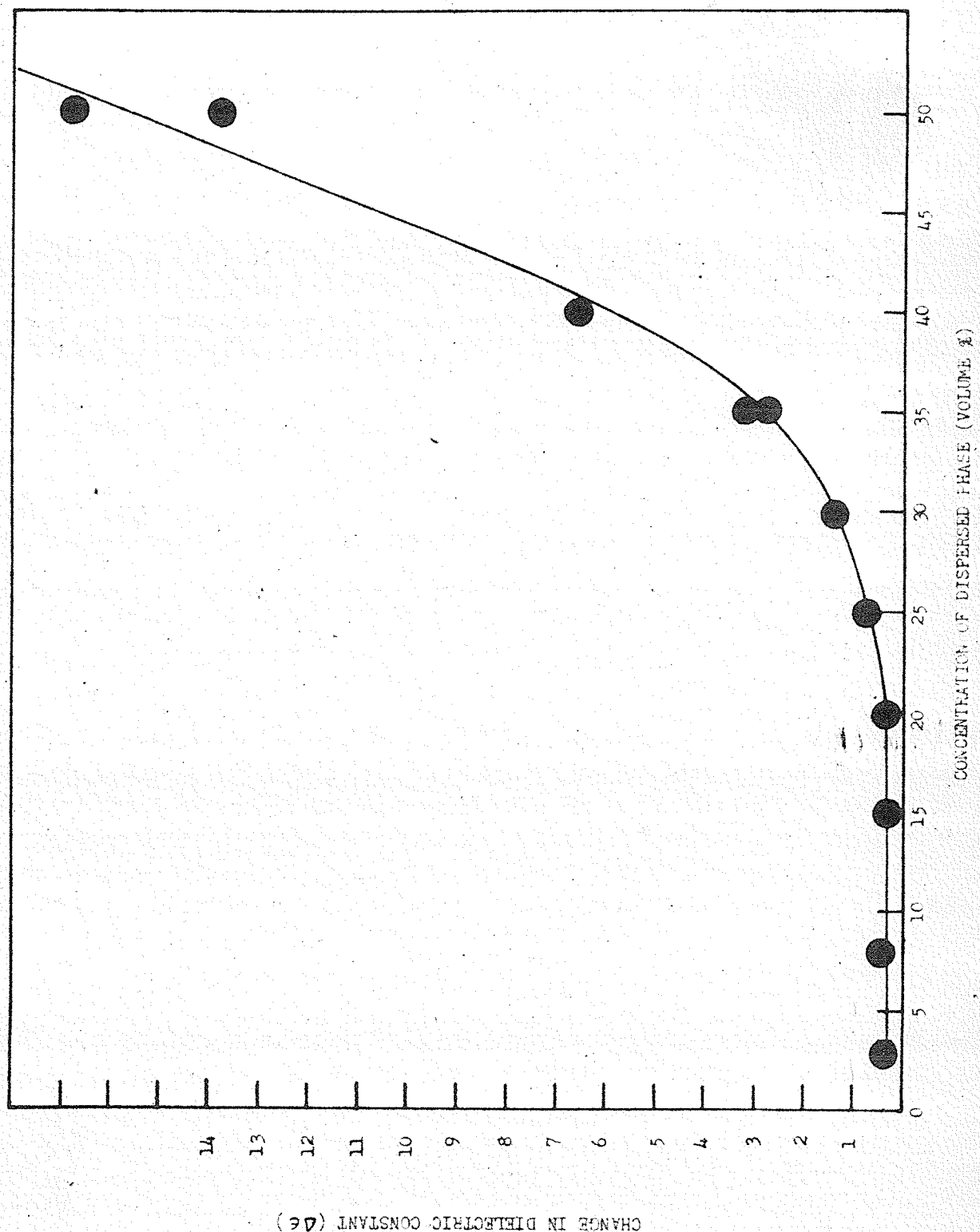
CHANGE IN DIELECTRIC CONSTANT (Δε)
0
1
2
3
4
5
6
7
8
9
10
11
12
13
14
0
5
10
15
20
25
30
35
40
45
50
CONCENTRATION OF DISPERSED PHASE (VOLUME %)

- FIGURE 25 -

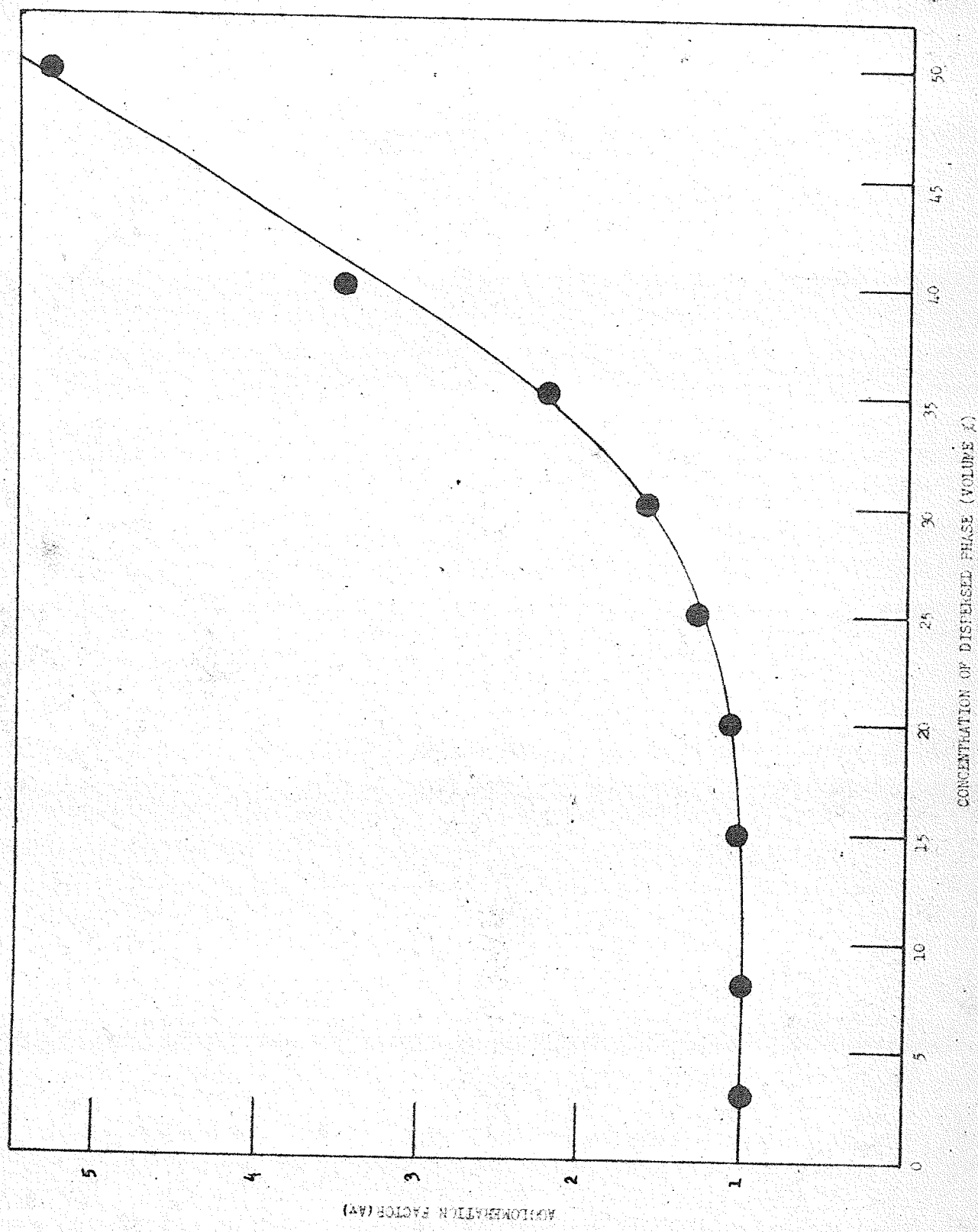
ADSIDEMATION FACTOR (AV)
1
2
3
4
5
0
5
10
15
20
25
30
35
40
45
50
CONCENTRATION OF DISPERSED PHASE (VOLUME %)

- FIGURE 26 -

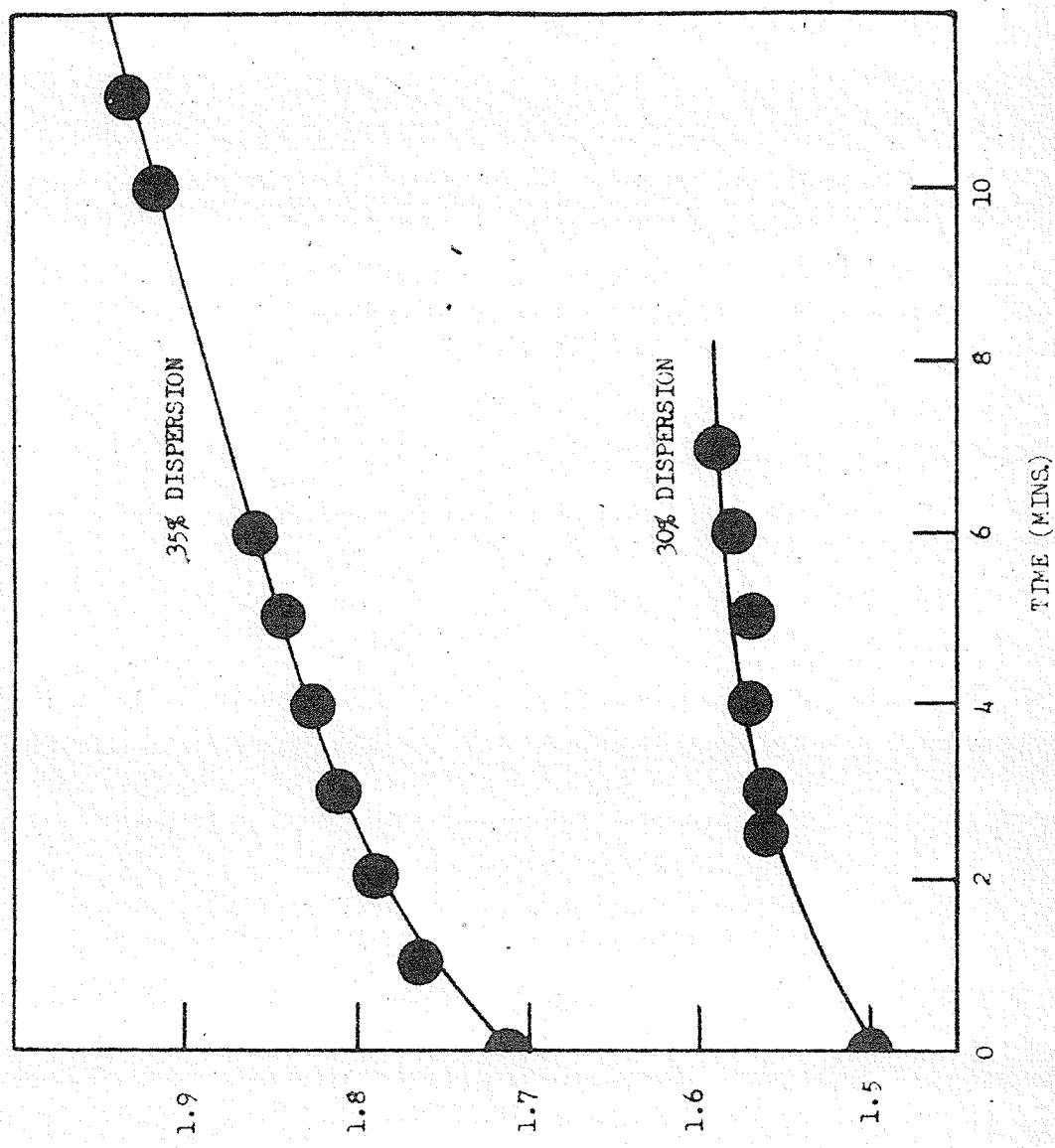
35% DISPERSION
30% DISPERSION
1.9
1.8
1.7
1.6
1.5
0
2
4
6
8
10
TIME (MINS.)
AGGLOMERATION FACTOR (Av)

- FIGURE 27 -

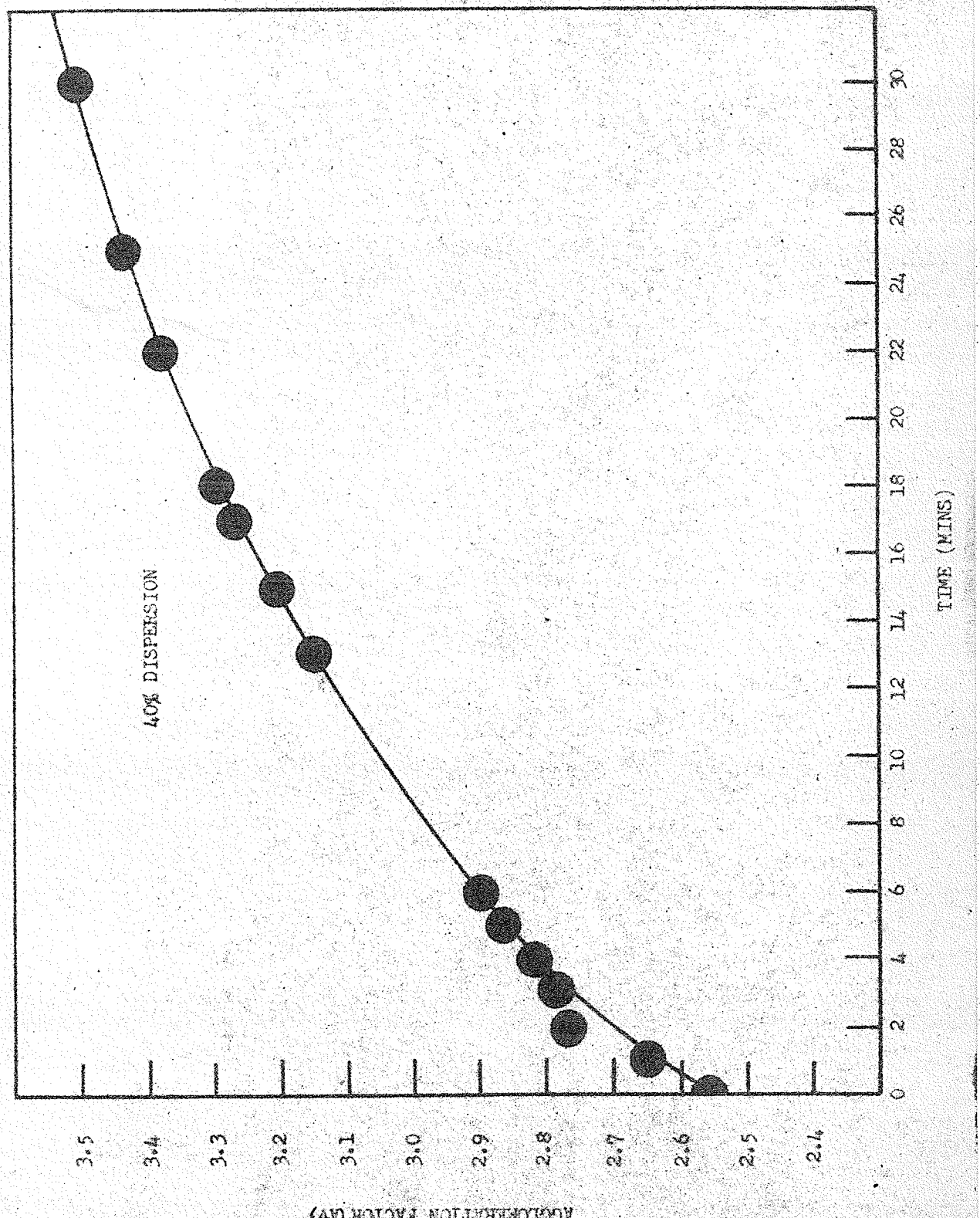
40% DISPERSION
AGGLOMERATION FACTOR (Av)
TIME (MINS)
3.5
3.4
3.3
3.2
3.1
3.0
2.9
2.8
2.7
2.6
2.5
2.4
0
2
4
6
8
10
12
14
16
18
20
22
24
26
28
30

- FIGURE 28 -

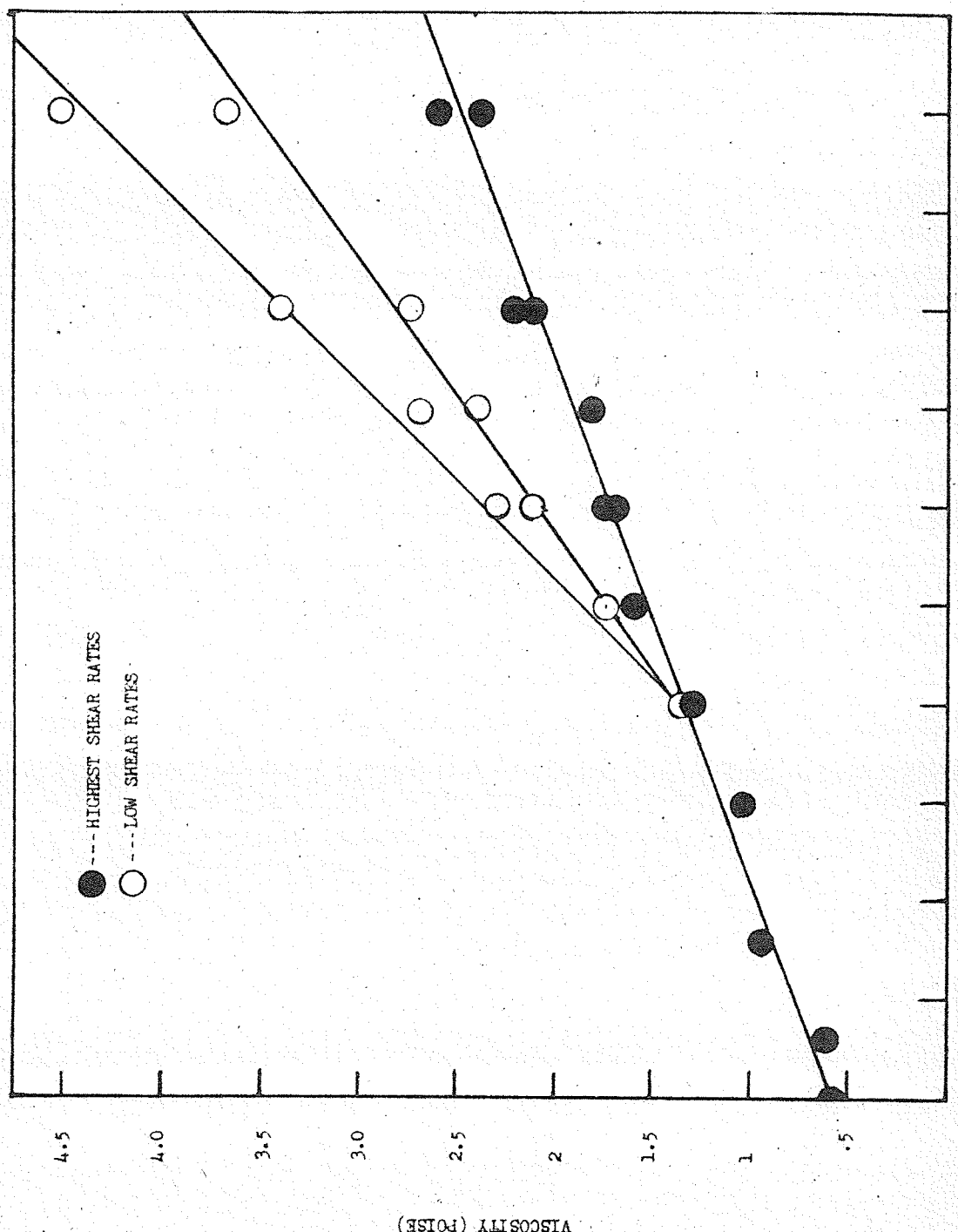
--- HIGHEST SHEAR RATES
--- LOW SHEAR RATES
VISCOSITY (POISE)
4.5
4.0
3.5
3.0
2.5
2
1.5
1
.5
0
5
10
15
20
25
30
35
40
45
50
CONCENTRATION OF DISPERSED PHASE (VOLUME %)

- FIGURE 29 -

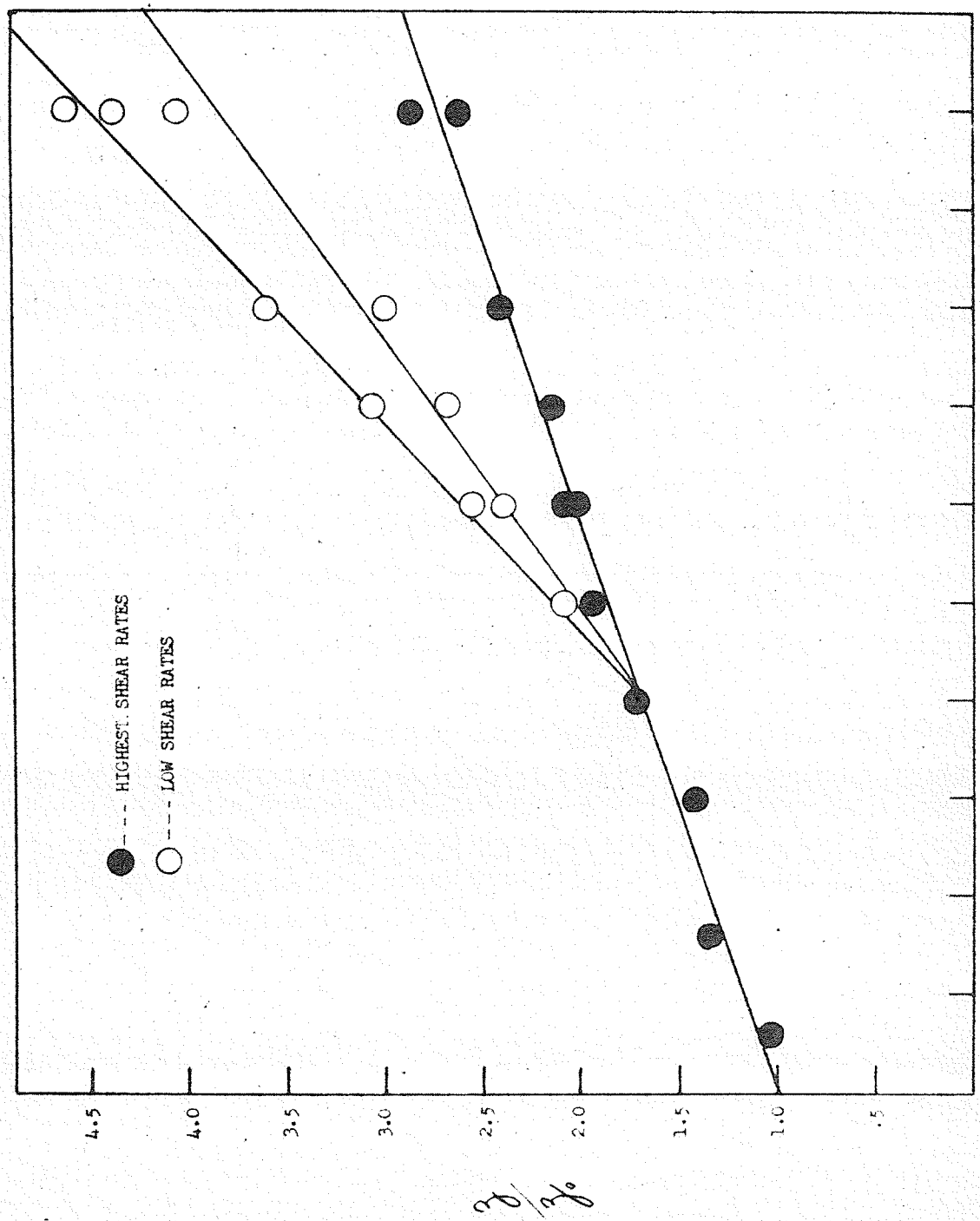
HIGHEST SHEAR RATES
LOW SHEAR RATES
4.5
4.0
3.5
3.0
2.5
2.0
1.5
1.0
.5
5
10
15
20
25
30
35
40
45
50
η/η₀
CONCENTRATION OF DISPERSED PHASE (VOLUME %)

- FIGURE 30 -

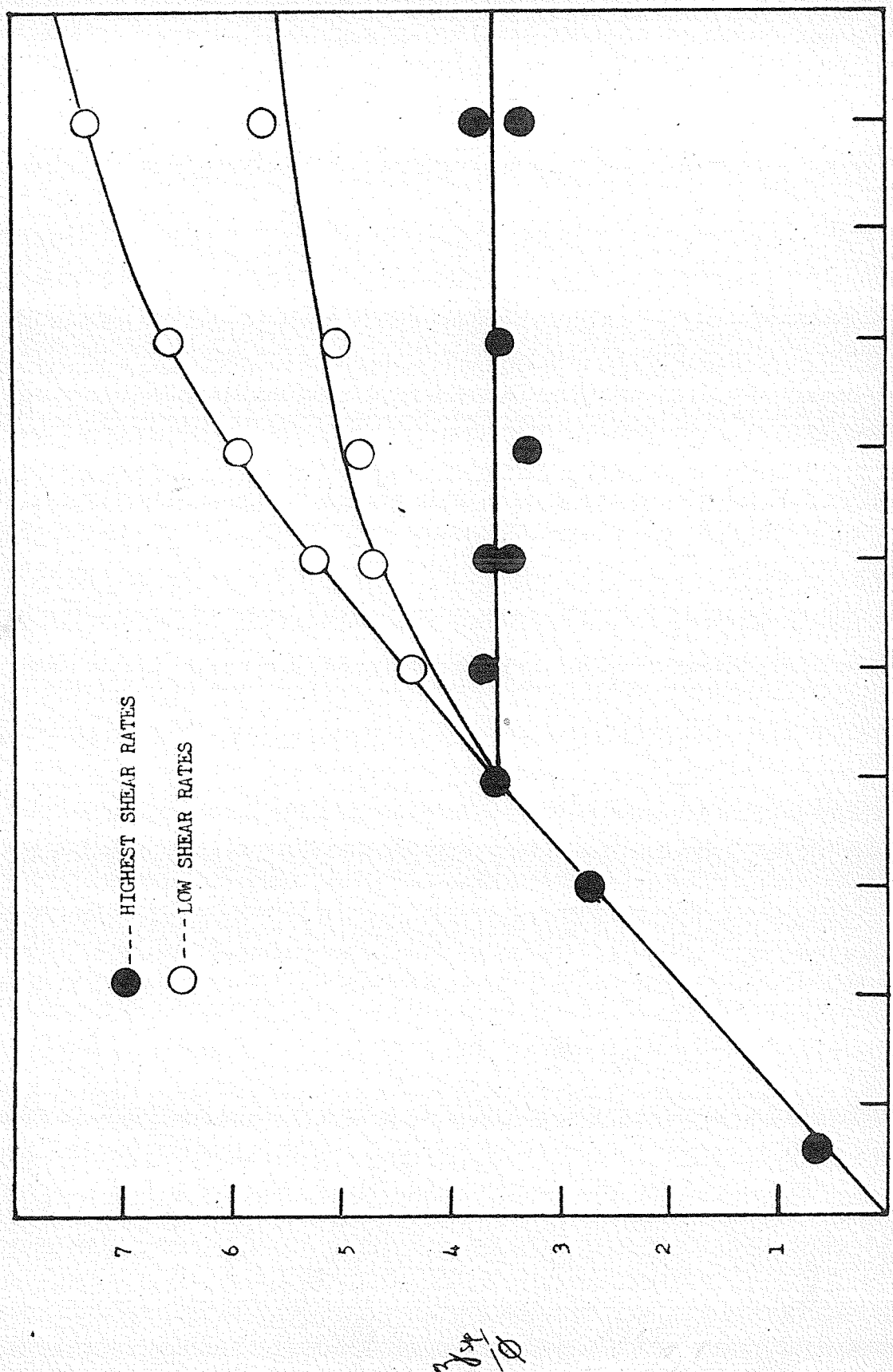
HIGHEST SHEAR RATES
LOW SHEAR RATES
7
6
5
4
3
2
1
0
.05
.10
.15
.20
.25
.30
.35
.40
.45
.50
ϕ
3.5*/ϕ

- FIGURE 31 -

DISCUSSION OF RESULTS

A linear relationship was found to exist between the dielectric constant of the emulsion subjected to high shear rates and the concentration by volume per cent of the dispersed particles when the dielectric constant of the dispersed is much higher than that of the medium (See FIGURE 24). A similar relationship for spherical particles was derived theoretically by Bruggeman. This relationship was characterized by a proportion factor 3. Voet also observed such a linear relationship with various dispersions. However, his datum on emulsions is very incomplete and at the higher concentration his agreement was poor. His proportion factor varied from 3 to higher values, up to 24. Further, he observed that systems having a shape nearest the spherical had the lowest proportion factor and as a result, he introduced a form factor which expressed the deviation from spherical shape. The larger the form factor the more the deviation from spherical shape.

Voet's (1) experiments on dispersions show that the change in dielectric constant is sensitive to the shape of the particles. Since the solid (spherical) particles of zinc could not change shape he attributed the deviation of the form factor from unity to particle agglomeration, that is, flocculation or formation of particle chains. In our experiments on emulsions then the observed changes in the dielectric constant can be attributed to two effects. (1) Change from spherical shape, and (2) particle agglomeration.

Rest values of the various dispersions calculated (see Table VI) with the simplified Bruggeman equation (Equation 2) agreed reasonably well with the experimental values which were obtained under shearing stresses (See Table V). This comparison is justified since the

Bruggeman equation was derived on the theory that the dispersed particles were independent of one another. The theory presented here would have the agglomerated structures broken up under shearing stresses resulting in the particles acting independently. Various shearing forces were necessary to obtain this end indicating different sizes or strength of the formed structures.

In addition to a form factor, experimental evidence points to the existence of an agglomeration factor which takes into account the difference between the dielectric constant of a dispersion when at rest and when subjected to shearing stresses. For dispersions up to 20% by volume of the dispersed phase the agglomeration factor was found to be unity indicating no particle agglomeration (i.e. particle acting independently) and thus resulting in Newtonian type of flow. (This was confirmed by the rheological data) (See FIGURE 12 and 13). FIGURE 26 shows a plot of the agglomeration factor with concentration. This data corresponds with that of FIGURE 25 which shows the change in dielectric constant with concentration. It was observed that within experimental errors there is no change in the dielectric constant at rest and when subjected to high shearing stresses up to a concentration of 20% by volume of the dispersed phase. With higher concentrations the change in dielectric constant rises very rapidly, as does the agglomeration factor. It was not found possible to relate the size of the agglomerate with the agglomeration factor. Voet observed by microscopical observation of dilute suspensions that upon agglomeration, particle chains were formed and it became evident that increased agglomeration necessarily led to an increased length of particle chains and was therefore connected with a more distant deviation from

spherical shape, which in turn caused the increase in the dielectric constant from which the agglomeration factor was calculated. This theory was accepted in this investigation because there appears to be no other reasonable explanation.

As said previously, the agglomeration factor was unity up to a concentration of 20%. Values for higher concentrations varied up to 5.3. Rates of shear up to 800 rpm were used. When particle agglomerates are subjected to shear they are partly broken up but in the presence of strong agglomeration forces particle chains will still exist even at moderate shearing stresses. This will lead to orientation and to a decrease in the dielectric constant and result in a somewhat decreased agglomeration factor without breaking up the structure. The most reliable measure of the state of agglomeration is taken at rest. FIGURES 27 and 28 show the increase in the agglomeration factor with time. Since the agglomeration factor increases with time it is evident that a structure build-up is taking place.

It was observed experimentally that very low shearing rates were necessary to obtain a decrease in the dielectric constant. However, the more concentrated emulsions required higher shearing rates to obtain the minimum value. This indicated a strong tendency to form particle agglomeration. (It should be noted that these changes in the dielectric constant could not be attributed to a temperature coefficient). Several plots (See FIGURES 20 to 23) show steps in the dielectric constant with increasing rpm. This can be accounted for by assuming structures of different strength being present. This assumption is supported by the fact that different rest values for different trials were recorded indicating different

structure formation. Thus a certain shearing force required to break up one structure would not be sufficient to break up another. The fact that the up curves and down curves have the same pattern seems to be further evidence in support of this. (See FIGURES 20 to 23). Hysteresis loops were observed in the lower concentration range. (See FIGURE 19). At present there appears to be no other explanation for these results except that they could be due to an orientation or a time effect.

When the shearing forces were discontinued the instantaneous value of the dielectric constant was not that of the dispersion at rest. The time required to reach the original value varied considerably. A period of 24 hours was required by several of the dispersions before the original value was reached. Even this duration of time was not sufficient in some cases. This might indicate the breaking up of a complicated structure which would require a long time to rebuild. The unreproducibility could also be attributed to the diversity in structure which reformed when the emulsion was at rest. If the shape of the particles was the sole factor in causing the observed decrease in the dielectric constant then upon removing the shearing forces the original rest value would be reached instantaneously. It would require an infinitesimal amount of time for a spherical particle which was distorted to say an ellipsoid to return to its original shape. However, the rebuilding of a broken structure would require a measurable period of time.

All the dielectric constant measurements were taken at a frequency of 10 kilocycles. There appeared to be no great changes in the readings when taken at 1 kilocycle and 100 kilocycles hence these were not recorded.

The rheological data which was obtained simultaneously with that of the dielectric data shows some enlightening results.

The dispersions up to 20% were observed to be Newtonian (See FIGURES 12 and 13.) This is in agreement with the dielectric properties where it was found that up to these concentrations the agglomeration factor was unity, indicating that the particles were acting independently. For dispersions of higher concentrations hysteresis loops (See FIGURES 14 to 18) were obtained indicating thixotropic systems. The plot of the viscosity and concentration of the dispersed phase (See FIGURE 29) is somewhat similar to that of the dielectric constant and concentration (FIGURE 24). In both cases the break occurs at 20%. The viscosity as calculated at the high shear rates appears to satisfy the Einstein equation. The slope of the straight line (FIGURE 30) however, is not 2.5 as predicted for spherical particles. The value calculated was 5.1 and the deviation from 2.5 can be attributed to a deviation of the particles from spherical shape. The viscosity was calculated at the high shear rates so that the particles if not acting independently exhibit a minimum relation for each other. (It should be noted that the proportion factor using the simplified Bruggeman equation turned out to be 5.1 resulting in a form factor of 1.7). Yield values were calculated (Table IX) for the thixotropic systems and were found to increase with increasing concentration.

The rheological data obtained for the oil alone showed it to be Newtonian in behavior under stresses of over 700 rpm. (See FIGURE 11). Since no thixotropic loop was obtained it follows necessarily that up to this shear rate the oil is not thixotropic.

On investigation of the dielectric and rheological behavior of

the dispersions over the investigated range it appears that the system changes at the concentration 20% from one of Newtonian to one of non-Newtonian. It was further observed that the viscosity was still changing after the dielectric constant had reached a minimum. This can only be explained by assuming that the shape of the particles has more effect on the viscosity than it has on the dielectric constant. That is the viscosity is more sensitive at high shear rates to the shape of the particles than is the dielectric behavior.

REFERENCES

1. VOET, A.J. Phy. and Colloid Chem. Vol. 51, p.1037. 1947.

2. GREEN, H. and WELTMAN, R.N. Alexander's Colloid Chem. Vol. VI: p.328.

3. BUCKINGHAM, E. Proc. Am. Soc. Testing materials 21, II 1154. 1921.

4. DEBYE, P. Polore Molekeln, S. Herzel Leipsig. 1929. -Lorentz Lorez and Clausius - Masotti relations.

5. BRUGGEMAN, D.A.G. Ann. Physik 24, 636 - 679 (1935).

6. GUILLIEN, R. Ann. Phys. 16, 205-252 (1941).

7. PARTS, A. Nature 155, 236, (1945).

8. FISCHER, E. Colloidal Dispersions. (1950 Rd).

9. COUETTE, M. Ann. Chem., 21, 433-510. 1890, or see HATSCHEK - Viscosity of liquids;Bell (1928) p.51.

10. BARR, - A Monograph of Viscometry. p.233.

11. WELTMANN, R.N. Inter. Chem. Rev., 2, 43-52, also GREEN, H., U.S. Patent 2, 365, 339 Dul9, 1940.

12. TAYLOR. Proc. Roy. Soc. A 157: 546. 1936.

13. TAYLOR. Phil. Trans. Roy. Soc. London A 223: 289 (1923).

14. BUCKHEIM, STUART and MENZ. Physik 112, 407 (1939).

15. GREEN, H. Industrial Rheology and Rheological Structures, Wiley Publication.

16. REINER and RIWLIN - Journal of Rheology. Vol. I (1928).

17. WELTMANN. Ind. Eng. Chem. 15, 424 (1943).

18. FREUNDLICK. Thixotropy, Herman et Cie Paris (1935).

19. GREEN and WELTMANN. Ind. Eng. Chem., Anal. Ed., 15, 201 (1943).

20. WELTMANN, J. Applied Phys., 14, 343 (1943).

21. GREEN and WELTMANN, Ind. Eng. Chem., Anal Ed., 18, 167 (1946).

22. EINSTEIN. Ann. Physik, (4) 19, 289, (1906) 34, 591 (1911).

23. COLLOID SCIENCE - Alexander and Johnson. Vol. II. Oxford Ed.

24. EMULSION TECHNOLOGY.

25. BENNETT. Practical Emulsions.

26. FISCHER.....Colloidal Dispersions (Wiley Publication).

27. GREEN.....Industrial Rheology and Rheological Structures.